Aalto University
School of Engineering

Anna Rumpunen

Suitability of a thermosyphon heat exchanger for cooling of power electronic components

Master's Thesis

Espoo 06.03.2015
Supervisor: Professor Pekka Ahtila, Aalto University
Instructor: Roman Jauhonen M.Sc. (Tech.)

Aalto University
School of Engineering

Aalto University, P.O. BOX 11000, 00076
AALTO
www.aalto.fi

Abstract of master's thesis

Author Anna Rumpunen

Title of thesis Suitability of a thermosyphon heat exchanger for cooling of power electronic components

Degree programme Energy and HVAC-Technology

Major Energy Technology **Code of professorship** Ene-59

Thesis supervisor Professor Pekka Ahtila

Thesis advisor Roman Jauhonen, M.Sc. (Tech.)

Date 6.3.2015 **Number of pages** 102 **Language** English

The development of power electronics continuously increases their power density and therefore creates challenges for their cooling. Conventional cooling methods, such as heatsinks, are no longer able to cope with the cooling of high heat densities, and therefore, new cooling methods are needed. Two-phase compact thermosyphon (COTHEX) cooling allows the cooling of higher heat densities without having to resort to using pumps. The standard COTHEX technology, however, cannot replace heatsinks due to their structure because it does not match with the cuboid shape of a heatsink. This thesis focuses on designing a thermosyphon concept for power electronics cooling that can replace a heatsink without the need to redesign the products in which they are installed.

In this thesis, three thermosyphon based cooling elements were designed, and their structures were optimized to provide as effective cooling as possible with thermal simulation. The thermal performances of the optimized elements and a conventional heatsink of same size were then compared to determine the solution which most effectively transfers heat. The best thermosyphon cooling method was selected, and its features were studied in more detail. The most suitable thermosyphon cooling element substantially improved the cooling of the power electronic device, semiconductor, compared to a conventional heatsink of the same size.

The selected thermosyphon construction was able to cool more effectively than the conventional heatsink at higher heat loads, higher surrounding temperatures and with lower air flows. The construction generates lower pressure drop and therefore allows higher air flow rates pass the finned structure of the cooling element. The coolant circulation enables stable heat distribution to the whole area of the baseplate in which the semiconductor is attached. Thus, thermosyphon technology provides heat transfer at the baseplate at a constant temperature, which offers many benefits. For example, even temperature distribution has a positive effect on the aging of semiconductor chips.

This thesis developed a new thermosyphon type and analysed its thermal performance. The new thermosyphon gave such positive results that it is highly recommended to replace conventional heatsinks with thermosyphon technology in power electronics cooling.

Keywords Power electronics, cooling, thermosyphon, heat exchanger, COTHEX, phase transition, heatsink, cooling element.

Tekijä Anna Rumpunen

Työn nimi Faasimuutoslämmönvaihtimen soveltuvuus tehoelektroniikkakomponenttien jäähdytykseen

Koulutusohjelma Energia- ja LVI-tekniikka

Pääaine Energiatekniikka **Professuurikoodi** Ene-59

Työn valvoja Professori Pekka Ahtila

Työn ohjaaja Diplomi-insinööri Roman Jauhonen

Päivämäärä 6.3.2015 **Sivumäärä** 102 **Kieli** Englanti

Tehoelektroniikan tehointensiteetti kasvaa jatkuvasti tekniikan kehittyessä mikä luo paineita tehoelektroniikan jäähdytykselle. Nykyisenä jäähdytysteknologiana käytetyt ripajäähdytteiset jäähdytyslevyt eivät enää kykene jäähdyttämään tarpeeksi tehokkaasti tehoelektronisia komponentteja ja siksi tarvitaan uusia jäähdytysmetodeja. Kompaktit faasimuutoslämmönvaihtimet (COTHEX) eli termosifonit mahdollistavat tehokkaamman jäähdytyksen ilman pumppuja. Jo käytössä oleva termosifonitekniikka ei kuitenkaan suoraan sovellu korvaamaan nykyisiä jäähdytyslevyjä, koska niiden muoto eroaa vahvasti suorakulmaisen särmiön muotoisista jäähdytyslevyistä. Tässä työssä suunnitellaan sellainen termosifonikonsepti tehoelektroniikan jäähdyttämiseen, joka voi korvata jäähdytyslevyn ilman että tuotetta, jonka sisälle se on asetettu, pitää muotoilla vahvasti uudelleen.

Työhön ideoitiin kolme erilaista termosifonitekniikalla toimivaa jäähdytyselementtiä ja niiden rakenne optimoitiin lämpöteknisesti lämpösimulointiohjelmien avulla. Optimoitujen jäähdytyselementtien ja samankokoisen jäähdytyslevyn jäähdytystehoja verrattiin keskenään, jotta löydettäisiin tehokkain tapa siirtää lämpöä pois tehoelektronisesta komponentista. Paras termosifonitekniikalla toimiva elementti valittiin voittajakonseptiksi ja sen lämmönsiirrollisia piirteitä tutkittiin tarkemmin. Elementti paransi tehoelektronisen komponentin, puolijohdemoduulin, jäähdytystä merkittävästi, kun sitä verrattiin samankokoiseen jäähdytyslevyyn.

Valittu termosifonirakenne jäähdytti paremmin niin korkeammissa lämpökuormissa ja ympäristön lämpötiloissa, kuin matalammissa jäähdytysilmamäärissä. Se tuottaa vähemmän vastapainetta ja siten päästää enemmän ilmaa lauhduttimen läpi perinteiseen jäähdytyslevyyn verrattuna. Termosifonin jäähdytysnesteen kierto mahdollistaa tasaisemman lämmön jakautumisen pohjalevyyn, johon puolijohdemoduuli on kiinnitettynä. Siten lämpötilajakauma pohjalevyssä on myös tasaisempi, mikä on todella toivottavaa puolijohteita käytettäessä. Termosifonitekniikan mahdollistama tasaisempi lämpötilajakauma pohjalevyssä esimerkiksi lisää puolijohteen käyttöikää.

Tässä tutkimuksessa keksittiin uusi termosifonirakenne ja sen jäähdytyskykyä tutkittiin. Se tuotti merkittäviä parannuksia puolijohteiden lämmönsiirrossa, joten on hyvin suositeltavaa soveltaa lämpösifonitekniikkaa tehoelektroniikan jäähdytyksessä jäähdytyslevyjen korvaamiseksi.

Avainsanat Tehoelektroniikka, jäähdytys, faasimuutos, lämmönsiirto, termosifoni, jäähdytyslevy, jäähdytyselementti

Acknowledgements

I wish to express my gratitude to my instructor, M.Sc. Roman Jauhonen for the great opportunity to develop the functionality of a significant product at the department of High Power Drives at ABB. Your advice had a major role in improving my work.

I also want to thank M.Sc. Teemu Heikkilä, Dr. Tero Viitanen and M.Sc. Tommi Liukko for their valuable insight during this study. Examining the potential of using a thermosyphon to improve the cooling of a frequency converter has been an inspirational and rewarding process. I thank my supervisor, Professor Pekka Ahtila, from the department of Energy Technology for sharing his experience and ideas regarding my research. I also wish to thank Timo and Bruno for their great assistance in the more practical aspects of the simulation process.

My special acknowledgements go to my close family for their comprehensive support and interest in my thesis study. I thank my father, Jyrki, for the new points of view. I also wish to express my gratitude to my mother, Leena. You have given your strong support for me during my thesis work and my whole studying career, for which I am truly grateful.

Most importantly, I wish to thank you, Jori, for standing by me throughout my thesis work and the eventful years in Otaniemi. I am thankful for your encouragement and the great improvement ideas you gave. Your patience and interest towards the study made this Thesis possible.

Espoo, 6.3.2015

Anna Rumpunen

Contents

Nomenclature

Latin Alphabet

Symbol	Meaning	SI units
A	area	m^2
a	thermal diffusivity	m^2/s
C	heat capacity	kJ/Ks
c_p	specific heat	J/kgK
D_h	hydraulic diameter	m
E	irradiance	W/m^2
f	friction factor	-
G	mass velocity	kg/m^2s
g	acceleration of gravity	m/s^2
H	height	m
L	length	m
l	latent heat	J/kg
M	molar mass	kg/mol
m	variable concerning fins	1/m
m	mass	kg
$\dot{m}$	mass flow	kg/s
n	number of objects	-
Nu	Nusselt number	-
P	perimeter	m
p	pressure	Pa
Δp	pressure drop	Pa
Pr	Prandtl number	-
q	heat flux	W/m^2
R	thermal resistance	K/W
Re	Reynolds number	-
s	thickness	m
T	temperature	K
ΔT	temperature difference	K
$\partial T/\partial x$	temperature gradient	K/m
V	volume	m^3
$\dot{V}$	volume flow	m^3/s
v	velocity	m/s
ν	kinematic viscosity	m^2/s
v	specific volume	m^3/kg
x	vapour quality	-
x	position along the conductive material	m
Δx	vapour quality change	-
z	position along the evaporator	m

Greek Alphabet

Symbol	Meaning	SI units
α	heat transfer coefficient	W/m^2K
Δ	difference	-
δ	boundary layer	m
ε	emissivity	-
ε	void fraction	-
η	efficiency	-
η	effectiveness	-
θ	temperature difference	K
λ	heat conductivity	W/mK
μ	dynamic viscosity	Ns/m^2
ξ	singular pressure drop coefficient	-
ρ	density	kg/m^3
σ	Stefan-Boltzmann constant	W/m^2K^4
Φ	heat power	W

Subscripts and abbreviations

Symbol	Meaning
∞	surroundings
b	base of the fin
c	condensation, coolant
ch	channel
cond	conduction
cr	critical
D	Dittus-Boelter
e	evaporator
f	friction
g	gravity
H	Heatsink COTHEX
l	liquid
M	Mounting base
max	maximum
min	minimum
PT	phase transition
R	Reference heatsink
r	radiation
s	surface, singular frictional pressure drop
sat	saturation
SC	semiconductor
T	Thermos
t	temperature
v	vapour
W	wall

AC	alternating current
CFD	computational fluid dynamics
CHF	critical heat flux
COTHEX	compact thermosyphon heat-exchanger
DC	direct current
FEM	finite element method
GWP	global warming potential
IGBT	insulated-gate bipolar transistor
MPE	multi-port extrusion
NTU	number of transfer units

1 Introduction

1.1 Backgrounds of the study

When it comes to the development of power electronics, it is clear that their power density is increasing. The components can be built into smaller assemblies due to development in electrical design. This creates challenges in their cooling. Power electronic components, such as semiconductors, create heat losses while under operation and the heat needs to be conveyed out of the components to prevent them from heating excessively. As the components become smaller, the area from which the produced heat is transferred becomes smaller. This makes it more challenging to convey heat out of the component. The current dominating heatsink technology struggles to meet with the today's demands for the cooling effectiveness. It should be ensured that a viable thermal design solution for the cooling of semiconductors in a given restricted space can be offered in the future as well.

Already now poor heat transfer of power electronic components constrain their usage. For example, in frequency converters each semiconductor has been determined a maximum amount of power that is allowed to be transferred through to keep the temperatures inside the semiconductors at a safe level. Even with restricted usage the semiconductors would benefit from lower temperature levels, because high temperatures in the components result in fast aging and eventually breaking of the component. For example, it is said that every 10 ^{0}C increase in the semiconductor chip's junction temperature reduces semiconductor lifespan by 50 % [1]. It is evident for safety and reliability reasons to improve the cooling of components in devices containing power electronics. Better safety and reliability results in savings on maintenance and will increase the customer satisfaction.

Compact thermosyphon heat exchanger (COTHEX) has proven out to be efficient in transferring heat especially from small areas of high heat density. It is a heat exchanger with gravity driven coolant circulation that benefits from high heat transfer coefficients of coolant's phase transition. The coolant boiling and condensing not only enable efficient heat exchange in small locations but it does it without the use of compressors or pumps. The boiling acts as a natural pump in the coolant circulation. Thermosyphons have already been studied to be beneficial for semiconductor cooling, for example by Perpina et al [2]. Another advantage of thermosyphon cooling is that the cooling occurs at constant temperature, because of heat absorption at phase transition. This allows better conditions for semiconductor usage and creates less strain due to temperature gradient inside the component. Compact thermosyphons using Multi-Port Extrusion (MPE), a type of small scale channels, for transfer of fluid should fit well for the semiconductor cooling purposes, because of their compactness and low material and fluid use.

The costs of using the compact thermosyphon technology in the cooling of the semiconductor may create a hindrance on its usage as the semiconductor cooling element.

The traditional heatsink offers most economical solution for the cooling. Yet, air cooling struggles to match the requirements for the cooling of semiconductors. Air cooling is feasible form of cooling for systems with low generated currents, but where there are high system powers and a low system voltage, the generated current in the circuit heats the semiconductors too massively. The effects of air cooling is intensified by using high pressure resistant fans that blow air at high velocity, but the solution creates noise problems as the huge fans need to provide the necessary air flow. Furthermore, the air cooling with heatsink technology can reach only a certain level of heat transfer effectiveness. After a certain point, increasing fan power no longer avails semiconductor cooling and new methods for more effective semiconductor cooling are needed.

Compact thermosyphons create far more value compared to the expenses used for the liquid cooling. The liquid cooling needs more components than thermosyphons and thus requires more installation time and maintenance. Liquid cooling needs components such as pipes, a pump, a cold plate, valves and sensors to measure flow and pressure of the liquid. Especially the pump generates expenses due to frequent need for its maintenance. Water cooling also brings water close to electrical parts, which means that elements have to be made from an expensive cupronickel alloy to eliminate the risk of leaks. All these components and materials create expenses that are not desirable for the development of cooling of semiconducting devices.

1.2 Objectives

This study concentrates on the cooling of power electronic devices with high power density. The objective of this thesis is to study thermosyphon technology for the cooling of power electronic components and to develop a thermosyphon cooling element that can replace the heatsink, which is currently used in cooling of electronics and power electronic devices such as frequency converters. The solution based on using thermosyphon technology should meet two different criteria. Firstly, the cooling performance of the thermosyphon has to be better than with heatsink. Secondly, the thermosyphon structure should match the one of heatsink, so that the thermosyphon could directly replace the heatsink in the application it is used in.

A finned cuboid-shaped aluminium heatsink that cools the ABB ACS880 r8i single drive’s semiconductor is used as the Reference heatsink and an optimal thermosyphon structure is designed to replace this heatsink. If the thermosyphon can be proven to cool semiconductor more efficiently, the designed thermosyphon meets the criteria of a successful design. The cooling performance of the thermosyphon and heatsink are defined using simulation programs. These programs are also used in the thermosyphon optimization process. This thesis concentrates on designing a suitable thermosyphon element to replace a heatsink on a theoretic level and does not take a stand on the manufacturability issues concerning thermosyphon manufacturability.

1.3 Delimitations

There are many methods available for cooling of power electronic devices. The most commonly used ones according to S. Kang [3] are air cooling, heat pipes, thermosyphons and liquid cooled cold plates. Semiconductor dissipates heat intensively and is often placed into a very compact place with the cooling element due to shortage in installation space. Therefore, a highly effective cooling method is needed. Thermosyphon meets this requirement and is chosen to be developed for cooling of the semiconductor.

The thermosyphon structure design has two delimitations that originate from the construction of the semiconductor and heatsink. The first delimitation for the cooling element is that the cooling element absorbs the semiconductors' heat with conduction. This means that the heat is transferred through solid material layers between the semiconductor and cooling element due to temperature difference between the layers. The semiconductor has a solid baseplate through which it emits heat and the cooling element has to have a baseplate to absorb the heat. Cooling elements that would absorb the heat directly with fluid circulation is not studied.

Other delimitation is that the cooling element has to emit its heat to the surroundings with finned structure as it is a component inside an application, such as frequency converter, and it is cooled with forced air flow. The heat can be transferred inside the cooling element from the baseplate to the finned structure either by conduction (heat transfer inside a solid material) or convection. Convection is determined as transfer of heat between solid material surface and fluid flow. Heatsinks transfer heat inside the cooling element using conduction and heat pipes, cold plates and thermosyphons transfer heat using primarily convection.

Thermosyphons utilize the high heat transfer coefficients of flow boiling and therefore should fit best for applications that require compact size and effective heat transfer. Due to requirement of compact size, this study focuses only on closed loop compact thermosyphons. The thermosyphon transfers heat with coolant that is on its two-phase state. Coolant is on a two-phase state when it is saturated and part of its content is in liquid phase and part in vapour phase.

One must note that heat pipe is a different device than thermosyphon, however. Their operation methods are based on different physical phenomena. Heat pipe is an enclosed pipe which has a narrow slotting on the inner surface, wire mesh or porous sintered structure and small amount of fluid. As the other end of the pipe is heated, the generated vapour moves to the cooler end of the pipe. In the cooler end the vapour condenses back into liquid and emits heat. The liquid moves back to the hotter end of the pipe due to the capillary forces in the inner pipe structure. Both thermosyphon and heat pipe use the heat of vaporization for heat transfer but the force that determines the flow direction is different. Thermosyphon applications base their operation on gravity and heat pipe applications on the capillary effect.

1.4 Research methods

This study concentrates on developing a functional thermosyphon application based on literature and by using simulation programs and 3D modelling. The study explains the working methods and properties of thermosyphon heat exchangers on theoretical level by utilizing the theory of heat transfer the literature has provided. The book Heat and Mass transfer is the dominating source of information when the thermodynamic features of the thermosyphons are discussed. These theories of heat transfer are applied when creating different thermosyphon cooling element structures.

The optimization of the thermosyphon concepts is conducted with simulation and modelling programs and simulation results give estimation on the effectiveness of each cooling element. This thesis does not conduct any experimental measurements. However, the credibility of the thermosyphon simulating program is validated with a development case that has succeeded in producing a functional thermosyphon cooling method for its semiconductor cooling. The simulations and testing measurements of the developments case are compared together, which will give proof that the thermosyphon thermal performance is in agreement with the predictions of the simulation program.

The modelling of the thermosyphons is conducted using Parametric Technology Corporation's (PTC) Creo Parametric modelling program. The program is commonly used as 3D parametric modelling tool. The 3D models are used to visualize the structures of the cooling concepts and as the basis of calculations in simulation programs. The 3D models are used in numerical computational fluid dynamic flow models to calculate their impact on the flow patterns inside the module. The 3D models are also vital in calculating the thermal properties of the cooling elements to visualize the structures of the cooling elements.

The fluid dynamics inside the frequency converter module are calculated using ANSYS Icepak. ANSYS, Inc. is a simulation software developer and its product, ANSYS Icepak, is CFD (Computational Fluid Dynamics) simulation software, which simulates fluid dynamics for electronics thermal management. The program calculates values for pressure, flow and temperature in a 3D model space. One can insert objects such as fans, heat exchanges and heat sources into the space and they can be determined features with thermodynamic properties. The aim is to create a simulation case that resembles the problem faced in the real life and to solve the problem by using the solver engine ANSYS Fluent.

The simulation space is meshed with a grid structure, which divides the total volume of the space into small elements. The grid is constructed in such way that it respects the boundaries of the objects inside the model space. The solver calculates pressure, speed (except in solid objects) and temperature for each element and therefore grid creation plays an important part on the accuracy of the modelling program. The program begins to calculate values for each element, which are in thermodynamic and hydrodynamic relation between each other when initiating the calculation. The program continues to

iterate increasingly accurate values for the elements based on previous results from the iterations until it reaches convergence. Convergence is reached when the relative error of the values in the elements is lower than the specified value given to the program by the user.

Corporate Research Centre of the ABB ltd. has developed a simulation program, COTHEX Designer, to calculate and optimize the thermal properties of compact thermosyphons. The software calculates temperatures, thermal resistance and pressure changes inside the thermosyphon fluid circulation loop. The research team has developed the tool by conducting measurements to thermosyphons by designing the tool to match the results of the measurements. They use correlations derived from literature and have developed new ones to produce more accurate results. The program, for example, utilizes experimental results from literature such as condenser heat transfer coefficient (Shah [4]), the heat transfer coefficient for air flow (Chang and Wang [5]) and void fraction (Chrisholm [6]). A proper heat transfer coefficient for boiling in minichannels could not be found from literature, so the research team developed one based on their measurement data.

The program uses finite element method (FEM) simulation to define the baseplate temperature distribution with means discussed by Jonathan E. Guyer, et al [7]. The program uses similar methods as ANSYS Icepak to iterate values for different sections inside the loop. The user provides a first guess for vapour quality, saturation temperature and mass flow of the fluid in the thermosyphon and calculates other values according to these values. The values should meet three convergence criteria, which are the mass, momentum and energy conservation. SIMPLEX algorithm, developed by George Dantzig in 1947, is used to reach convergence in the conservation results.

2 Backgrounds

2.1 Semiconductors

Semiconductor device converts the electricity fed into a desired form utilizing the electronic properties of semiconductor materials. Semiconductor consists of two different components: Insulated Gate Bipolar Transistors (IGBT) and diodes. Diodes allow the current to move only in one direction and thus convert the electricity passively. IGBT is a semiconductor device with four semiconducting material layers. It is used as an electronic switch and because it can be opened and closed at will, it operates in the semiconductor device as an active component in electricity conversion. The diodes and IGBTs are connected together as seen in Figure 1 and by opening and closing the IGBTs the current can be converted to a desired state. In the figure, IGBT is marked in a blue circle and diode marked in a red circle.

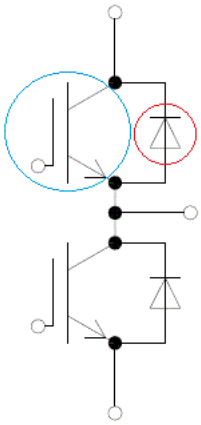

Figure 1. Circuit diagram of a dual IGBT module

Using semiconductors generate heat to some amount due to the fact that the components in the semiconductors are unideal. Both IGBT and diode chips produce heat with two different methods. Heat is generated while in operation and when switching on and off. The total heat generated by the semiconductor chips is the sum of these two heat generation methods. Bond wires that connect the diodes and IGBTs generate small amounts of heat as well.

While the diodes and IGBTs are on-state, a small voltage occurs over the chips and thus generates heat losses. The momentary losses in the components, IGBTs and diodes, can be calculated by using equation 1:

$$\Phi = UI \ , \tag{1}$$

where Φ is the heat generated, U is the voltage over the component and I is the current passing through the component.

The heat losses generated by switching on and off the IGBTs depend strongly on the switching frequency. The switching frequency f_{sw} depicts the amount of switching on and off in a time unit and the time of one switching cycle T_{sw} is the inverse of switching frequency. During one switching cycle, the IGBT is once turned on and once turned off. During a switch on and off, a significant voltage occurs over the IGBT chip and simultaneously a strong current passes through the chip. This creates a vast amount of heat loss in a short time.

The total heat generated is the sum of these three elements; constant heat loss at operation, switch on and off heat loss and heat loss in the bond wires. The heat is conducted to the surroundings, mostly towards the semiconductor's baseplate although a small amount of the heat transfers into the bus bars that connect the semiconductors into other components. However, in this study all the heat generated is expected to be transferred through the baseplate. The method of heat transfer from the semiconductor device to the thermosyphon baseplate is discussed in the Chapter 3.3.1.

2.2 Thermosyphons

Thermosyphons are heat exchanging devices that circulate a substance through natural convection. In other words, the movement of the coolant occurs due to change in the density of the coolant, without an external source. The change in density of the coolant occurs in thermosyphon applications because of rise in the coolant temperature or phase transition. The portion of the coolant which is less dense rises and the denser portion falls. This phenomenon creates a force which drives the coolant to movement. As the circulation of the coolant occurs naturally, the thermosyphons do not use external surface forces, such as pumps. As the difference in the coolant densities is the driving force for the movement, the thermosyphon is dependent on the gravitational field and thus requires to be placed in such orientation as it is designed.

The thermosyphons studied in this thesis circulate fluid inside a closed loop in which it is in constant transition phase between liquid and vapour. This type of flow is called two-phase flow and it is characteristic for it to have physical properties of both fluid and vapour. The liquid and vapour are expected to be at their saturated state and so the heat absorbed and emitted by the coolant is transmitted completely to coolant's phase transition. The reason for keeping the coolant in its saturated state instead of allowing the coolant to transfer heat in other states (subcooled or superheated) is that the heat transfer is most efficient at saturated state. Other major reason is that the temperature difference between the coolest and the hottest spot at cooling element baseplate is at its lowest when refrigerant is at a saturated state. Chapter 3.4.2 discusses these reasons and their importance more in detail.

The main reason for keeping the coolant in constant phase transition is that the heat is then transferred most efficiently. Heat transfer coefficient α determines the effectiveness of heat transfer. It is the fraction between heat flux q and temperature

difference ΔT as stated in the equation 20. Large value for the heat transfer coefficient predicts good ability to cool, because it stands for that the temperature difference between refrigerant and baseplate is small relative to the heat flux directed to the cooling element.

The heat from the semiconductors is first transferred inside the cooling element to the condenser area and then out of the cooling element. The cooling out of the element in this study is conducted with forced air flow. Figure 2 states typical heat transfer coefficients in different heat transfer methods and it shows that gas flow between tubes has a heat transfer coefficient up to values of 350 W/m^2K, however, it can be enhanced further with powerful fans that force the air flow to move even faster. Heat transfer coefficient can reach up to 3000 W/m^2K with the fans. In that case the heat transfer occurs with forced convection. Heat transfer out of the cooling element is conducted with forced air flow produced by fans and cannot be changed in the study.

The heat transfer methods inside the cooling element can be affected, though. Conventional heatsinks rely on conduction to transfer the heat from the semiconductor to the cooling element's finned structure that dissipates the heat. The heat transfer coefficient inside the cooling element can be increased with fluid circulation inside the cooling element, in which case convection also transfers heat from the semiconductor to the finned structure. The fluid circulation may be executed with forced convection, for example with cold plates, which are frequently used in liquid cooled electronics. However, even higher heat transfer coefficients can be achieved with phase transition, such as boiling and condensation.

The coolant both boils and condensates in the thermosyphon cooling element fluid circulation loop and therefore it can transfer heat most efficiently of all the methods of heat transfer. Figure 2 states that boiling and condensation have the highest values for the heat transfer coefficient in heat transfer. Typical heat transfer coefficient values for both boiling and condensation is in the magnitude of 10 000 W/m^2K. Therefore, thermosyphon applications have higher potential for heat transfer than any other type of cooling element.

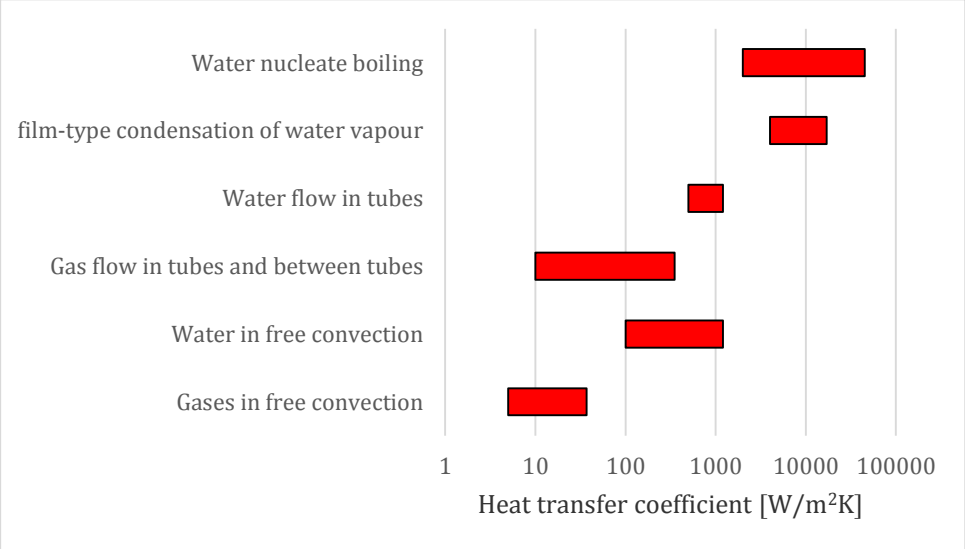

Figure 2. Typical heat transfer coefficient values for different cooling methods

In boiling, heat is fixed into vaporization due to the fact that the molecules require energy in order to break loose from the bonds that tie them together into liquid form. Another factor that increases the heat transfer coefficient with phase transition is that boiling phenomenon speeds the flow circulation. The bubble generation in boiling dramatically decreases the fluid's density and thus creates a force that moves the fluid upwards. This is called bubble pumping effect. The heat transfer coefficient of flow boiling is the sum of forced convection flow in pipes due to bubble pump effect and the absorption of heat of bubble generation. Therefore, flow boiling creates the highest possible heat transfer coefficients and is the most efficient method to transfer heat via convection.

Thermosyphon heat exchanging devices utilize the high temperature level of the heat by turning part of the heat into work that forces the working fluid to circulate in the system at a fast pace. Therefore, the bubble generation can be seen as the working force in the thermodynamic cycle of the thermosyphon operation. The work is done to overcome the decelerating forces that occur due to frictional pressure drops in the pipes. Other forces that affect the thermodynamic cycle of the thermosyphon are gravitational forces and condensing. Chapter 3.5 concentrates more on the thermo- and fluid dynamic properties of the thermosyphons.

The laws of thermodynamics and limitations in installation space strongly affect the design of the thermosyphon applications. Chapter 0 discusses the mechanical aspects of the design of compact thermosyphons for the cooling of power electronic devices.

Thermosyphons have already been utilized in frequency converters' semiconductor cooling. ABB has patented a compact thermosyphon for semiconductor cooling as seen in Figure 3.

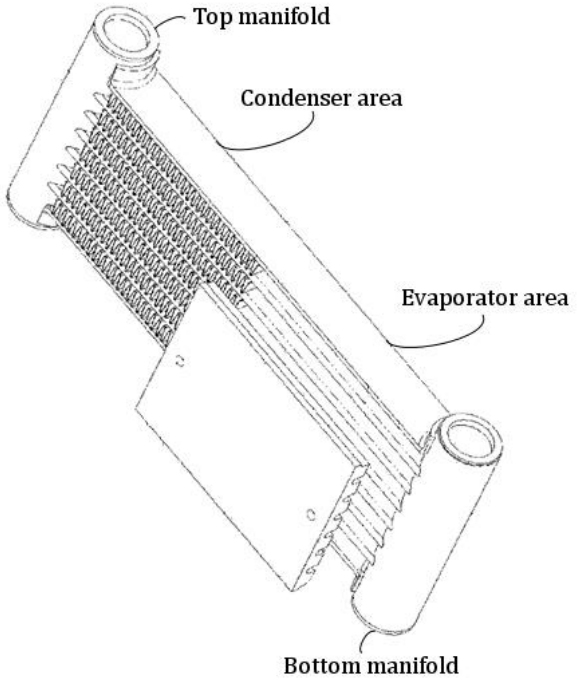

Figure 3. Standard COTHEX for cooling of power-electronics components: EP 2031332 A1 [8]

The thermosyphon in Figure 3 operates by vaporizing fluid in the evaporator area. The vapour flows towards the top manifold inside minichannels that are in multiport extrusion (MPE) tubes. The vapour travels through condenser area in which it emits heat and the top manifold gathers the vapour and subjects its flow downwards back to the condenser area. The vapour condenses in the minichannels and falls to the Bottom manifold. The evaporator area then pumps and vaporizes the fluid back into the circulation from the bottom manifold. This compact thermosyphon is referred as standard COTHEX in this study.

This structure of standard COTHEX can only be used for the semiconductor cooling when the air flows to the condenser in horizontal direction and a flat planar space is available for its placement. Therefore, it cannot be used directly to replace the heatsink as it instead needs a cuboid shaped space through which fan blows air parallel compared to the baseplate of the cooling element. This means that this kind of thermosyphon cannot be used directly to replace a traditional heatsink as it cannot be placed in similar locations where the heatsinks are installed.

Thermosyphon applications show much potential for the electronics cooling. If a thermosyphon can be designed and optimized in such way that the construction of the thermosyphon does not create thermal resistance excessively, the power electronic components will have lower temperature levels than with other cooling methods. Thermosyphon has potential to transfer heat more efficiently than any other cooling method discussed.

3 Theory of heat transfer

3.1 Heat transfer in general

Heat transfer is defined as the energy which crosses boundaries from a system to another and this transport of heat occurs due to the temperature difference between the systems. The first law of thermodynamics states that energy never disappears. With heat transfer this means that the change in the internal energy of a closed system is equal to the amount of heat supplied to the system, reduced by the amount of work done by the system on its surroundings. The second law of thermodynamics states the direction of heat transfer: heat always flows over the boundary of the system to the direction of the lower temperature level. Heat transfer occurs always when there are temperature differences inside a system or between them. Three modes of heat transfer can be distinguished: radiation, conduction and convection.

Thermal radiation takes place between surfaces. All surfaces radiate, but the surfaces that are at lower temperature level than other surfaces receive more heat than they emit, therefore gaining heat altogether. Conduction is transfer of energy inside a material or through material layers due to a temperature gradient, which is temperature difference within a certain length of material. Convection is heat transfer due to temperature difference between solid material's surface and a fluid that is in motion. These methods of heat transfer usually occur simultaneously but often one of these methods dominates.

3.2 Radiation

Thermal radiation is electromagnetic radiation which is transmitted between surfaces. Radiation is generated by charged particles in a matter, which are in constant thermal motion. The particles elevate into energy level above an arbitrary baseline energy state and fall back to their baseline energy state. When the particles are above the arbitrary baseline, they hold energy which they will emit when they fall back to the baseline energy state. The energy emitted from this excited state is in form of electromagnetic waves and therefore needs no substance for its transfer. Gaseous and liquid substance hardly absorbs this kind of energy and therefore it can be said that the heat is transmitted only between surfaces.

All forms of matter emit electromagnetic waves. When radiation energy hits the surface of any matter, a part of it is absorbed and the rest of it is reflected or transmitted to surroundings. The radiation is absorbed by a very thin layer of matter in the surface layers of an object. The absorbed energy is turned back into heat and conducted into inner layers of an object and as a result the temperature increases inside the matter. As all objects' surfaces constantly radiate heat and absorb heat, the sum of these energies determines whether the total heat exchange by radiation is positive or negative in a given

position of surface. The change in the temperature inside the matter is dependent on the direction of total heat exchange.

The amount of thermal radiation between two surfaces is dependent on the quality of the surfaces, the temperature difference between them and their location. The intensity of radiation, irradiance, is the total power sent by the surface divided by its area. The irradiance has the dependency on the temperature of the surface according to equation 2:

$$E = \varepsilon \sigma T_s^4 \ , \tag{2}$$

where ε is the emissivity of the surface, $\sigma = 5.670 \times 10^{-8}$ is the Stefan-Boltzmann constant and T_s is the temperature of the surface.

Emissivity ε measures the quality of the surface. Material which absorbs heat well has an emissivity close to value 1 and material that reflects most of the heat has an emissivity close to value 0. The emissivity of the objects is always something between these two values.

The total radiative thermal power Φ_r between a small radiating surface and a large surrounding surface can be stated to be according to equation 3:

$$\Phi_r = \varepsilon \sigma A (T_s^4 - T_\infty^4) \ , \tag{3}$$

where A is the area of the radiating surface and T_∞ is the temperature of the surroundings.

With this equation the magnitude of radiation power is now determined for the heatsink and the semiconductor studied of this thesis. To determine the magnitude of thermal radiation power, we may simplify and treat the heatsink as a cuboid that radiates heat from all of its surfaces. Its outside measures are 0.186 m x 0.0865 m x 0.27 m and therefore it has a total area of $A_{r,H}$=0.179 m^2, where H stands for heatsink. The emissivity of untreated aluminium is ε_H=0.06. The temperature of the surroundings can be assumed to be T_∞=40 ^{0}C, as it is a typical surrounding temperature for the heatsink in extreme operation conditions. In such situation, the temperature of the cooling element can be approximated to be $T_{s,H}$=80 ^{0}C. The radiance power for the cooling element is therefore $\Phi_{r,H}$=3.6 W. The semiconductor has a white plastic exterior with outside measures of 0.150 m x 0.02 m x 0.17 m. The total radiation area is A_{SC}=0.0383 m^2, where SC stands for semiconductor. The emissivity can be assumed to be ε_{SC}=0.8. The temperature of the semiconductor surface can be approximated to be $T_{s,SC}$=90 ^{0}C and the temperature of the surroundings is the same T_∞=40 ^{0}C. The radiance power for the semiconductor is therefore $\Phi_{r,SC}$=13.5 W. The total radiance power is therefore $\Phi_{r,H}+\Phi_{r,SC}$=17.1 W, which is less than 1 % of the maximum total heat loss of 2 kW generated in typical use of semiconductors in power conversion.

In reality the fins increase the radiation surface area and thus increase the radiation power. Yet, most radiative power generated by the fins may reflect or be absorbed into

adjacent fins. The radiative power could be increased by painting the cooling elements black and by optimizing the cooling element structures so that it would be more favourable for the radiation. It is clear though, that the most effective way to increase the radiative heat transfer is to increase the temperature of the object's surfaces or to decrease the temperature of the surroundings. As the equation 3 indicates, the radiative power correlates with temperature significantly ($\Phi_r \sim T^4$). Decreasing the surrounding's temperature is not usually possible as it is dependent on issues that cannot be controlled. Increasing the cooling element's temperature is rather a questionable solution, because increasing cooling element's temperature will also result in increased semiconductor temperature and decreasing the semiconductor temperature was the primary goal of this study.

The calculation indicates that radiation is not a major component in the heat transfer of the semiconductor cooling element and therefore it is ignored in the thesis.

3.3 Conduction

3.3.1 Conduction through material layers

Heat conduction is the transfer of energy inside a material or through material layers due to a temperature difference. There are two different physical methods of conduction. First method is heat transfer between atoms and molecules. The heat migrates through movement and vibrations of the atoms and molecules. The particle that is on a higher energy level, in other words at higher temperature, transfers some of its energy to a particle of a lower level. Thus, the movement and vibrations of particles spread to other particles causing the heat to transfer. The second method is transfer of heat inside metal alloys and other electricity conducting substances via the movement of free electrons. Because the cooling elements are made of aluminium metal alloys, this form of conduction plays a significant part of the conduction. Yet, metal alloys conduct heat less efficiently than pure metals due to errors in the material's crystal grating. The errors in the grating hinder the movement of free electrons and therefore lower the alloy's ability to conduct. These kinds of errors are for example non-metallic particles inside the crystals.

The substance's ability to conduct heat is determined with conductivity. Conductivity is very faintly dependent on the temperature of the substance and therefore the material's ability to conduct in heat transfer calculations is simplified to be a material property, a constant, predetermined for each material. Chapter 4.1.3 discusses more about metal alloys' conductivities.

Heat power travelling through a certain cross-sectional area is called heat flux and it can be presented with Fourier's conduction equation 4, which is in one-dimensional and stationary (independent of time) case:

$$q_x = -\lambda \frac{\partial T}{\partial x} \ , \tag{4}$$

where q_x is the heat flux in one dimensional case, λ is the material's heat conductivity and $\frac{\partial T}{\partial x}$ is the temperature gradient.

If the heat transfer is assumed to be linearly distributed, the heat flow Φ_{cond} for conduction can be stated to be according to equation 5:

$$\Phi_{cond} = -\lambda A \frac{\partial T}{\partial x}, \tag{5}$$

where Φ_{cond} is the heat flow via conduction and A is the cross-sectional area.

Each material of certain thickness has some thermal resistance, which measures material's resistance to heat flow resulting to temperature difference between sections of material. Thermal resistance can be defined by applying the analogy of Ohmic law in the equation 6:

$$R_{cond} = \frac{\Delta T}{\Phi} = \frac{s}{\lambda A} \tag{6}$$

where ΔT is the temperature difference and s is the thickness of the material.

Heat is conducted from semiconductors to the cooling element baseplate and to the evaporation tubes from which the coolant receives the heat. Figure 4 depicts the component material layer through which the heat is conducted. Insulated-gate bipolar transistors (IGBT) and diodes generate heat and conduct it to the baseplate of the semiconductor module. The baseplate of the semiconductor module conducts the heat to thermal grease and the thermal grease conducts the heat to the surface of the baseplate of the cooling element. The thermal grease is designed to replace the micro-sized air layer which would otherwise take place in between the baseplates of the semiconductor and cooling element. Subsequently, the heat travels from the cooling element baseplate to the surface of the evaporation tubes that hold the coolant. From there the heat is conducted to the inner surface of the evaporation tubes whereupon the heat is emitted to the coolant fluid via convection. Convection is discussed in Chapter 3.4.

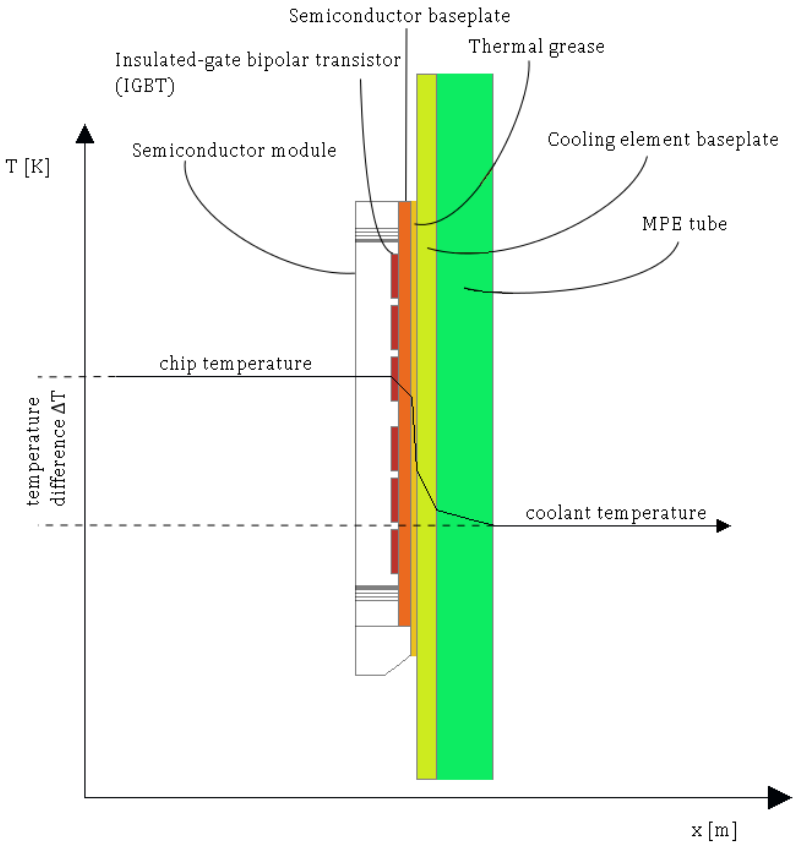

Figure 4. Cross-section of a semiconductor and temperature distribution inside it

Figure 4 depicts how the temperature decreases as the heat is conducted through each component layer. The reason for this is that each layer has some thermal resistance. The thermal resistance of the wall-like layers, such as insulated-gate bipolar transistors, diodes, semiconductor baseplate, thermal grease and cooling element baseplate, can be calculated with the equation 6 and the total heat resistance of the system is the sum of these components.

Some components are placed next to each other so that the heat transfer is divided between them. The heat transfer acts then in a similar manner as the components were connected in parallel. These kinds of components are IGBTs and diodes and evaporation tubes. For them the total thermal resistance is the resistance of an individual component divided by the number of components.

The total thermal resistance is the sum of each material's thermal resistance. In the case of conducting the heat from semiconductor to the cooling element baseplate, the total heat resistance is according to the equation 7:

$$R = \frac{s_{chip}}{\lambda_{chip}(A_{diode}n_{diode}+A_{IGBT}n_{IGBT})} + \frac{s_{SB}}{\lambda_{SB}A_{SB}} + \frac{s_{TG}}{\lambda_{TG}A_{TG}} + \frac{s_{CB}}{\lambda_{CB}A_{CB}} \quad (7)$$

where chip stands for semiconductor chips, IGBT stands for insulated-gate bipolar transistors, SB stands for semiconductor baseplate, TG stands for thermal grease, CB stands for cooling element baseplate, n_{diode} is the number of active diodes and n_{IGBT} is the

number of active IGBT chips. The thickness and conductivity for the semiconductor chips are identical and therefore they are presented with the same subscript.

The total amount of heat conducted is:

$$\Phi = \frac{\Delta T}{R} = \frac{\Delta T}{\frac{s_{chip}}{\lambda_{chip}(A_{diode}n_{diode}+A_{IGBT}n_{IGBT})}+\frac{s_{SB}}{\lambda_{SB}A_{SB}}+\frac{s_{TG}}{\lambda_{TG}A_{TG}}+\frac{s_{CB}}{\lambda_{CB}A_{CB}}} \quad (8)$$

where ΔT is the temperature difference between the semiconductor chips and the cooling element baseplate.

3.3.2 Conduction in the fins

The heat is transferred out of the cooling element by blowing air through a finned structure, which is connected to the condenser. The coolant condenses inside the condenser by emitting heat to the condenser tube walls. The walls conduct the heat to the finned structure, from where the heat is absorbed into the air flow. The purpose of the fins is to enlarge the cross-sectional area of the cooling area and thus making the heat transfer more effective as stated in equation 21.

Yet, this enlargement of area is only partially effective, because the thermal resistance in the fins cause the fins to have a temperature difference between the tip and the base of the fin. The longer the fins are, the larger the temperature gradient is. This temperature gradient causes the effect that the temperature difference between the cooling air and the tip of the fin is smaller than the temperature difference between the cooling air and the base of the fin. The fin efficiency η describes this effect and is explained more thoroughly later in this chapter.

The fin efficiency calculation is possible if the temperature distribution inside the fin is known. To be able to calculate the temperature distribution, some assumptions have to be made:

1. The temperature only changes in one direction, which is from the base of the fin to the tip.
2. The fin material has constant thermal conductivity.
3. The heat transfer coefficient α at the fin surface is constant.
4. The temperature of the air surrounding the fin is constant.

These assumptions are usually true with the exception of the assumption 3, which assumes that the heat transfer is constant over the surface of the fin. A generic fin that has been attached to a plate is depicted in Figure 5.

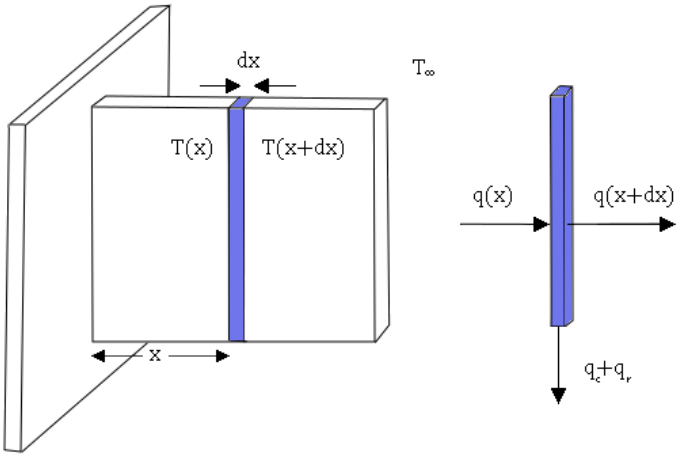

Figure 5. Energy balance for a fin element of length dx

Energy balance of the fin element heat flow with the length of dx in stationary situation is:

$$q(x) = q(x + dx) + q_c + q_r \,, \tag{9}$$

where q(x) is the heat flux conducted to the fin element, q(x+dx) is the heat flux conducted out of the element, q_c is the heat flux dissipated by convection and q_r is the heat flux dissipated by radiation.

The heat left to be conducted to the following element can be described by inserting the equation 5 into equation 9:

$$q(x + dx) = q(x) + \frac{\partial q}{\partial x} dx = -\lambda \frac{\partial T}{\partial x} A + (-\lambda) \frac{\partial^2 T}{\partial x^2} dx A \,, \tag{10}$$

where A is the cross-sectional area of the fin.

The heat dissipated by convection and radiation can be described to be:

$$q_c + q_r = \alpha (P dx)(T(x) - T_\infty) \,, \tag{11}$$

where $\alpha = \alpha_c + \alpha_r \approx \alpha_c$ is the total heat transfer coefficient, P is the perimeter of the fin, T(x) is the temperature of the fin at the point x and T_∞ is the temperature of the surroundings. The heat transfer coefficient for radiation is negligible for reasons stated in the Chapter 3.2.

Inserting the equations 10 and 11 into the equation 9 and integrating it will form a solution with some undefined constant values for the energy balance equation. By adding some boundary conditions, the constant values can be defined. First boundary condition states that in the point x = 0, in other words at the base of the fin, the temperature is

$T(x=0) = T_b$. Second boundary condition depends on how the fin is attached to the cooling element.

If the fin is only attached from the base of the fin, meaning that the tip of the fin is loose, the second boundary condition states that in the spot x = H, where H is the height of the fin, ergo at the tip of the fin the heat conduction is approximately zero and therefore $\partial\theta/\partial x\,|_{x=H} = 0$, where $\theta = T - T_\infty$ is the temperature difference between the base of the fin and its surroundings.

If the fin is attached from both ends, and the fin is heated at both ends with equal amount of power, the heat flow in the middle of the fin is zero. Therefore the second boundary states that $\partial\theta/\partial x\,|_{x=H/2} = 0$.

By inserting these conditions to the solution of the integrated energy balance equation, we get the heat conducted from the base of the fin. Two different equations can be determined for the heat load conducted through these two different fin attachment cases. If the fin is only attached from the base of the fin, the heat load equation can be stated to be according to equation 12:

$$\Phi_{b,1} = \theta_b m \lambda A tanh(mH) \tag{12}$$

and if the fin is attached from both ends, the heat load equation can be stated to be according to equation 13:

$$\Phi_{b,2} = \theta_b m \lambda A tanh(\tfrac{1}{2} mH)\ , \tag{13}$$

where m is a variable defined by the features of the fin and its surroundings. The generic equation for the variable m is:

$$m = \sqrt{\frac{\alpha P}{\lambda A}}\,. \tag{14}$$

The variable m needs to be defined for each fin structure used in the different cooling concepts. All the cooling elements in this study have fin structures that consist of plates. When s is the thickness and H is the height of the fin, the following equations apply for the plate fins that are substantially higher compared to their thickness: $A = s \cdot H$, $P = 2H + 2s$ and consequently $P/A = 2(s+H)/sH \approx 2/s$. Therefore, the variable m is for the plate fins:

$$m = \sqrt{\frac{2\alpha}{s\lambda}}\,, \tag{15}$$

where s is the thickness of the fin.

The efficiency of the fins can be calculated using the equation 16:

$$\eta = \frac{\Phi_b}{\Phi_{b,max}}\,, \tag{16}$$

where $\Phi_{b,max}$ is the maximum heat load.

The maximum heat load that can be conducted through the fin would occur when the temperature of the fin is constantly in the fin's base temperature T_b. This would mean that the fin would have infinite thermal conductivity. The maximum heat load can be calculated with equation 17:

$$\Phi_{b,max} = PH\alpha\theta_b \tag{17}$$

By inserting the equations 12 and 17 into equation 18, the fin efficiency equation 18 for the fins only attached from their base is defined as:

$$\eta = \frac{tanh(mH)}{mH}. \tag{18}$$

Inserting the equations 13 and 17 into equation 18, the fin efficiency equation 19 for the enclosed fins attached and heated from both ends is defined as:

$$\eta = \frac{tanh(\frac{1}{2}mH)}{\frac{1}{2}mH}. \tag{19}$$

3.4 Convection

3.4.1 Convection in general

In a flowing fluid, heat is not only transferred by conduction but with macroscopic movement of the fluid. Part of the heat travels via conduction due to temperature gradient in the flow and part as enthalpy and kinetic energy bound in the mass of the fluid. This is called convective heat transfer and it can be described as the superposition of thermal conduction and energy transfer by the flowing fluid.

In the case of heat transfer of a thermosyphon, convection occurs in two different locations. Firstly, the cooling air absorbs heat from the fins located in the thermosyphon condenser area and moves the heat away from the element surroundings. Secondly, the coolant inside the thermosyphon channels transfers heat via convection. The effectiveness of the convection is enhanced with boiling and condensing of the coolant which both are special cases of convective heat transfer.

Let us study heat transfer with convection that occurs between a surface and flowing medium when they are in different temperature levels. Figure 6 presents the velocity and temperature curves of the fluid flow. As seen from the figure, at the heated surface x = 0 the velocity of the fluid v(0) is zero and the heat is transferred only with thermal conduction. The velocity increases with the function v(x) and the heat transfer similarly shifts from conduction over to the convection method of heat transfer. The fluid and the surface create a boundary layer in which the velocity of the flow increases from zero to v_∞. This boundary layer is called hydrodynamic boundary layer δ. Similarly the temperature decreases with the function T(x) and the heat transfer is shifted from conduction over to the convection. The fluid and the surface create a boundary layer in which the temperature of the fluid decreases from the wall temperature T_W into temperature T_t that approximates the surrounding temperature T_∞. This boundary layer is called temperature boundary layer δ_t. Figure 6 presents the velocity v (left) and temperature T (right) curves in a fluid as a function of distance from the wall.

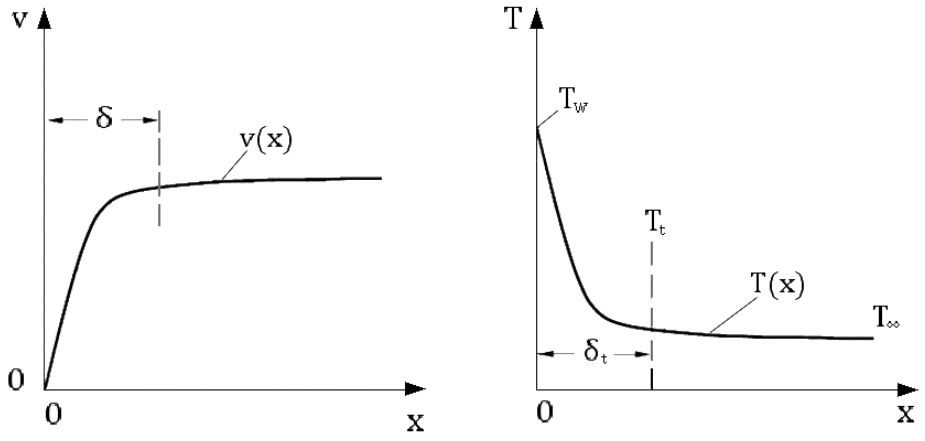

Figure 6. Velocity and temperature curves of fluid flow respect to distance from surface, which emits heat [9, p. 11]

The convection can be divided into two different types according to the character of the flow. The convection can be described as natural, if no external influence such as a pump or fan increases the flow velocity. In such case the mass transfer of the convection occur because the temperature difference generates differences in the density of the fluid material and thus forces the fluid to movement. The convection can be described as forced, if the fluid flow is generated with an external force.

There are also convection processes that are based on the phase transition. In the phase transition process the major amount of the heat is transferred with latent heat generated in the phase transition such as boiling or condensation. Both boiling and condensation result in huge heat transfer efficiencies which is the main idea for the effectiveness of compact thermosyphon heat exchanger applications. Boiling and condensation will be discussed in the Chapters 3.4.2 and 3.4.3.

Regardless of the type of convection, the heat flux from the surface to the coolant can be described with the equation 20:

$$q = \alpha(T_W - T_\infty) \,, \tag{20}$$

where q is the heat flux, α is the heat transfer coefficient, T_W is the temperature of the heat transfer surface (wall) and T_∞ is the temperature of the surroundings.

The convective heat can be calculated by multiplying heat flux with heat transfer area and fin efficiency (should the calculation be made for the whole cooling element) as the equation 21 states:

$$\Phi = A\eta q \,, \tag{21}$$

where Φ is the heat load, A is the heat transfer area and η is the fin efficiency.

Heat transfer coefficient α determines the effectiveness of heat transfer. The external conditions, such as flow type and flow rate, have strong influence on its value. Two dimensionless quantities: Reynolds number Re and Prandtl number Pr depict these external conditions. Reynolds number depicts characteristics of the flow. The flow may be laminar, turbulent or in transition zone between the given two. When the value for Reynolds number is less than 2300 for flow inside a pipe, it can be assumed to be fully laminar. When the value of the Reynolds number is over 4000, the flow in a pipe can be assumed to be turbulent. Laminar flow can be described as flow in which the parallel layers of the fluid do not mix together and as a result there is no disruption between the layers. Turbulence is the inverse of laminar flow. It is unsteady, aperiodic motion in which the fluid experiences fluctuations and mixing of matter, energy and momentum.

As the thermosyphons are cooled using air flow generated by fans, the air flow can straightforwardly assumed to be turbulent. For coolant flow, coolant's boiling creates a

bubble pumping effect, thus causing the flow to be turbulent as well. For these reasons this study concentrates only in explaining the characteristics of the forced turbulent flow.

Reynolds number is defined as the ratio of inertial forces to viscous forces and therefore quantifies the relative importance of these flow forces for the flow conditions. Reynolds number can be calculated with equation 22:

$$Re = \frac{vD_h}{v}, \tag{22}$$

where v is the mean velocity of the fluid, D_h is the hydraulic diameter for geometry of the fluid flow area and v is the kinematic viscosity of the fluid material.

The kinematic viscosity is ratio of the dynamic viscosity μ to the density of the fluid ρ. The dynamic viscosity is a measure of a fluid's resistance to flow, which is constant for each material. The velocity v can be calculated using equation 23:

$$v = \frac{\dot{m}}{\rho A}, \tag{23}$$

where ṁ is the mass flow of the fluid, ρ is the density of the fluid and A is the cross-sectional area the flow travels through. The hydraulic diameter D_h can be calculated using equation 24:

$$D_h = \frac{4A}{P}, \tag{24}$$

where P is the wetted perimeter of the cross-sectional area.

The other dimensionless quantity, Prandtl number Pr, is defined as the ratio of kinematic viscosity to thermal diffusivity. Thermal diffusivity measures the material's ability to conduct energy respect to its ability to store energy. Prandtl number defines the ratio of heat transfer between conduction and convection. When Pr is much smaller than the number 1, thermal diffusivity dominates and when Pr is much larger than the number 1, kinematic viscosity dominates. Prandtl number is calculated using equation 25:

$$Pr = \frac{v}{a} = \frac{c_p \mu}{\lambda}, \tag{25}$$

where a is the thermal diffusivity $a = \frac{\lambda}{\rho c_p}$, c_p is the specific heat of the fluid, μ is the dynamic viscosity and λ is the thermal conductivity of the fluid.

Many empirical correlations have been created to predict the heat transfer coefficient for the convective heat transfer. All correlations are dependent of the context of the fluid flow. One has to determine where the convection occurs, for example, in a pipe, channel or on a flat plate. Also, the type of the flow needs to be determined because the

correlations only apply when the Reynolds and Prandtl numbers have their value in a certain area specified for each correlation.

In order to calculate the heat transfer coefficient of the turbulent convective flow, a dimensionless Nusselt number Nu is used to define the relation between the correlations. Nusselt number can be described in two different ways. First description gives the relation to the heat transfer coefficient.

$$Nu = \frac{\alpha D_h}{\lambda}. \quad (26)$$

The second description binds the Nusselt number to the Reynolds and Prandtl numbers. This description requires knowledge of the flow types and the location it occurs in.

When the convection occurs in the cooling fins, the Nusselt number can be described with equation 27 that is constructed for cases with a flat plate in turbulent flow:

$$Nu_x = 0.037 Re_x^{4/5} Pr^{1/3}, \quad (27)$$

when $0.6 < Pr < 60$. [10]

Combining the equations 26 and 27 will result the convective heat transfer coefficient of the turbulent flow for a fin:

$$\alpha = \frac{0.037 Re^{4/5} Pr^{1/3} \lambda}{D_h}. \quad (28)$$

Icepak, that is used to simulate the dynamics of the air flow in a frequency converter module with the cooling elements, uses a different heat transfer model for the convective cooling of the fins. Icepak utilises The Zero Equation Model to calculate the heat transfer coefficients. The calculation method is described in the Appendix 1.

The Nusselt number for the convection for coolant inside the MPE tubes' channels can be calculated with Dittus-Boelter equation 29:

$$Nu_D = 0.023 Re_D^{4/5} Pr^n, \quad (29)$$

where n = 0.4 for heating (evaporator channels), n = 0.3 for cooling (condenser channels) [11] and when $0.6 \leq Pr \leq 160$, $Re_D > 10\,000$ and $L/D_h > 10$, where L is the length of the tube. [10] By combining the equations 26 and 29, the convective heat transfer coefficient for the channels is created:

$$\alpha = \frac{0.023 Re_D^{4/5} Pr^n \lambda}{D_h}. \quad (30)$$

The phase transition requires an additional heat transfer coefficient component to be added to the heat transfer coefficient equation due to the fact that heat is not only transferred with movement of the fluid but also with heat absorption and emission to bubble generation. The heat transfer coefficient for boiling and condensation is described in the Chapters 3.4.2 and 3.4.3.

Regardless of the type of the flow, the heat Φ_{PT} transferred with phase transition can be described with the equation 31:

$$\Phi_{PT} = \dot{m}_{PT} l \, , \tag{31}$$

where PT stands for phase transition, $\dot{m}_{PT}$ is the mass flow of the material transiting its phase and l is the latent heat released in vaporization.

3.4.2 Boiling

Boiling is the rapid vaporization of a liquid, which occurs when a liquid is heated to a temperature which equivalent vapour pressure is at or above the pressure of surroundings. The liquid has then reached its boiling point and the vaporization occurs inside the liquid, thus forming bubbles that rise upwards.

Most bubbles nucleate in the heated walls and when the size of the bubble is sufficient, the vapour bubble detaches from the walls leaving a vapour nuclei to produce a new bubble. The amount of heat that is emitted by the walls defines the speed of bubble formation. Bubble formation in larger scale determines the flow pattern of the boiling, which plays an important role in the effectiveness of the heat transfer.

Comprehensive and all inclusive theories of the boiling have not been formed, which means that the study concentrates only on the experimentally discovered relationships between different parameters of boiling, more specifically on boiling as it may occur in the compact thermosyphon applications. The boiling takes place in vertical channels of a small diameter and the type of the flow discussed is turbulent forced convection.

The pressure difference caused by boiling determines the flow behaviour. The system pressure decreases along the heated surface due to added heat input. Heat input increases the vapour content in the pipeline according to equation 48. Increasing amount of vapour corresponds to decreasing amount of liquid. Vapour quality x measures this and is presented in the equation 32:

$$x = \frac{\dot{m}_v}{\dot{m}} \, , \tag{32}$$

where $\dot{m}_v$ is the mass flow of the fluid in vapour phase and $\dot{m}$ is the total volume flow of the fluid.

Due to increase of vapour content, the system pressure decreases as stated in the equation 43. Pressure drop in the system simultaneously superheats the liquid, which raises the rate of evaporation. This phenomenon is called flashing and it often occurs in the forced two-phase flows in heated channels. The nominal system pressure determines the boiling temperature along with the fluid's own material properties. These kind of constantly changing parameters; vapour quality, system pressure and boiling temperature, have a strong effect on the heat transfer coefficient. Hence, it can be said that boiling in the heated tubes is a dynamic process whose properties the heat transfer coefficient and the flow patterns strongly depend on.

Figure 7 presents flow patterns with the regions of heat transfer that occur in a pipe of a small diameter and the temperatures of the wall and fluid. Characteristics of the flow patterns and the behaviour of the temperature in the wall surface and fluid are explained in the following paragraphs.

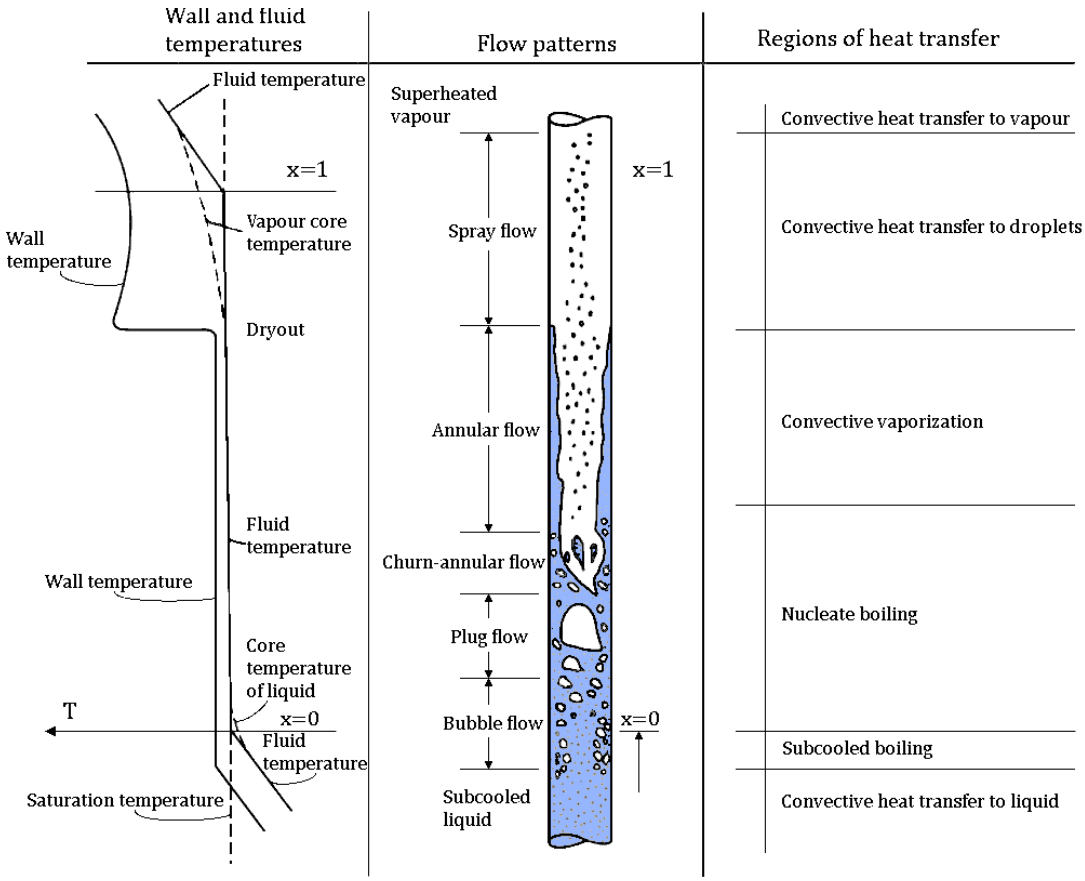

Figure 7. Flow patterns in a vertical, heated tube [9]

Let us examine a case in which a subcooled liquid enters a heated pipe, is boiled in its saturated state, and leaves the pipe as superheated vapour. Subcooled liquid is liquid at temperature below its saturated temperature. Heating of the subcooled liquid happens with typical convective heating explained in the Chapter 3.4.1. All heat goes to increasing the temperature of the liquid and hence, it is characteristic for this type of flow to have no

bubbles in the liquid. Vapour bubbles do form in the heating surfaces but they quickly condense back to liquid as they leave the heated wall and reach the core of the liquid. As the temperature increases the bubbles start to persist; first close to the wall in the subcooled boiling phase, and as the temperature increases they become more and more dispersed in the liquid flow. This phase is called bubble flow and it can only exist with very small amounts of vapour in the liquid. Bubble flow phase is typical for flows with high velocity and high pressure and therefore not experienced as a dominating flow pattern in small channel thermosyphon applications. However, bubble flow phase can be experienced in the thermosyphon as a very brief boiling state that turns quickly into plug flow boiling had the liquid been subcooled at some point. [9]

When the core of the liquid is heated to the liquid's saturation temperature, the heat is transferred with nucleate boiling and temperature remains constant. Saturation state is the point all heat is directly converted into phase transition and consequently, the temperature of the fluid remains constant. The bubble flow turns into plug flow as the vapour bubbles coalesce into larger bubbles. The bubbles expand until they fill almost the entire tube section and they develop a shape of a bullet due to the restrictions caused by the tube wall. Elongated confined bubble flow, similar to plug flow but with elongated spherical top and bottom bubbles, can be observed in channels of diminutive diameter such as in the compact thermosyphon. Elongated confined bubble flow is presented in Figure 8 and it has been studied to be the dominant flow pattern in the compact thermosyphon channels under typical operation values. [12] These bigger bubbles are often followed by a stream of small bubbles interspersed into the liquid.

Figure 8. Elongated confined bubbles in a small scale tube [13]

At high mass velocities the bubble structure disintegrates producing churn flow. The flow has a very unstable character that consists of large irregular vapour fragments. The heat transfer turns from nucleate boiling to convective vaporization as the phase transition from liquid to vapour occurs in the interface of the liquid and vapour. The bubbles have turned into one large segment of vapour in the core of the tube containing liquid droplets and the fluid has formed into a liquid film at the tube's wall. This boiling state is called

annular flow. One character of this flow type is that the vapour interspersed with droplets in the centre of the tube moves forward in higher velocity than the liquid film at the tube's wall. [9]

When the heating continues the liquid film degreases leaving in the end only vapour that contains droplets. This is called spray flow. The droplets vaporize until only vapour is left and further heating superheats the vapour into gas. [9] The flow has experienced dryout when the liquid film ceases to exist and only spray flows in the channels. Wall temperatures increase rapidly at dryout, which makes the cooling conditions beyond dryout unstable. When the last droplets have evaporated, heat is only transferred to the system with forced convection to the superheated vapour.

Forces pushing the fluid into movement inside the heated tubes determine the pattern of the flow and thus heat transfer region of the boiling. One important variable is the tube cross-sectional area. Also flow rates of the vapour and liquid phases and their densities contribute to the flow pattern. Figure 9 shows the regions of the flow patterns in a flow pattern diagram. In compact thermosyphon heat exchangers the coolant fluid flows inside Multi-Port Extrusion (MPE) tubes with diminutive internal channel diameters. It has been studied, that for the upflow boiling of R134a in vertical mini-channels, nucleate boiling was found to be the dominant mechanism of region of heat transfer [14], [15]. The plug and churn annular flows are said to be the dominant flow patterns in such conditions. Figure 9 presents the flow boundaries for different flow patterns.

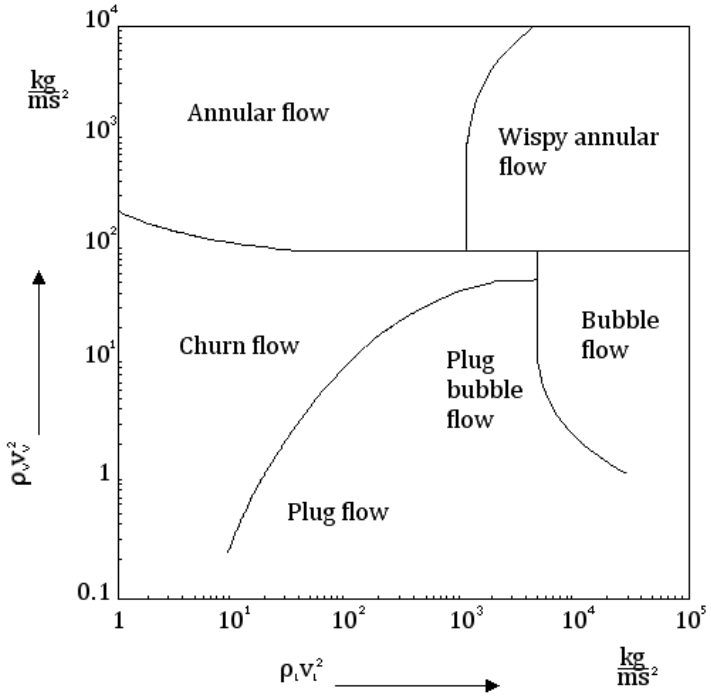

Figure 9. Flow pattern diagram for vertical, two-phase flow [16]

The x-axis presents the forces moving in the liquid phase and y-axis presents the forces moving in the vapour phase. The forces contributing to liquid flow can be calculated with equation 33:

$$\rho_l v_l^2 = \frac{\left[\left(1-\frac{\dot{m}_v}{\dot{m}_l}\right)G\right]^2}{\rho_l} \quad , \tag{33}$$

where ρ_l is the density of the liquid, v_l is the velocity of the liquid, $\dot{m}_v$ is the vapour flow rate, $\dot{m}_l$ is the liquid flow rate and G is the mass velocity. The force contributing to vapour flow can be calculated with equation 34:

$$\rho_v v_v^2 = \frac{\left[\frac{\dot{m}_v}{\dot{m}_l}G\right]^2}{\rho_v} \quad , \tag{34}$$

where ρ_v is the density of the vapour and v_v is the velocity of the vapour. The mass velocity G can be calculated as fluid's flow rate per unit area:

$$G = \frac{\dot{m}}{A_{ch}} \quad , \tag{35}$$

where A_{ch} is the cross-sectional area of the channel.

A large uncertainty has to be acknowledged for Figure 9 flow map as it has been developed only for adiabatic flows and the decisive forces in the different flow regions are not known with sufficient certainty. Regardless, the transition between the boundaries of the flow patterns is never accurate in practice and yield to subjectivity of the observer. For these reasons the flow map is given for a rough estimate of what kind of flow patterns may be experienced when testing empirically.

Boiling has been studied empirically in compact thermosyphon channels and the equation 36 has been created by Corporate Research Centre of the ABB ltd for the heat transfer coefficient α in the nucleate boiling region:

$$\alpha = 0.5\left(K\left(\frac{p}{p_{cr}}\right)^{n_1} M^{-0.5} q^{n_2} G^{n_3} - \alpha_c\right)\left(1 - tanh\left(F(x - x_{cr})\right)\right) + \alpha_c \quad , \tag{36}$$

where K = 1720.7, $p = p_{sat}$ is pressure at the saturation point, p_{cr} is the critical pressure, n_1, n_2 and n_3 are constant values defined in empirical measurements, M is the molar mass of the coolant, q is the heat flux, G is the mass velocity, α_c is convective heat transfer coefficient defined by equation 30, F = 3.1567 and x_{cr} = 0.9147.

Boiling at the evaporator part of the cooling element is however, only part of a larger heat transfer process in the thermosyphon fluid circulation. Hence, the other parts of the fluid circulation loop have a great impact to the coolant boiling. Therefore the operation of the evaporator should be studied as a part of the circulation loop to fully understand boiling in the thermosyphon cooling. Boiling as a part of fluid circulation loop is discussed in the Chapter 3.5.

3.4.3 Condensation

When vapour reaches contact with a wall of a lower temperature level than the saturation temperature of the vapour, the vapour turns into liquid at the surface of the wall. The liquid is called condensate and it is subcooled because it has emitted some of its heat to the wall. The subcooled liquid induces further vapour to condense on its surface and thus the condensing accelerates. The condensate subsequently falls down in the condenser due to having larger density than vapour. Thus the condensate leaves the condenser area and allows more vapour to condense on the cooled surface.

The course of this condensing process can be subdivided into several steps, in which a series of resistances have to be overcome in similar manner as in conduction of heat explained in the Chapter 3.3.1. The fraction of these individual resistances in the total resistance can vary a great deal. Three resistances in series have to be overcome:

1. The thermal resistance in the vapour phase when the vapour travels to the condenser wall
2. The thermal resistance during the conversion of the vapour into the liquid phase when the vapour condenses
3. The resistance of heat transport in the liquid phase when the liquid travels further.

Of these resistances, the thermal resistance in the liquid plays the major role, although in the event of the vapour being superheated the thermal resistance in the vapour has to be considered as well. In other events, it is low due to good mixing. The conversion of vapour to liquid phase has a rather small resistance. The resistance during the conversion from vapour into liquid consists of two elements. Firstly, the temperatures at the phase interface between vapour and liquid needs to drop in order of condensation to occur and secondly, particles resist phase transition.

The condensation can take place in various ways. When the liquid phase fully wets a vertical surface, filmwise condensation occurs, whereas in dropwise condensation the liquid wets the solid surface only partly. In the case of having condensate tubes in vertical position, the type of flow is film condensation. The condensate film can be in laminar or turbulent flow as shown in Figure 10:

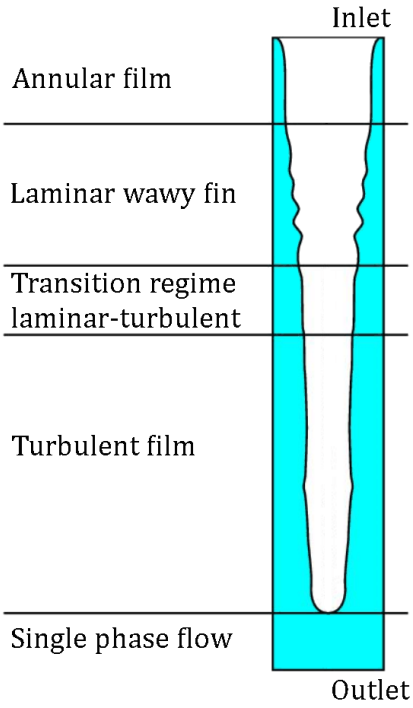

Figure 10. Flow regimes of film condensation [17]

Figure 10 shows the flow regimes in a vertical tube of a small diameter. As the vapour condenses on a vertical tube wall a liquid film develops and it flows downwards due to gravitational causes. When the vapour velocity is low and the liquid film is very thin, the liquid film is in a laminar flow and has a flow pattern of annular film. The heat is then mainly transferred via conduction.

Empirical experiments, for example the studies of Dukler and Bergelin [18], show that waves can develop even in a flow that is clearly laminar (Re < 30). The waves can be observed in all kinds of surfaces, rough and polished. The irregularities in the rate of condensing have been studied to create the waves. One might assume that keeping the stream to the condenser homogenous would improve the heat transfer, but quite on the contrary the waves have been studied to improve the heat transfer.

The velocity of the condensate increases downstream, due to gravitational acceleration. The Reynolds number of the flow increases accordingly, as predicted in equation 22. The wavy film flow regime eventually turns into turbulent flow when the Reynolds number exceeds the value of 4000. The heat transfer coefficient increases accordingly when the flow accelerates.

In the case of condensation in thermosyphon condensers, the influence of the vapour flowing along the condensate with same velocity has to be taken into account. Correlations have been found from empirical studies on how the heat transfer coefficient is related to the vapour quality, Reynolds number and Prandtl number. Condensation can be described with equation 37 presented by Shah [4]. It contains the relationship of equation 29 although the exponent of the Prandtl number is increased from 0.3 to 0.4. The

first term in the equation 37 takes into account convective heat transfer in turbulent single phase flow and an additional term in the square bracket take into account the phase transition and the effect of vapour flow. The Nusselt number for condensation is:

$$Nu = 0.023Re^{0.8}Pr^{0.4}\left[(1-x)^{0.8} + \frac{3.8(1-x)^{0.04}x^{0.76}}{\left(\frac{p}{p_{cr}}\right)^{0.38}}\right] \quad , \tag{37}$$

when following requirements are met: $100 \leq \mathrm{Re} \leq 63\,000$, $1 \leq \mathrm{Pr} \leq 13$, $10.8\ \mathrm{kg/m^2s} \leq G \leq 210.6\ \mathrm{kg/m^2s}$ and $3\ \mathrm{m/s} \leq v \leq 300\ \mathrm{m/s}$. [4]

The equation 37 for Nusselt number was not primarily developed for small channels. Yet, it has the best approximates when defining the heat transfer coefficient for the condensation of the coolant, because it is applicable down to very low mass velocities (~10 $\mathrm{kg/m^2s}$).

The heat transfer coefficient for condensation can be calculated by combining equations 26 and 37:

$$\alpha = \frac{0.023Re^{0.8}Pr^{0.4}\left[(1-x)^{0.8}+\frac{3.8(1-x)^{0.04}x^{0.76}}{\left(\frac{p}{p_{cr}}\right)^{0.38}}\right]\lambda}{D_h} \quad . \tag{38}$$

The pressure of the two-phase flow changes due to phase transition in similar manner as with the case of boiling. Condensation decreases the vapour content of the mixture as stated in the following chapter's equation 49. Reduced vapour content increases the system pressure as stated in the equation 43. Condensation at the cooling element condenser is however, only one part in the fluid circulation loop. The other parts, sections, of the fluid circulation loop have a great impact to the coolant condensation and therefore the operation at the condenser should be studied as a part of the whole circulation loop to fully understand thermosyphon cooling. Condensation as a part of fluid circulation loop is discussed in the next chapter.

3.5 Thermosyphon as a heat exchanger

To fully understand the working principles of a compact small channel thermosyphon, the heat transfer in thermosyphon loop as a whole entity needs to be studied. This means that the features of fluid flow and system pressures inside the thermosyphon need to be studied. The working principles of the thermosyphon as a heat exchanger have to be considered as well. Significant attributes in the flow study are: flow rate of the fluid, saturation temperature, vapour quality and pressure drop in each section of the loop. Number of Transfer Units (NTU) Method is used to determine thermosyphon cooling abilities as a heat exchanger.

The fluid flow and its pressure drops can be predicted with Homogeneous flow model as it has been studied to have sufficiently accurate results. [19] It is one of the simplest prediction methods for estimating pressure drop when concerning two-phase flow. Homogeneous flow model treats the two-phase mixture as a single fluid with mixed properties of both vapour and liquid. The properties of the mixture, such as the density are described by using the vapour quality x as the variable that defines the portions in which the homogenous flow carries vapour and liquid. The density of the homogenous flow can be described using equation 39:

$$\rho_{TP} = \frac{1}{x v_v + (1-x) v_l} \quad , \tag{39}$$

where TP stands for two-phase flow and *v* is the specific volume of the fluid.

The homogenous flow assumes that vapour and liquid velocities are equal which may not in reality be true. However, the dominant flow type in the case of MPE tubes with channels of small diameter is elongated confined bubble flow and these bubbles extend to fill the whole cross-sectional area of the channel, thus pushing liquid plugs upwards. Therefore, in the case of compact thermosyphons, the velocities of liquid and vapour can be assumed to be equal and a homogeneous flow model can be used. [20]

Compact small channel thermosyphon consists of six sections. There are laws of physics concerning the mass, momentum and energy that contribute in each section. Additionally, each section has a relation to the next one in a way that ensures continuum between the sections and stable conditions in the loop as a whole. Figure 11 depicts these six sections:

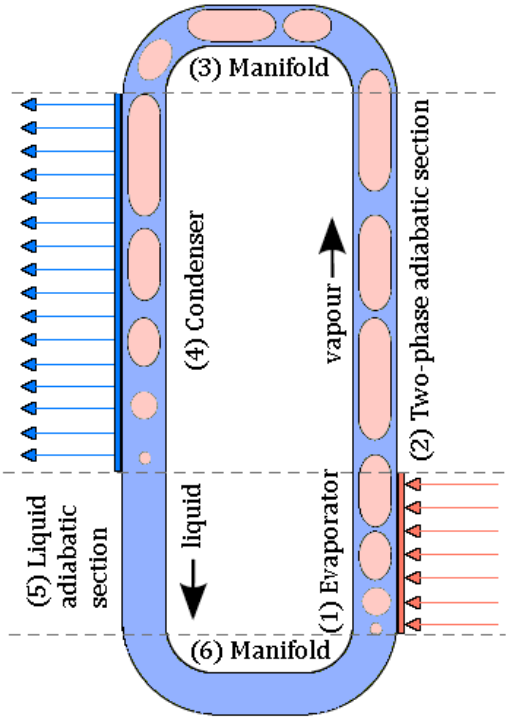

Figure 11. Thermosyphon heat exchanger fluid circulation loop [20]

Three major forces affect the fluid flow in the thermosyphon loop: accelerative, frictional and gravitational, and the forces create both negative and positive pressure drops. These pressure drops add or subtract pressure to the system pressure which is determined by the temperature of the coolant.

In the evaporator section 1, heat is absorbed from the heat source, such as semiconductor, into the thermosyphon coolant circulation. The coolant inside the pipe begins to boil as heat is absorbed into it. Chapter 3.4.2 discusses fluid flow boiling in more detail. In boiling, the density of the two-phase vapour liquid mixture decreases as the proportion of the vapour in the mixture increases. This creates a pressure drop that forces the two-phase fluid into upward movement. The increase in vapour quality accelerates the movement and the elongated confined bubbles growing in the vertical evaporator push the fluid mixture upwards. Simultaneously, the gravity force decreases pressure and forces the flow downwards as well.

The accelerative forces from heating affect the fluid as long as it moves upwards from evaporator to the two-phase adiabatic section 2. In this section the heat no longer accelerates the flow and it slowly decelerates due to frictional and gravitational forces that affect the flow movement by decreasing the pressure of the system. The fluid continues to move towards the manifold, that gathers all the fluid and distributes it to the condenser. As it reaches the manifold, the fluid flow turns to horizontal direction and the gravity no longer affects the flow. Therefore, in the manifold section 3 the only forces affecting the flow are frictional decelerating forces.

When the two-phase flow reaches the condenser section 4, it emits its heat and begins to condense back into liquid. Condensation of the fluid is discussed in Chapter 3.4.3. The condensation emits heat, which is conducted from the tube walls to the condenser fins. The fins emit heat to the surroundings via forced convection of air flow as discussed in Chapter 3.3.2. As the density of the mixture increases, the pressure of the fluid increases and creates an accelerative force that pushes the fluid to move downwards. Gravitation also increases the system pressure, thus accelerating the fluid flow downwards.

The saturated liquid continues to flow downwards in the liquid adiabatic section 5 into a manifold section 6. The gravity increases the system pressure until it reaches the manifold, where the direction of the flow turns horizontal. The manifold feeds the evaporator saturated two-phase fluid and thus begins a new round in the fluid circulation loop.

The pressure inside the loop is constantly affected due to friction and gravitation. The roughness of the pipe walls creates constantly frictional pressure drops, while curves, expansions and shrinkages in the manifolds create singular frictional pressure drops. Gravitation however, both increases and decreases the pressure inside the loop depending on the direction of the flow. When the flow moves upwards, the gravitation decreases the system pressure and when the flow moves downwards, the gravitation increases the system pressure. In horizontal flow, the gravitation naturally does not have an effect on the pressure.

There are convergence criterions to be met in the loop. The fluid mixture's mass flow inside every section needs to be exactly the same, because no mass is lost or acquired when fluid travels inside the closed loop from section to another. The total pressure drop Δp, which is the sum of the pressure drop components from all of the sections, needs to be zero. Also, the amount of energy absorbed into the loop and emitted from the loop needs to be equivalent. Otherwise the conservation equations of the loop would not be met and the loop would not converge, in other words be in balance. The Table 1 presents conservation equations for mass, pressure drops and energy distribution in the thermosyphon loop:

Table 1. Conservation equations application matrix

Section	Mass	Pressure drop				Energy
		a	g	f	s	
(1) Evaporator	1	+1	+1	+1	0	1
(2) Two-phase adiabatic section	1	0	+1	+1	0	0
(3) Manifold	1	0	0	+1	+1	0
(4) Condenser	1	-1	-1	+1	0	-1
(5) Liquid adiabatic section	1	0	-1	+1	0	0
(6) Manifold	1	0	0	+1	+1	0
Convergence	$m = m_0$		$\Delta p = 0$			$Q_c = Q_e$

The numbers in the matrix stand for following: 1=applies, +1=applies with positive effect, -1=applies with negative effect and 0=does not apply. The letter a stands for pressure drop occurring due to acceleration of the fluid, g stands for pressure drop of gravity, f stands for pressure drop of friction in the pipes and s stands for singular frictional pressure drops. [20]

The total mass of the coolant is the sum of the mass components from each section. The mass of the fluid in any section can be defined with equation 40:

$$m_{(i)} = V_{(i)}(\varepsilon\rho_v + (1-\varepsilon)\rho_l) \ , \tag{40}$$

where V is the volume of the fluid, ε is void fraction and densities ρ_v and ρ_l are valued at the fluid's saturation temperature. The void fraction is the fraction of the channel volume that is occupied by the vapour phase. When considering homogenous flow the void fraction can be defined with equation 41:

$$\varepsilon = \frac{V_v}{V} = \frac{\rho_v x}{\rho_l(1-x)+\rho_v x} \quad . \tag{41}$$

The flow rate ṁ of the coolant determines the mass velocity of the flow as stated in the equation 35. To meet the convergence criterion, the flow rate should be equal in each section to ensure continuum between sections. Both accelerative and frictional pressure drops have dependency of the mass velocity and therefore they are the parameters that define the velocity of the fluid flow in the loop.

The total pressure drop in the given section, $1 < i < 6$, can be calculated with equation 42 and it consists of pressure drop components defined in the equations 43, 44, 45 and 46 and. One must take into account whether the effect of the pressure component is positive, neutral or negative on the whole pressure system level as the pressure drop components can increase the system pressure, have no effect at all, or decrease it in the given section. The directions of the effects are determined in the Table 1. The total pressure drop in a certain section $\Delta p_{(i)}$ is according to equation 42:

$$\Delta p_{(i)} = \frac{\Delta p_a + \Delta p_f}{1+G^2 x\frac{dv_v}{dp}} + \Delta p_g + \Delta p_s \ , \tag{42}$$

where dv_v/dp is a constant evaluated at $1.3\cdot10^{-7}$ [14].

The pressure drop components in each section can be described according to the equations 43, 44, 45 and 46. Their effect on the system needs to be taken into account according to the Table 1. For example, pressure component with value of +1 increases pressure drop, thus decreasing the system pressure in the given section. Negative value of -1 again decreases pressure drop and therefore increases the system pressure. The values of pressure drop components are calculated using equations 43, 44, 45 and 46:

$$\Delta p_a = G^2(v_v - v_l)\frac{dx}{dz}L_{(i)}\ , \tag{43}$$

$$\Delta p_g = \rho_{TP} g L_{(i)}\ , \tag{44}$$

$$\Delta p_f = \frac{G^2}{2\rho_{TP}D_h}\cdot 4 f_{TP} L_{(i)}\ , \tag{45}$$

$$\Delta p_s = \frac{G^2}{2\rho_{TP}}\cdot \xi\ \ , \tag{46}$$

where G is the mass velocity of the coolant, dx/dz is the change in vapour quality within a certain vapour travel length, $L_{(i)}$ is the length of the section, g = 9.81 is the gravitational acceleration, f_{TP} is a frictional value and ξ is the singular pressure drop coefficient.

For compact thermosyphon applications the frictional value can be determined as function of the Reynolds number and it is according to equation 47:

$$4f_{TP} = 0.316 Re_{TP}^{-0.25} \text{ and} \tag{47}$$

the Reynolds number is determined according to the equation 22. The value of the singular pressure drop coefficient depends on the flow velocity as well, but also on the curves, expansions and shrinkages that change the flow direction and behaviour.

Calculating the vapour quality change Δx is necessary to define the accelerative pressure drops in the evaporator and the condenser. The vapour quality change for the evaporator can be determined with equation 48 and the quality change for the condenser with equation 49:

$$\Delta x_e = \frac{\Phi_e}{\Phi_{PT}}\ , \tag{48}$$

$$\Delta x_c = \frac{\eta C_c (T_{sat} - T_c)}{\Phi_{PT}}\ , \tag{49}$$

where η is the effectiveness of heat exchange, C_c is the heat capacity of the coolant flow, T_{sat} is the coolant saturation temperature in the given pressure and T_c is the temperature of the condenser. The heat induced to the cooling element Φ_e can be calculated with equation 1 and the heat absorbed into phase transition Φ_{PT} can be calculated with equation 31.

The heat capacity of the coolant flow C_c is calculated by multiplying the coolant's mass flow with its specific heat according to equation 50:

$$C_c = \dot{m}_c c_p\ . \tag{50}$$

where $\dot{m}_c$ is the flow rate of the coolant and c_p is the specific heat of the coolant.

The effectiveness η is determined with the Number of Transfer Units (NTU) Method. It is defined as the fraction of the actual heat transferred and the maximum possible heat transferred. The actual heat transferred is the heat absorbed into air flow that transfers the heat out of the cooling element. Therefore, the effectiveness can be calculated with equation 51:

$$\eta = \frac{\Phi_{air}}{\Phi_{max}} \ . \tag{51}$$

Heat transferred by the air flow can be described with equation 52:

$$\Phi_{air} = C_{air}\Delta T \ , \tag{52}$$

where C_{air} is the heat capacity of the air flow and ΔT is the increase of temperature in the air. C_{air} can be calculated with equation 50 by using values specified for air and air flow rate instead.

These equations will result to determining effectiveness of the thermosyphon heat exchanger with equation 53:

$$\eta = \frac{C_{air}(T_{cold,out} - T_{cold,in})}{C_{min}(T_{hot,in} - T_{cold,in})} \ , \tag{53}$$

where C_{min} is the heat capacity of the flow with smallest value in the heat exchanger.

In the case of a thermosyphon, the minimum heat capacity is either the heat capacity of cooling air flow or the coolant flow in the loop. The temperature descriptions are determined in Figure 12.

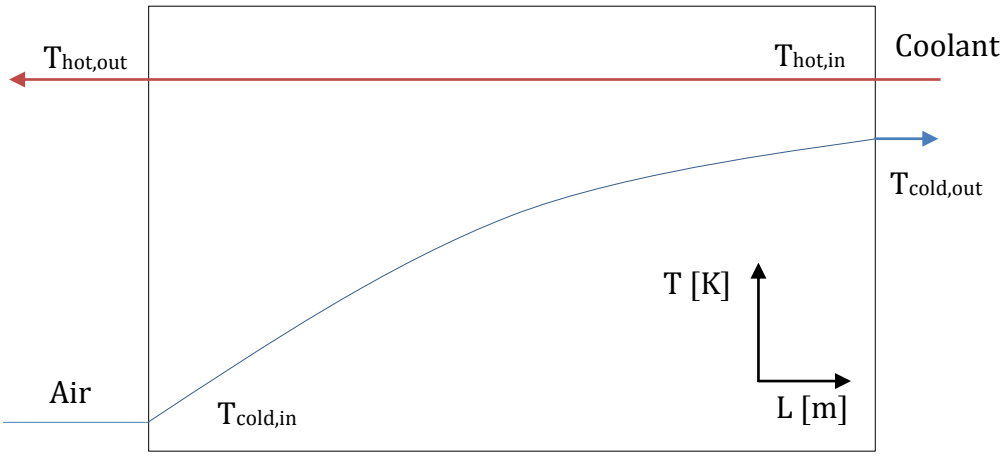

Figure 12. Temperatures of the heat flows flowing into and out of a heat exchanger

The area marked with black outlines indicates the enthalpy boundary of the thermosyphon heat exchanger. The coolant flow and its temperature are indicated with red line and the air flow and its temperature with blue line. Inside the thermosyphon

enthalpy boundary the coolant flow transfers its heat to the air flow. As a result, the temperature of the air flow increases and the vapour content of the coolant flow decreases.

The total pressure drop in the loop Δp is the sum of the pressure drops in each section $\Delta p_{(i)}$. To meet the convergence criterion, the total pressure drop should equal zero. Figure 13 gives an example of the pressure distribution in the sections inside a typical compact thermosyphon loop derived from simulations of this study.

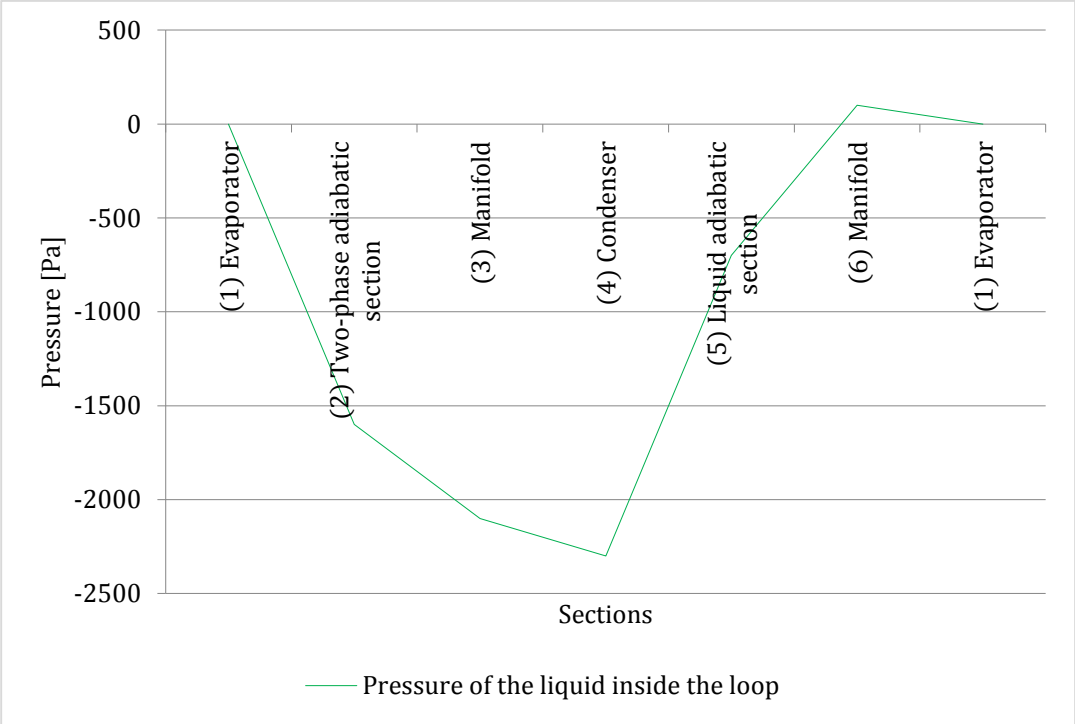

Figure 13. Pressure distribution of coolant inside a thermosyphon loop

The simulation methods for calculating the pressure distribution in the thermosyphon loop are explained in the Chapter 1.4.

The thermosyphons are designed to operate so that the coolant is in its saturated state. As the Chapter 3.4.2 discusses, the heat transfer coefficient has its highest values when the fluid is on its saturated state and transfers heat with nucleate boiling. When the heat transfer coefficient is high, the thermal resistance of the cooling element is low. With low thermal resistance the temperature difference between the semiconductor chips and the cooling element is small and heat transfer can be said to be highly efficient. Therefore, the thermosyphons are designed to operate so that the coolant is in its saturated state when thermosyphon operates on the typical heat load range. Figure 14 depicts the cooling element thermal resistance, states of the fluid and regions of heat transfer relative to heat flux directed to the cooling element baseplate.

The fluid might be in superheated state if heat flux pointed to the thermosyphon is oversized or the amount of fluid, in other words coolant filling ratio, is undersized. In this case the thermosyphon could experience dryout, which is the maximum vapour quality

beyond which hot spots occur. At dryout all the fluid has vaporized and only some spray may travel through the tubes. The working conditions of the thermosyphon are stable with heat fluxes smaller than the heat flux experienced at dryout but with greater heat fluxes excessive heat will create damage. Dryout can be avoided by keeping vapour quality below 50 % for a fixed heat flux. The heat flux at the point of dryout is called critical heat flux (CHF), which determines the point above which the thermosyphon will experience thermal runaway. The thermal runaway makes the operation conditions beyond CHF unstable and poses a thread for material damage. As there is no fluid to be heated in the heat fluxes above CHF, the wall temperatures rise uncontrollably. CHF is usually reached with fluxes above the value 100 kW/m^2 and therefore, heat flux values above it should be avoided.

If the operation conditions reach the fluid critical point, the differences in the material properties between liquid and gas phases no longer exist. This leads to a situation where gravity based thermosyphon can no longer operate as the differences between densities of vapour and liquid have ceased to exist. This stops the circulation of the fluid in the thermosyphon loop. While there is no circulation, no convective heat transfer can occur within the fluid.

The fluid might be in subcooled state if the thermosyphon heat flux pointed to the thermosyphon is undersized or the filling ratio is oversized. The heat transfer coefficient is lower in subcooled state, because the heat transfer occurs only with convective heat transfer. If the heat flux is so small that the gravity cannot overcome the viscosity of the fluid, the circulation does not occur. This is called the viscous limit. Figure 14 depicts the relations between these definitions.

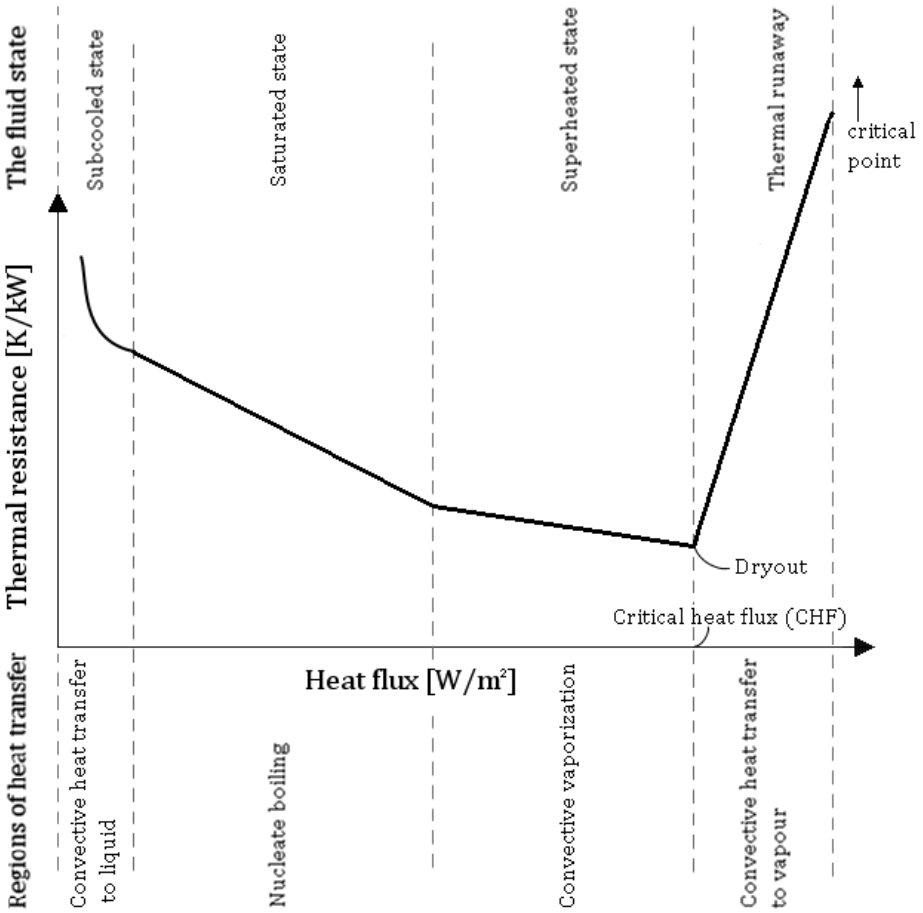

Figure 14. The effect of the heat flux for the thermal resistance of thermosyphon

The cooling element thermal resistance is remarkably lower in fluid's subcooled state and with heat fluxes above CHF. Consequently, it would be advisable to keep the semiconductor's heat flux at a range that keeps the fluid under these states. However, keeping the fluid at its saturated state will offers some benefits compared to the fluids superheated state. The fluid is at constant temperature when nucleate boiling occurs and therefore keeps the thermosyphon wall temperatures at constant level. At convective vaporization, vapour may occasionally reach contact with tube walls, which generates hotspots at the wall. This creates strain on the thermosyphon structure. Also, the maximum temperature difference at the baseplate surface increase constantly with increased heat flux. The temperature difference creates strain on the semiconductor itself and to the attachments that keep the semiconductor connected to the cooling element baseplate. Therefore, one should aim to keep the coolant at its saturated state.

This theory of heat transfer gives the guidelines to designing a functional semiconductor cooling concept to replace a conventional finned heatsink. The following Chapter 4 not only needs to consider the rules of thermodynamics in the thermosyphon heat transfer but also restrictions concerning the space the thermosyphon can occupy. The restrictions concerning space and position of the thermosyphon strongly affect the thermosyphon design. New thermodynamically feasible thermosyphon designs which meet the requirements regarding the space and heat transfer limitations in this study are presented in the following chapter.

4 The cooling concepts

4.1 Mechanical structure

4.1.1 Structure design

In this study I propose a new thermosyphon design, which will replace the conventional heatsink currently used for the ABB ACS880 r8i single drive's semiconductor cooling by filling the same space reserved for the conventional heatsink. This heatsink is referred as the Reference heatsink in this thesis and its cooling performance is used as the basis all the comparing between the cooling technologies. Three different thermosyphon concepts are designed to replace the Reference heatsink used in the frequency converter and later the one with best cooling performance is chosen as the winning concept. The heatsink and the thermosyphon have to be of similar size, because the thermosyphon should fit into the same space as the heatsink. Similar size also enables comparing between the cooling performances of the cooling technologies. There are three semiconductors in each frequency converter, all of which are cooled by a separate cooling element but this thesis concentrates on developing one cooling element that cools one semiconductor.

The Reference heatsink is constructed using traditional extruded aluminium profiles. They are called lamel profiles and they are attached to each other by pressing them together using a pressuring tool designed specifically for the job. After the pressing, the heatsink is sawn down to fixed size of 186 x 86.5 x 250 mm. The thickness of the baseplate is 19 mm. The semiconductor module is placed on the cooling element baseplate inside the hatched area shown in Figure 15. Planarity for the hatched area should be 0.025, for it is important that the baseplate of the semiconductor module is as firmly in contact with the surface of cooling element as possible. Firm contact enables better conduction of heat between the cooling element and semiconductor. Thermal grease is inserted between the semiconductor baseplate and cooling element baseplate to ensure the lack of air between the baseplates. The semiconductor is attached to the cooling element baseplate using standard screws.

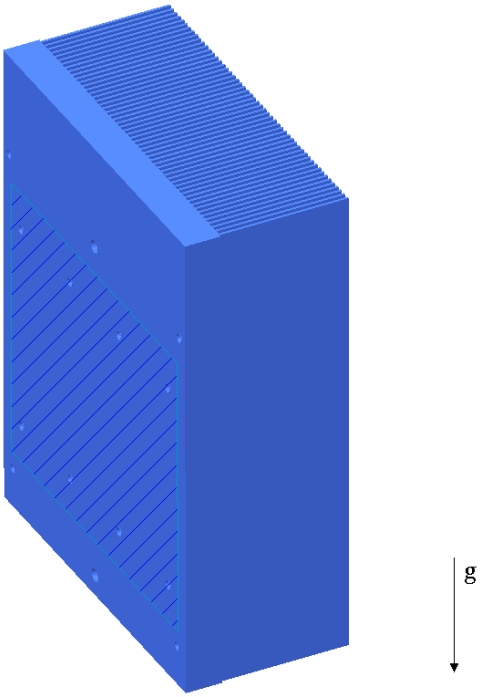

Figure 15. Reference heatsink

The frequency converter in this development study contains three cooling elements. The elements are attached into the converter module with an attachment plate and bus bars for AC (alternating current) and DC (direct current) are connected to the semiconductors creating a firm construction between semiconductor devices and other components of the converter module. Figure 16 shows the attachment of the components to the semiconductor and the direction of the cooling air flow.

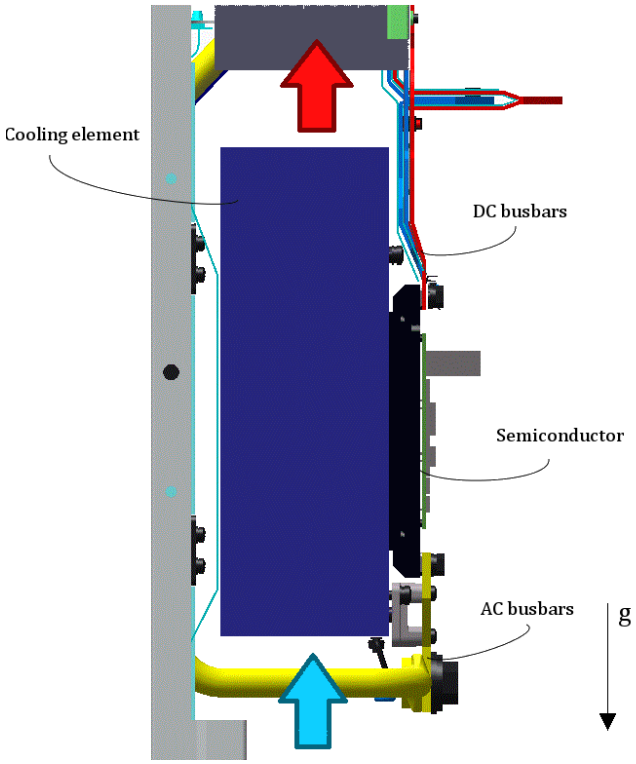

Figure 16. The structure of the semiconductor attachments and the direction of the air flow.

The arrows in Figure 16 indicate the direction of the air and heat flow. Air flows through the cooling element in vertical direction, which means that the cooling fins of the thermosyphon need to be directed in such way that the air flow travels vertically through the cooling surface area. Air arrives to the cooling element's fins at the temperature of the surroundings and leaves the element at a higher temperature.

Figure 16 shows that there is some additional space in the top parts of the cooling element, which can be utilized for semiconductor cooling. The maximum size of the thermosyphon can be 186 x 86.5 x 270 mm when the additional space taken into account. Larger size in any direction will result in reaching contact with other components, such as the other two cooling elements and AC and DC bus bars.

The restrictions for the size of the cooling element show, that the cross-sectional area for heat transfer for the cooling air is undersized for the cooling needs using the current heatsink. The equations 12 and 13 for the fins' conduction of heat to the surroundings show that the cross-sectional area plays an important role for heat transfer. However, abundance in space at the direction of the air flow does not make much of a difference unless it can be utilized in some way to increase the cooling area.

Previous studies indicate that the air flow rate travelling through the condensing area of the cooling element is inadequate with the heatsink. The cooling element fins create great amount of pressure drop which results that the fins receive little cooling air. Therefore, the focus in the mechanical design is to maximize the condensing area of the cooling element and to lessen the pressure drop created at the condenser.

One important aspect for maximizing the cross-sectional area of heat transfer is to minimize the thickness of the cooling element's baseplate. The MPE tubes, which transport the coolant, have to fit into the same baseplate however, and this means that the thickness of the baseplate has to be at least the same height as the MPE tubes. The MPE tubes have to be placed in such way that they do not interfere with the screw holes of the semiconductor. One thermosyphon manufacturer produces them in two different heights: 18 mm and 21 mm. The tubes can be assembled into the baseplate with three different pitches: 10 mm, 11 mm and 14 mm. The pitch of the MPE tubes is determined as the distance between two MPE tubes located next to each other as seen in Figure 17.

To create a baseplate with minimum thickness, the MPE tubes need to be located so that they do not overlap the screw holes. The distance between the screw holes cannot be changed, because they are used to attach the semiconductors. The different tube pitches left only one reasonable choice on how to place the tubes. The placement of the tubes (green) and screw holes (red) is shown in Figure 17 along with the tube pitch. Tube pitch is determined as the distance between two tubes.

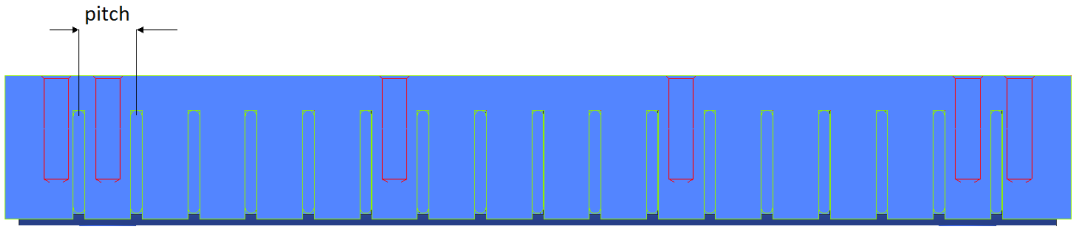

Figure 17. The position of MPE tubes and screw holes inside the baseplate

The only reasonable pitch for the tubes seems to be 10 mm and as the tube pitch and the space limitations of the Reference heatsink determine the number of evaporator tubes in the evaporator, the number of tubes can be the maximum of 17 as seen in Figure 17. Three thermosyphon concepts are developed and optimized according to these restrictions in the Chapter 4.2.4 by taking into account the nature of the space for the cooling element.

4.1.2 The cooling concepts

In this study I examine three different cooling concepts. These concepts are studied, optimized and compared with each other to find the best possible cooling method for the semiconductor. The Delimitations chapter discussed the restrictions of the structure of the thermosyphon concepts. Two main restrictions were found: installation space and semiconductor requirements. Firstly, the thermosyphon concepts have a closed loop circulation and are constructed by using multiport extrusion (MPE) with microscopic channel sizes due to very limited installation space. To achieve high heat transfer intensity, the concepts will utilize effective heat transfer of phase transition between liquid and vapour in their flow circulation. Secondly, all of the concepts will use baseplates as conducting surfaces, because the semiconductors require planar surfaces to be attached on. The cooling elements have to emit their heat to the surroundings with cooling fins in vertical direction as the heat transfer out of the cooling element is conducted with vertical forced air flow.

The first concept inspiration comes from the thermosyphon already used in ABB modules shown in Figure 3. It cannot be used directly, because the thermosyphon is designed to be cooled in horizontal air flow. Yet, by angling the condenser compared to the baseplate we can create a usable structure. This structure is shown in Figure 18.

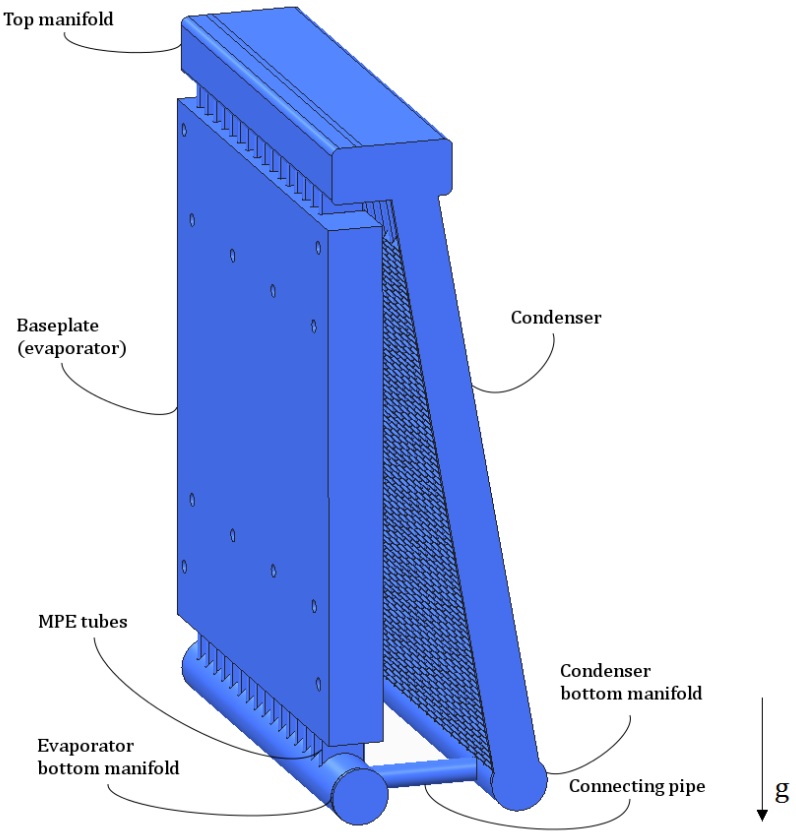

Figure 18. Concept one, Thermos thermosyphon

In bottom manifold of the evaporator, coolant is a mixture of saturated liquid and vapour with low vapour quality. Manifolds are containers, which are used in the thermosyphon applications to gather and distribute coolant from fluid channels. The coolant flows into MPE tubes' channels to the evaporator due to pressure difference between the evaporator and the manifold. Boiling has created low pressure into the evaporator and so it draws coolant to replace the fluid that has left the evaporator. The baseplate functions as the evaporator in all of the thermosyphon applications. Inside the baseplate's MPE tubes the semiconductor's heat is absorbed into the coolant and it begins to boil. This creates a force that makes the coolant travel to the top manifold. From there it travels inside the condensing MPE tubes and emits heat to the cooling fins and condensates back to lower vapour quality. This area is called the condenser. The condenser fins emit the heat to surrounding air that flows through the fins. The condenser bottom manifold gathers the fluid and sends it back to the evaporator bottom manifold through the connecting pipes.

This concept has increased its heat transfer area by positioning the condenser so that it uses the whole cuboid shaped space. It is a vast improvement of a similar L-shaped thermosyphon used in the patent EP 2682957 A1 [21], which is only able to use approximately 35 % of the heat transfer area in the similar sized space.

The condenser fins in this concept are optimized in such way that the condenser creates a small pressure drop and at the same time withholds maximum amount of fins.

As Figure 19 shows, should the fins be positioned perpendicularly (Figure 19 picture b.) respect to the condenser MPE tubes, the air flow would have to make a great inclination when passing through the condenser. When air has to swift its course dramatically, large pressure drops occur. If the fins are positioned in an inclination respect to the condenser, as in Figure 19 a, the air will shift its course in a smaller degree thus creating smaller pressure drop. The red arrows in Figure 19 depict the air travel path through the condenser. The air flows shift their course twice when passing the condenser fins and the inclinations of the air flow path in Figure 19 b. are much greater than in Figure 19 a.

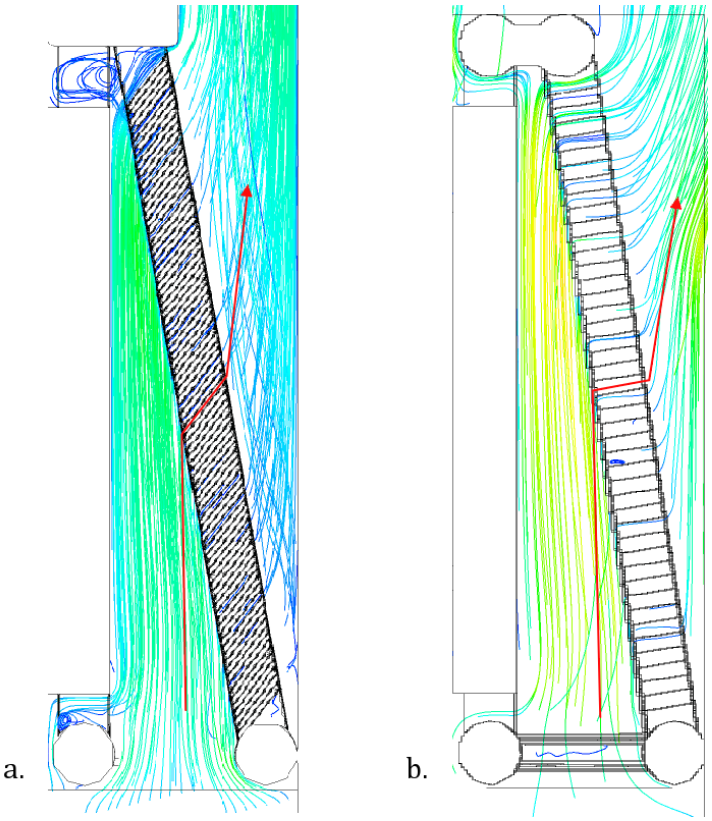

Figure 19. The shift of air flow when air travels through condenser fins; a. shift of flow with inclined fins and b. shift of flow with perpendicular fins compared to the condenser MPE tubes

Inclined fins will reduce the created amount of pressure drop in the element and therefore increase the amount of air flow travelling through the condenser. Increased air flow will result in greater heat transfer in the condenser area, which directly means that the thermosyphon is able to cool more effectively. However, high inclination in the fins means that less fins fit into the condenser structure and a smaller amount of fins decreases the amount of heat transferred in the cooling element. Therefore, the degree of inclination of the fins respect to the condenser has to be a compromise between maximising the amount of fins and minimising the generated pressure drop in the element. Further studies regarding the optimal degree of inclination of the fins should be made to reach more optimized fin structure and thus, better cooling performance.

The second concept is inspired by conventional heatsinks and it has been patented by ABB Oy for patent number EP 2383779 B1 [22]. The concept benefits of both cooling

methods of conventional heatsinks and thermosyphons. It is more affordable compared to thermosyphons. Yet, it transfers heat within the cooling element more efficiently than in the case of a conventional heatsink, due to the fact that it has highly convective coolant flow absorbing heat in its baseplate. The structure of the second thermosyphon concept, Mounting Base, is shown in Figure 20.

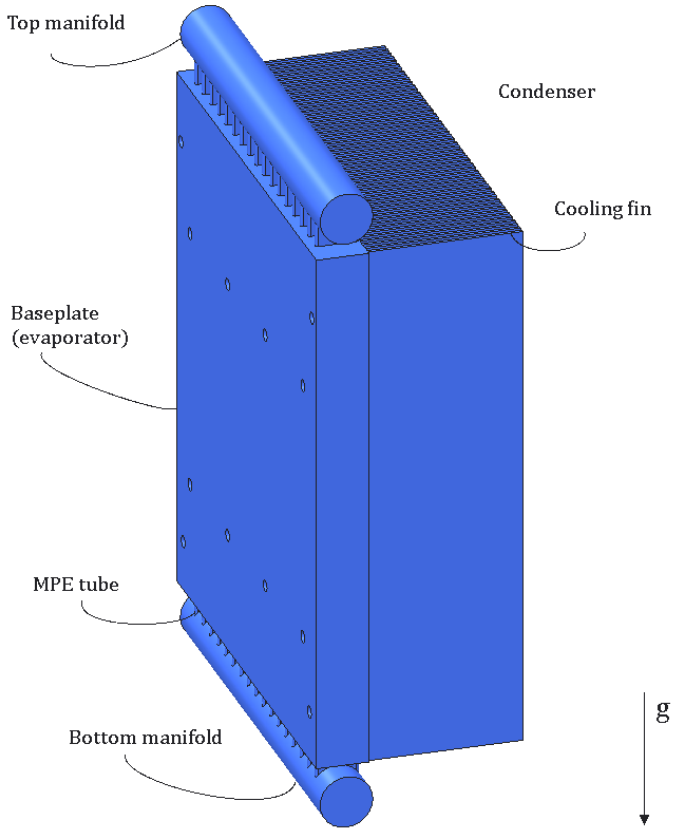

Figure 20. Concept two, Mounting base thermosyphon

The fins in this Mounting base concept are extruded aluminium fins similar to ones used in conventional heatsink. The coolant travels in the MPE tubes inside the baseplate and the manifolds collect the coolant, sending it back to circulation. The channels inside the MPE tubes can work both for evaporating and condensing depending on the circumstances inside the thermosyphon. The main idea is that the channels that are closer to the heat source inside the MPE tube act as the evaporating channels and the channels that are closer to the cooling fins act as the condensing channels. Figure 21 presents the cross-section of the Mounting base thermosyphon baseplate to demonstrate the working principle of the evaporating and condensing channels inside the MPE tubes.

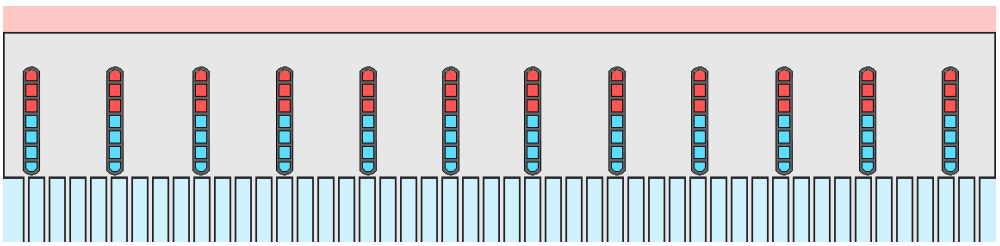

Figure 21. The working principle of a Mounting base thermosyphon

The MPE tube channels that are marked red in Figure 21 indicate the channels, in which the fluid evaporates. These channels receive most heat from the semiconductor through thermosyphon baseplate, because they are closest to the evaporator surface. The channels marked in blue indicate channels in which the coolant condensates and emits its heat to the condenser fins. The blue channels emit heat most efficiently due to the fact that they are located closest to the cooling fins.

The coolant rises to the MPE tube channels from the Bottom manifold due to pressure drop in the evaporator. The coolant rises through the channels located close to the surface of the baseplate and starts to boil. The boiling fixture arrives to the Evaporator top manifold, which gathers the high vapour quality coolant together from the channels. From there it travels to the channels located closer to the cooling fins and condenses. The low vapour quality coolant falls down to the Bottom manifold, which gathers the coolant and sends it back to the evaporator. Thus begins the new cycle of the coolant circulation. The working principles of this thermosyphon are explained in detail in patent EP 2383779 B1. [22]

The third concept is also inspired by conventional heatsinks, but in this concept MPE tubes replace the extruded fins. The structure of the second thermosyphon is shown in Figure 22. Coolant travels inside a hollow baseplate and boils. The boiling occurs in the baseplate inside channels that carry the coolant upwards to the connecting pipes through the perforated blocks. The pipes and blocks connect the coolant flow to the vapour compartment. Inside the vapour compartment the coolant spreads and moves to the MPE tube channels. The coolant flows inside the MPE tubes in horizontal direction and emits condensing heat to the surfaces of the MPE tubes and cooling fins. Louvered air fin plates are attached between the MPE tubes to increase the cooling efficiency. The low vapour quality coolant is gathered in the condensate compartment located next to the baseplate. Gravity forces the coolant to drop to the bottom parts of the condensate compartment. From there the coolant is conveyed back to the evaporator through a connecting block, which connects them together. The perforated connecting block is located in the bottom parts of the condensate compartment and Baseplate and cannot be seen in Figure 22.

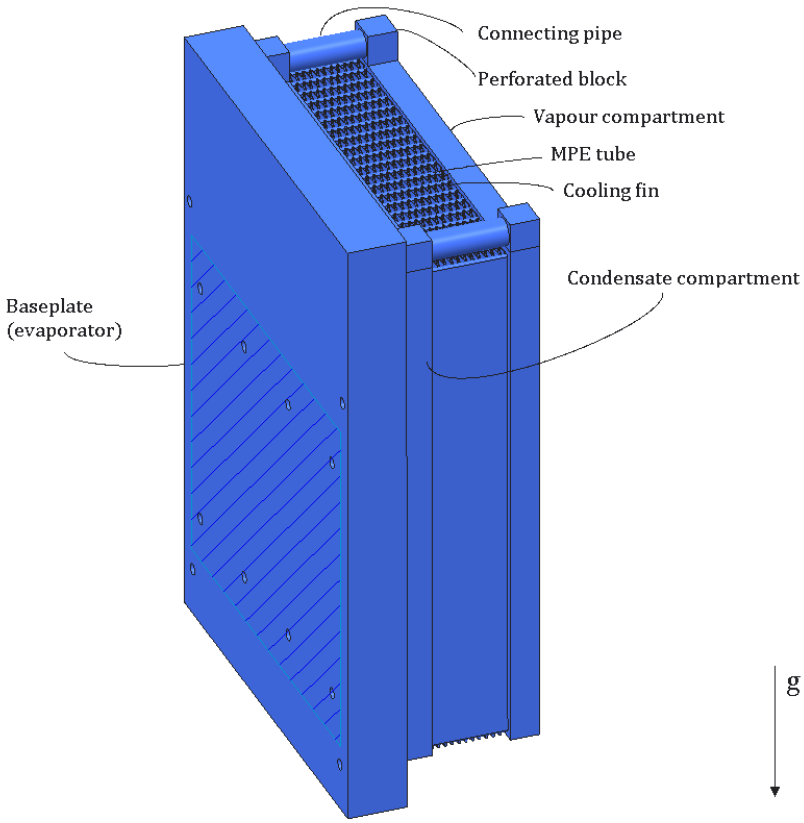

Figure 22. Concept three, Heatsink COTHEX

The third concept is very complex and thus difficult to manufacture. The complexity may create thermal resistance inside the thermosyphon and thus increase the temperature difference between the semiconductor chips and the coolant. Yet, the concept has already proven functional in previous studies and it has been successfully manufactured.

4.1.3 Material

Both the thermosyphon applications and extruded aluminium heatsinks are made of aluminium alloys. Typical alloy for extruded cooling elements is AW-6060-T5. However, in thermosyphon applications it is not suitable due to its high magnesium concentration which makes brazing much more difficult. Therefore, thermosyphon assembly parts are made of AA-3003 alloy. AA-4045 is used to attach the separate thermosyphon parts together. The attachment of the parts is conducted by pressing them together and placing them into an oven. In the oven, material AA-4045 melts and attaches the components together. The temperature inside the oven is kept constant in such a temperature that AA-3003 stays solid, whereas the AA-4045 melts and brazes the solid components together as it has a lower melting point.

The Reference heatsink is made of an aluminium alloy EN AW-6063 or EN AW-6060. These alloys have good strength properties after heat treatment, good corrosion resistance and they are inexpensive compared to copper. Therefore, these alloys are most popular when producing extruded profiles.

When developing cooling elements the properties of the material have a great influence on cooling. The thermal conductivity of the cooling element material is one of the major components that dictate the heat resistivity of the cooling element. The higher the cooling element's conductivity is, the less the cooling element will have thermal resistivity. Yet, the expensiveness and the abilities to shape the material play a very important role. Figure 23 depicts thermal conductivities of some metals. The aluminium alloys used for the cooling elements are marked in blue and other metals in red colour.

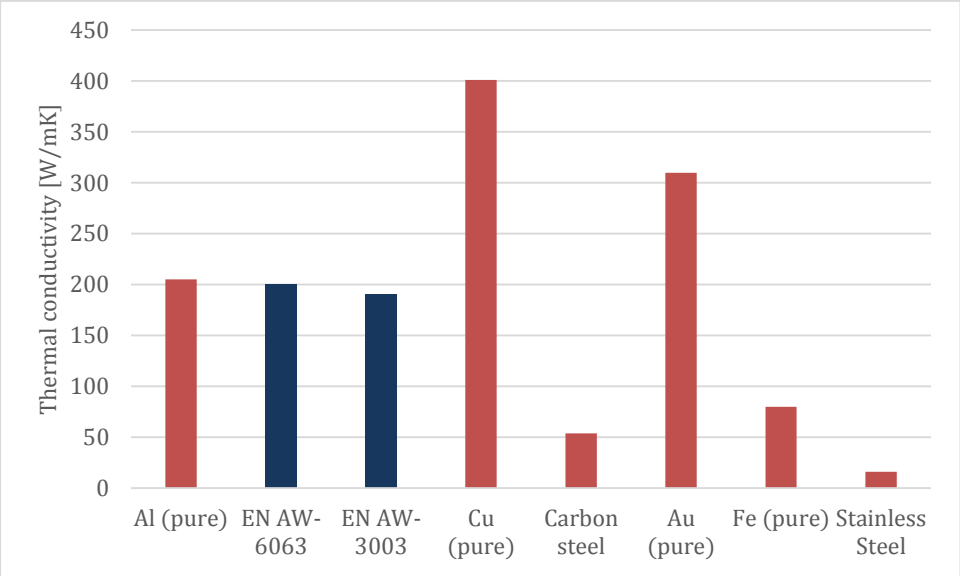

Figure 23. Thermal conductivities of some common metals (red) and the metals used in the cooling elements (blue) [23], [24]

The best material in the view point of thermal performance of these metals is copper. The major disadvantage for using copper though, is its value. When copper costs 7 USD/kg and Aluminium 1.7 USD/kg [25] it is more feasible to use aluminium as the manufacturing material even though the thermal conductivity is twice better for the copper.

4.2 Thermodynamic optimization

4.2.1 Thermodynamic design

In order to know which concept proves out to achieve the best cooling performance, the cooling abilities of all of these concepts need to be tested. It is impossible to test these concepts by building several test set ups and conducting measurements not only due to limited resources but also because the optimization of the concepts require countless trials to reach the optimum cooling performance. Thus, in this study I examine the different structures using simulation software. The simulations are used to optimize best possible solution that meets the requirements concerning the cooling element. However, the thermosyphon concepts are optimized keeping in mind that the concepts can be manufactured and that way the simulated cooling performance can actually be achieved.

Two simulation programs are used for simulation. ANSYS Icepak is used to determine how much fluid passes through the fins of the cooling element and how much pressure drop the cooling elements cause. The other simulation program is COTHEX Designer, which calculates the temperatures and heat transfer abilities such as thermal transmittance, and resistivity. It also gives values for pressure drops inside the thermosyphon, which gives an indication of the magnitude in fluid flow in the loop. The working principles of the simulation programs are discussed in the Chapter 1.4 and the calculation methods are based on the theories of fluid dynamics and thermodynamics previously discussed in the Chapter 3.

When optimizing the cooling concepts and simulating their abilities to cool the heat source, we need to define what is the measure, we want to optimize. Because the chips inside the semiconductor are most likely the first components to suffer damage when experiencing overly high temperatures, we assume that the temperatures inside the chips are the most important values that need to be optimized. The temperatures inside the chips are called junction temperatures and these are used when optimizing the structure of the cooling elements.

To be able to optimize the cooling concepts and compare them together, standard conditions have to be defined. There are three parameters that need to be defined: standard heat load, standard air flow through the condensers of the cooling elements and ambient temperature. The standard conditions are discussed in the following chapter.

After the determination of the standard conditions the cooling elements can be optimized to meet the best possible cooling power under these conditions. The thermal performance of the cooling elements can be optimized by designing some important structures and parameters in the cooling elements. These structures and parameters are:

1. number of condensate tubes
2. coolant type
3. coolant filling ratio
4. fin length
5. fin pitch.

Some parameters cannot be optimized. For example, the number of evaporator tubes and their height is strongly dependent on the tube manufacturing possibilities. In addition to this, the positions of the screw holes in the baseplate are to remain fixed, as stated in the Chapter 4.1.1. Then again, the height of the evaporator tubes defines the thickness of the baseplate. Fins usually have a standard thickness in typical thermosyphon applications and therefore are not optimized.

4.2.2 The standard conditions

Standard conditions have to be determined in order to optimize the cooling concepts and then to compare them together under similar conditions. Three parameters are given values: ambient temperature, heat load and air flow through the condensers of the cooling elements.

The ambient temperature is the temperature inside the frequency converter module and therefore the temperature cooling air in the converter module. The temperature in which the frequency converter module works typically in customers' applications can be used as the ambient temperature. A typical converter working temperature is approximately 40 ^{0}C and therefore it is used as the ambient temperature in this study. However, the frequency converter should be able operate properly in a temperature range of 0 ^{0}C to 50 ^{0}C [26], and the cooling element should be simulated also under these ambient temperatures to ensure proper operation temperatures.

The cooling power of the cooling elements is determined using a worst-case analysis when it comes to semiconductor heat losses. Therefore, we define the highest achievable power that can be produced with semiconductors and use it as the standard heat load. Maximum semiconductor heat losses in the frequency converter usage is 2088 W. With this case the heat losses are generated in the bond wires and IGBT and diode chips. In typical frequency converter usage however, the largest amount of heat loss occurs in the IGBT chips. To make the simulations more straightforward, I assume that all of the heat losses are generated in the IGBT chips. Because there are 18 IGBT chips in the semiconductor, the amount of heating power generated in one chip is 116 W.

The most useful way to compare the cooling capabilities of each cooling concept under standard air flow is to compare them in a situation as if they would be inside the frequency converter. Each cooling concept allows a different amount of air to flow through their condensers due to the fact they all create a different amount of pressure drop. Therefore, the amount of the air flowing through the condensers of the cooling elements in the frequency converter typical fan operating point is used as the standard air

flow. This way the pressure drops that the cooling concepts create can be taken into account. The method for defining standard air flow is explained in the following chapter.

4.2.3 Fan performance and pressure resistance curves

The converter modules need cooling in order to work properly. The electrical components create excessive heat when they are operated and the heat needs to be conveyed out of the module to prevent the components from overheating. The cooling method used in the frequency converter module applications is forced air flow with fans inserted to the bottom of the module. The fans blow air upwards through the module and as the air bypasses and collides with components, the heat from their immediate surroundings and their surface is caught into the air flow. The heated air travels out from the top parts of the module.

Some converter modules are inserted into cabinets that contain other electrical components and converter modules. These converters that are inserted into cabinets suffer from higher temperatures because a great deal of the cooling air circulates inside the cabinet and it takes more effort for the heat to travel out of the cooling system. To make the simulation more straightforward however, we assume that the converter module in the simulation environment is not inside a cabinet, but stands on its own.

As the air collides with components inside the converter module, the impact changes the direction of the air flow. Due to the impact and the shift of direction, components create pressure drops that are all characteristic for each component. That is also the case for the cooling elements. Each cooling element concept changes the air direction and produces pressure drops in different ways and with different amounts. Therefore, in order to know the cooling abilities of each cooling element concept, we need to know how much air travels through the condenser fins in actual frequency converter usage. Because the cooling elements create different amounts of pressure drop, the amount of air travelling through the condenser fins is different for each concept. Also, due to the fact that the cooling elements create a different amount of pressure drop with certain amounts of air flow compared to each other, the amount of pressure drop the converter module produces is highly dependent on the cooling elements used in the module.

To better understand how the components create pressure drops inside the converter module, I constructed a simulation environment, which consists of objects of similar geometry as in the actual converter module. The simulation environment is created in the Icepak software in which all components are visualized in a three dimensional environment. I designed the cooling elements with Creo Parametric program and rest of the structures of the components are extracted from CAD –documents created by the ABB Drives Mechanical Design Engineering team. All CAD -objects are converted into Icepak -objects that have thermal features. The results of the simulations can be visualized with colours where each colour indicates a certain value of measured parameter. Figure 24 illustrates the simulation set up and results calculated by the Icepak software.

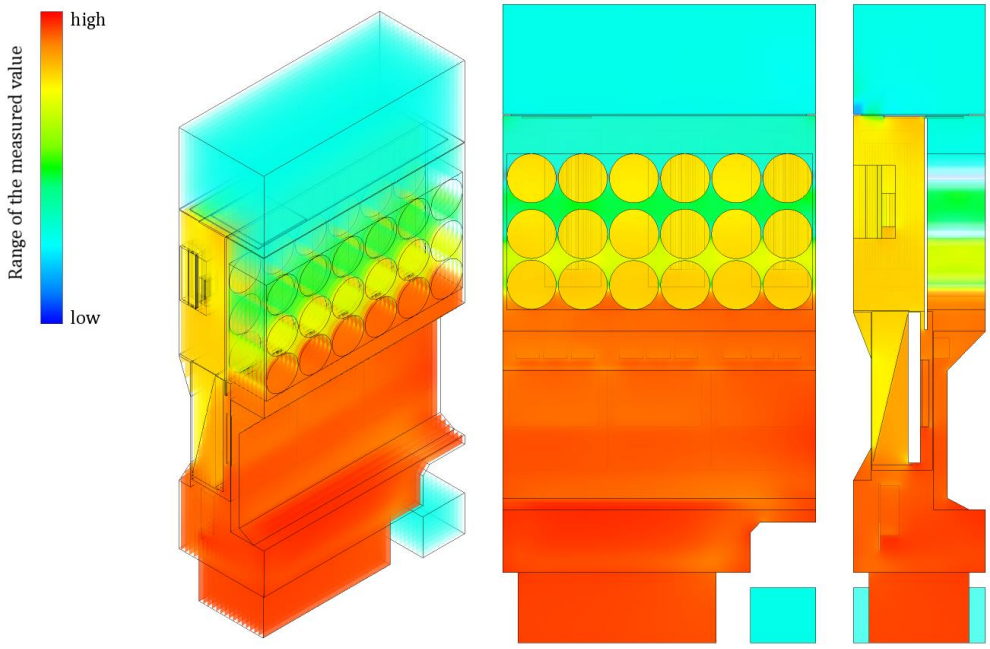

Figure 24. Layout of a converter module and simulation results presented in ANSYS software

I used the software to calculate how much the converter module and the cooling elements individually create pressure drops when certain amount of air is pushed through the converter module. The simulations resulted in pressure resistance curves for the cooling elements and the whole converter. Resistance curve for the whole converter is called system resistance curve and the resistance curve for the cooling elements are called cooling element pressure drop curves. The simulations are performed so, that system resistance and cooling element pressure drop curves are simulated for each cooling element concept. While simulating different cooling element concepts, the layout of the converter module stays otherwise intact except for the cooling elements that are changed in the simulation module.

A simulated fan, that is able to blow a certain amount of air through the module regardless of the system resistance, was placed underneath the converter module in the simulation software. As the fan blows a constant amount of air through the module, Icepak is able to calculate pressure drops generated by each object inside the module. By doing this I was able to determine both the whole system resistance and the cooling element pressure drop. By making various simulations with different air flows blown through the module, the system resistance curve and cooling element resistance curve could be determined. By including a fan performance curve into the graph, we can determine the fan's operating point from the intersection point of the system resistance curve and the fan performance curve as seen in Figure 25. Fan operating point determines the pressure drop and air flow in the module when the fan is operated on full power.

The standard air flow discussed in the Chapter 4.2.2 is the air flow travelling through cooling element fin structure at the operating point. The operating point is determined by

using a fan performance curve of one of standard fans used in the converter module. The fan selected for the simulation can withstand the least amount of pressure drop and therefore is the weakest performer of all the fans used in the converter module. As the fan is able to endure the least pressure drop generated by the objects inside the module, it is evident than with this fan the amount of air travelling through the cooling elements is smallest. Thus, is the temperatures inside the cooling elements highest compared to the other fans and blowers used in the converter module. It is important that the thermosyphon cooling element needs to perform better than the cooling element used at the moment in the module, especially when using this fan. Figure 25 is an example of a fan performance curve with a system resistance curve.

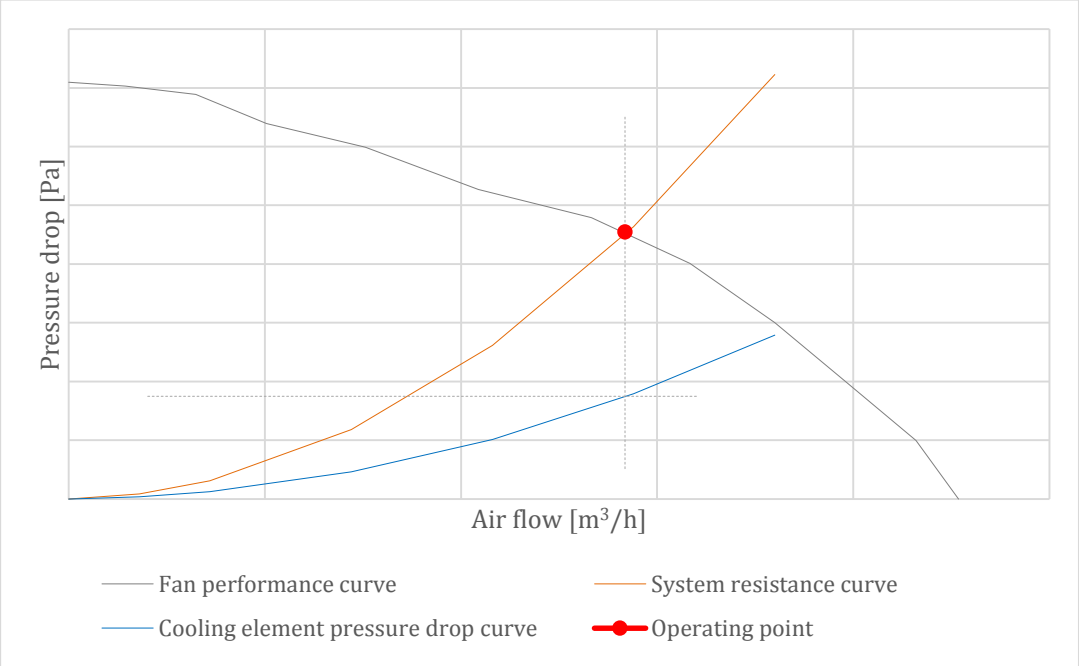

Figure 25. Defining operation point of the system with fan performance and system resistance curve

The operating point describes the amount of air blown through the module and the pressure drop created by all of the objects inside the module and it is in the intersection of the fan performance curve and system resistance curve. The amount of pressure drop created by the cooling element can be determined by drawing a straight vertical line, from the operating point and can be seen in the figure as dashed grey vertical line. The pressure drop of the cooling element can be determined from the intersection point of the vertical dashed grey line and the cooling element pressure drop curve. The horizontal dashed grey line indicates the cooling element pressure drop in the fan operating point. The air flow through the cooling element cannot be determined from Figure 25 as the cooling element's pressure drop curve is determined as a function of air flow blown through the whole converter module. The volume flow through one cooling element can be determined from the simulation results when knowing the cooling element pressure drop.

After defining the amount of air travelling through the cooling element, we are able to optimize the cooling elements and determine the cooling efficiency of each cooling element. The results of these fluid dynamical simulations are presented in Chapter 6.1.2.

4.2.4 Condensing tubes

The number of condensing tubes is determined for Thermos and Heatsink COTHEX with an assumption that the coolant filling ratio is 50%. Previous studies concerning compact thermosyphons have concluded that the filling ratio of 50 % is often close to the optimal filling ratio and therefore it can be used to determine optimal number of condensing tubes. The mounting base has its condensing channels in the baseplate, which means it cannot be optimized and is not considered in this chapter. Filling ratio is determined as the fraction of the fluid filled into the system compared to the maximum mass of fluid that can be inserted into the thermosyphon. By inserting the dimensions of the thermosyphon defined before in Chapter 4.1.1, the optimal amount of the condensate tubes can be determined using the COTHEX Designer. Figure 26 is an example of temperature levels in thermosyphons having a varying number of condensate tubes.

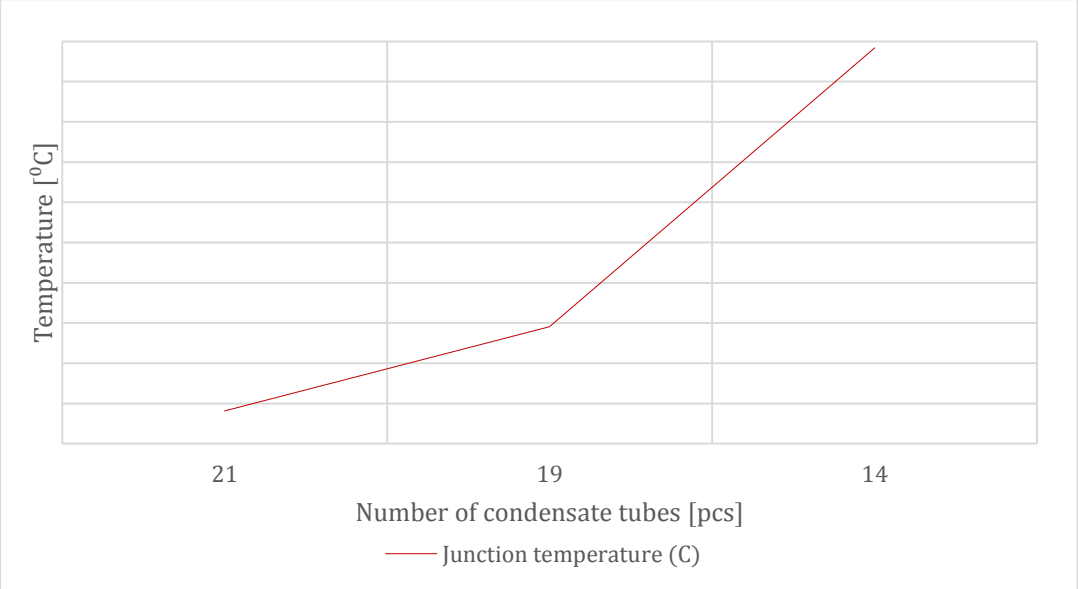

Figure 26. Defining the optimal amount of condensate tubes for the condenser

It is clear, that higher amounts of condensate tubes will result to better cooling performance and thus, lower temperature levels at the cooling elements. This means that increasing the number of condensing tubes will improve the cooling performance of the thermosyphon. Theories regarding the thermosyphon operation discussed in Chapter 3.5 support these findings. Bigger amount of condensate tubes means that the coolant has larger cross-sectional area for heat transfer in the condenser channels. Consequently, the mass velocity of the fluid in the channels is smaller and the frictional pressure drop in the condenser is lower, as equation 45 for frictional pressure drop predicts. The lower amount of frictional pressure drop in the thermosyphon fluid circulation enables better cooling efficiency. This means that the condenser should be installed as many condensate tubes as possible.

The amount of the condensate tubes in the condenser depends on how closely the tubes can be installed. The distance between two condensate tubes is called tube pitch and manufacturing requirements dictate that it has to be 10 mm. Maximum width of the cooling element is 186 mm and therefore Thermos and Heatsink COTHEX can have maximum of 18 condensate tubes installed. As there is need for additional space for supporting structure in the sides of the condenser, a realistic number for MPE tubes in the condenser is 17.

4.2.5 Coolant

There are many things to be considered when choosing the right coolant for the thermosyphon. The ideal coolant is dielectric, non-flammable, non-toxic, has low global warming potential (GWP), long lifetime, is reasonably priced and most importantly is efficient at transferring heat.

There is no ideal coolant and therefore choosing the right coolant is always a compromise. When choosing a coolant for the thermosyphon, its efficiency is the highest priority. It is also preferable that the selected coolant can be used in the future without an extra fee due to possible upcoming regulations for high carbon footprint. The coolant should also be easily replaceable to another coolant if needed. It is always important that the coolant is easily available. The most suitable coolants for these thermosyphon cooling purposes are R245fa and R134a. Their operating range fits best for the compact thermosyphon temperature and pressure range and they achieve the lowest possible temperature levels in the thermosyphon operation. Their lifetime is long, 7.6 years for R245fa and 13.0 years for R134a [27]. This is desirable, since the thermosyphon would not need to be replaced due to expiration of the cooling liquid. As an example of this, frequency converter's lifetime is designed to be at least 10 years. Yet, the GWB is high for both of these fluids: 930 for R245fa and 1300 for R134a [27].

Water would be a strong candidate due to its strong heat transfer capabilities, low expense, availability and environmentally friendliness but is not considered here as a cooling option. Water is not compatible to be used with aluminium alloys of which the thermosyphons are composed of due to corrosion, growth of bacteria and freezing in low temperatures. Water, which always has got some impurities, reacts with the alloy electrochemically and produces corrosion on the metal surface. The surface of unclad AL3003 alloy experiences pitting corrosion and thus, creates small pits that deepen within time. The alloy has a mean pit depth of ~250 μm after four weeks [28], which means that if the water is used as the coolant, the MPE tube channel walls with depth of 0.4 mm would be corroded to have holes within a month. The main reason however, is that the frequency converter may occasionally experience temperatures below zero Celsius and the coolant would consequently freeze. Therefore, only the coolants R245fa and R134a are considered as the thermosyphon coolants.

The cooling efficiency between these coolants is quite similar as can be seen in Figure 27, which was conducted to Thermos cooling concept. The figure depicts the junction temperature of the cooling element with different coolant filling ratios. The temperature difference between the coolants types at filling ratio of 50 % is 2 ^{0}C according to Figure 27. The difference is therefore insignificant when considering the absolute temperature levels of the thermosyphon.

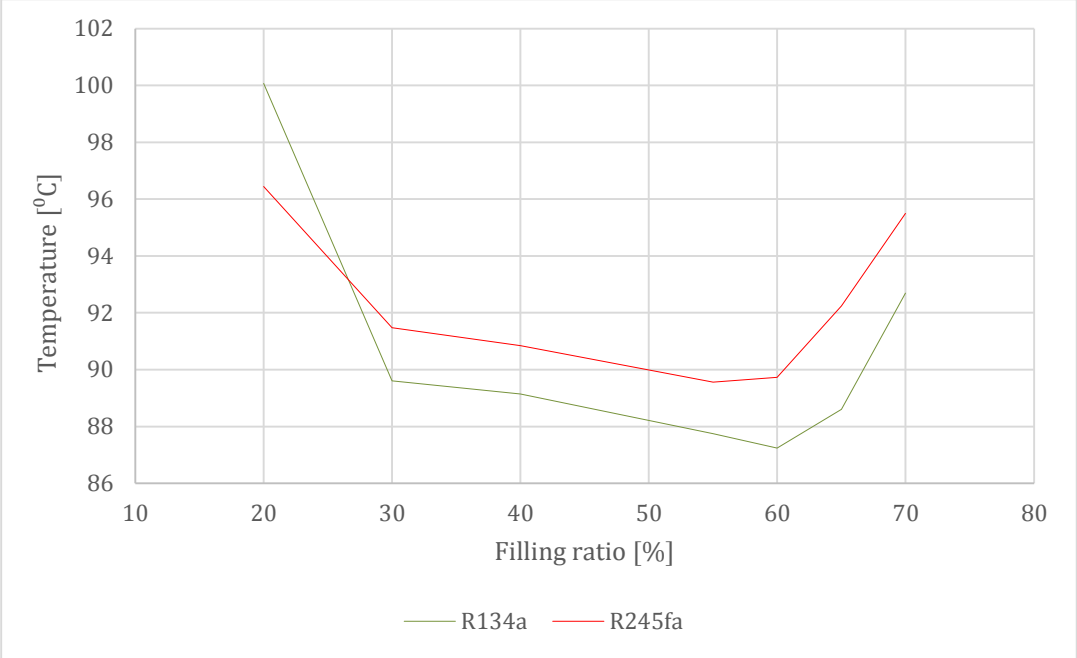

Figure 27. The temperatures of the Thermos thermosyphon with the considered coolants

The price is also an insignificant factor when choosing the right coolant between R134a and R245fa for the cooling concepts. As the thermosyphons can only carry coolant the maximum of 1 kilogram, the price difference between the R-134 and R245fa is the maximum of 13 € in the thermosyphon. As the thermosyphon costs hundreds of euros and the whole frequency converter module thousands of euros, the coolant price is not an important factor compared to these expenses.

In the end the main factor defining the coolant to be used is the availability of the liquid. R134a is widely available whereas R245fa has substantially less providers. On the other hand, R134a has a high GWP and might have to be replaced due to future EU regulations. Fortunately a suitable replacing coolant HFO-1234ze with lower GWP of 6 has been developed. Therefore, R134a is used for the time being and upgraded in the future for the more environment friendly coolant.

Defining the optimal coolant filling ratio for Thermos and Heatsink COTHEX is conducted similarly by using the number of 17 condensate tubes. The ambient temperature of 40 ^{0}C and ambient heat load of 2088 W was used. The optimal filling ratio was determined from the junction temperature curves.

When considering the optimal filling ratio, there are two phenomena that need to be avoided. A low filling ratio might result in dryout in the evaporator, which will lead to superheating the coolant. In the case of dryout, the heat transfer coefficient decreases thus increasing the thermal resistance of the evaporator and therefore increasing also the temperatures of the thermosyphon. A high filling ratio might result in subcooling of the coolant in the evaporator, which increases the temperatures in the thermosyphon application as discussed in the Chapter 3.5.

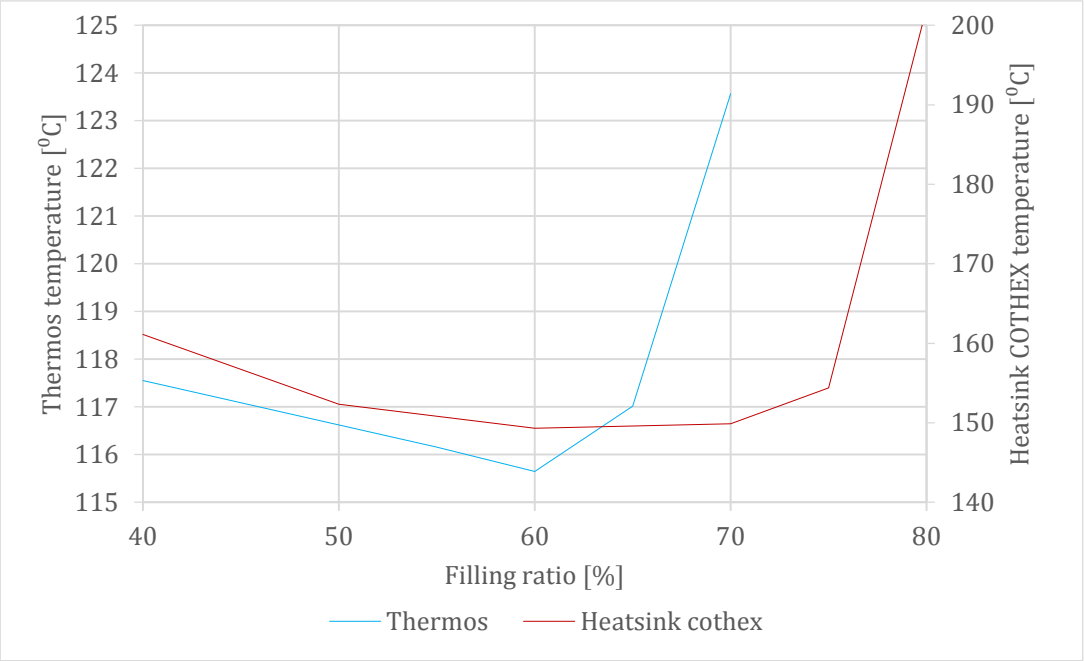

Figure 28. Defining the optimal coolant filling ratio for Thermos and Heatsink COTHEX cooling concepts

Figure 28 shows that the optimal filling ratio for Thermos cooling concept is 55 %. The curve begins to ascend rapidly with filling ratios larger than 60 % and therefore it is essential that the cooling element is filled accordingly to avoid high temperatures. The optimal filling ratio for the Heatsink COTHEX is 60 % and because the temperatures ascend slowly with filling ratios both smaller and larger than the optimal ratio, the filling ratio does not make a great difference when optimizing the cooling element.

COTHEX Designer could not be used for the thermal optimization of the Mounting base thermosyphon concept as it was not designed for thermosyphons having lamel fins in the condenser. As a result of this, an optimal coolant filling level could not be determined for the Mounting base thermosyphon. The cooling properties for the Mounting base thermosyphon were calculated by other means and are explained in the Chapter 6.1.

4.2.6 Fins

There are two types of fins used in the cooling concepts studied in this thesis. One type is the lamel fin, used in the Reference heatsink and in the Mounting base thermosyphon. The other fin type is called the louvered air fins and it is used in Thermos and Heatsink COTHEX thermosyphons. The fins can be optimized by determining the optimal fin height and fin pitch. Figure 29 depicts the fins and their pitch and height.

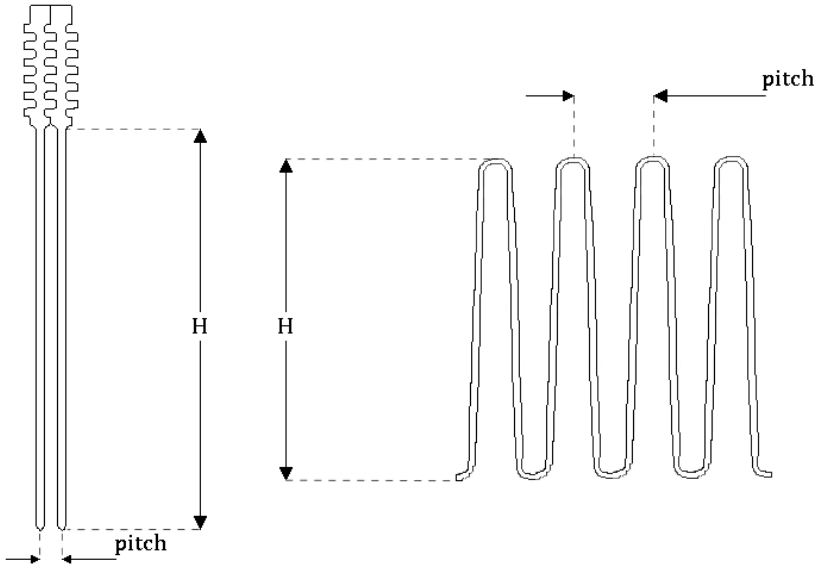

Figure 29. Fin pitches and fin heights of the lamel and louvered air fin types

Lamel fins are extruded aluminium profiles, lamel profiles, and they are attached to each other with a pressurising tool that presses the base parts of the fins together forming a finned structure with a baseplate. These fins are only attached from their base and therefore their thermodynamic heat dissipation efficiency can be calculated with equation 18. The louvered air fins are manufactured by bending a plate into the shape depicted in Figure 29. Louvers are placed on the sides of the fins to increase the turbulence of the bypassing air. Bigger turbulence stands for a larger Reynolds number, and by increasing the Reynolds number, the convective heat transfer increases as stated in equation 28. Louvered fins represent the fins that are attached and also heated from both of their ends and their thermodynamic heat dissipation efficiency can be calculated with equation 19.

The distance between two cooling fins that are located next to each other is called the fin pitch. For lamel fins used in the Reference heatsink and in the Mounting base thermosyphon concepts, the fin pitch is easily defined to be the distance between the centre lines of lamel profiles as presented in Figure 29. For bent plates used in the Thermos and Heatsink COTHEX cooling concepts, the fin pitch is the distance between the adjacent top or bottom parts of the bent plate. The height H of the fin can be determined to be the distance between the tip of the fin and the base of the fin or in the case of enclosed fin the distance between top and the bottom parts of the fin.

The height of the lamel fins can be determined from the boundary rule of having maximum height of the cooling element to be 86.5 mm. As the baseplate takes 25 mm for the Mounting base thermosyphon, the fins can be the maximum height of 61.5 mm. When knowing that the convectional cooling power increases when raising the height of the cooling fins as stated in equations 12 and 15, it can be said that the longer the fins are, the better the cooling efficiency is. Figure 30 presents the cooling power of the fins calculated using these equations 12 and 15.

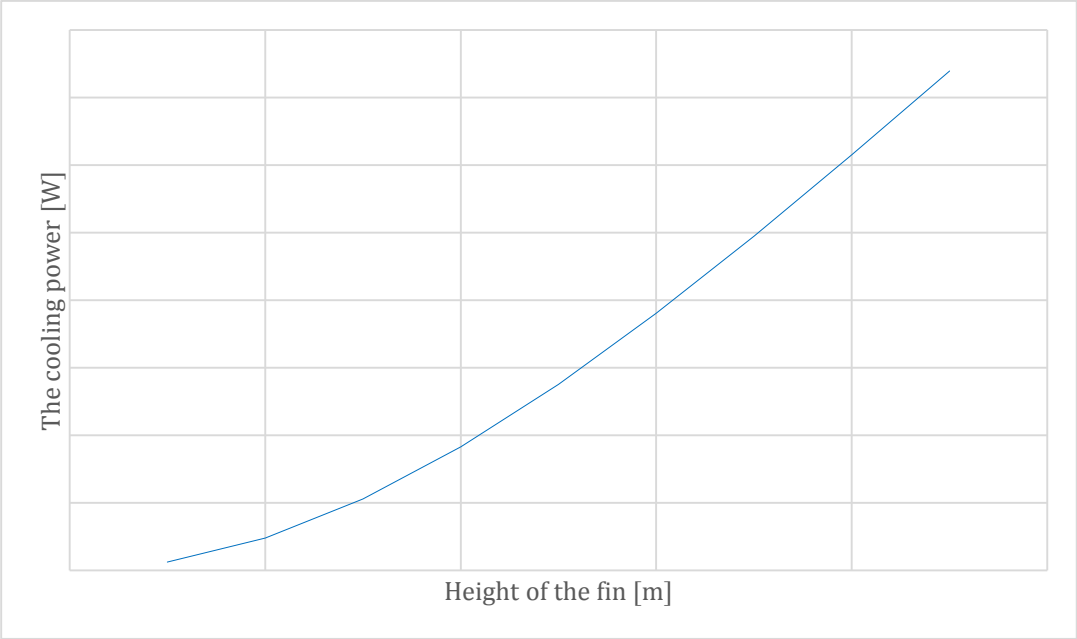

Figure 30. Cooling power of the fin respect to its height

This means that the optimum length of the fins for the Mounting base thermosyphon with these boundary rules is 61.5 mm.

For louvered air fins in Thermos and Heatsink COTHEX cases, the amount of condensate tube determine the height of the fins. As stated in Chapter 4.2.4, the optimal number of condenser tubes for the Thermos and Heatsink COTHEX is 17 with the condenser tube pitch of 10 mm. The thickness of the tubes is 2 mm and therefore the fin height is 8 mm.

The fin pitch should also be optimized. The boundary rule for the minimum value of the fin pitch comes from the manufacturing issues for both fin types. The bending machine of the supplier for the louvered air fins is able to bend the plate into fins pitches between the values 2.5 mm and 5 mm. The lamel fin profiles can have the thickness of 1 mm and the distance between them can be 2 mm, meaning that the minimum theoretical fin pitch for the lamel fins is 3 mm. The lamel fins can be thicker and have more distance between them quite unlimitedly. Therefore there is no boundary rule for the maximum fin pitch for the lamel fins. The fin thickness of the louvered air fins is 0.14 mm.

One might assume that the bigger the amount of air travelling through the condenser, the lower temperatures the cooling element will reach. This is not entirely true as the amount of heat transfer area has also a great impact on the cooling performance. Increased air flow will raise the velocity of the air through the condenser fins according to equation 23. That will increase the Reynolds number as stated in the equation 22, which will lead to higher heat transfer coefficients in the fins, as shown in equation 28. However, to increase the air flow through the condenser, the fin structure has to be modified in such way that it will create a smaller pressure drop. Due to the fact that fins create the largest amount of pressure drop, the amount of fins has to be reduced. This means that the total fin cooling power is smaller, because there are fewer fins to emit heat. Therefore, the optimal fin pitch needs to be solved using simulations. The cooling element pressure drop and air flow are calculated using Icepak and the thermal performance with COTHEX Designer. The optimal fin pitch for the Thermos thermosyphon cooling elements is stated in Figure 31.

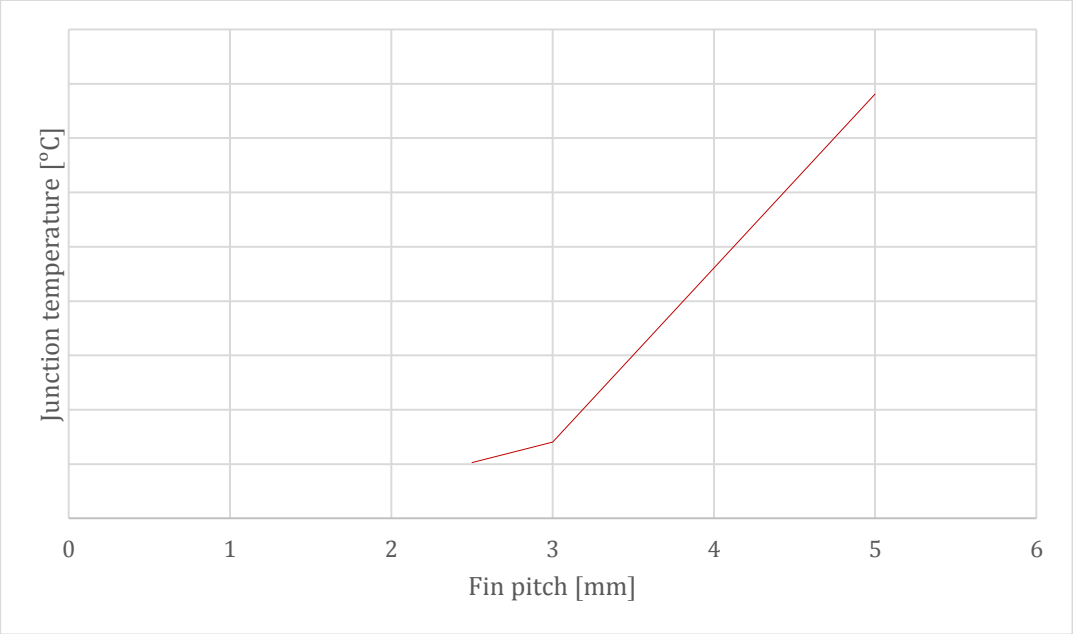

Figure 31. Defining optimal fin pitch for the cooling elements

Figure 31 show that a small fin pitch will result to low junction temperature level. Therefore, it is clear that with these thermosyphon concepts the smallest fin pitch creates best thermal performance. Therefore, Thermos and Heatsink COTHEX will use fin plates with fin pitch of 2.5 mm and fin height of 8 mm.

The cooling fins of the Mounting base cooling element use same lamel fin construction as used with the Reference heatsink. The construction has been optimized for the frequency converter usage and therefore it can be assumed that it will provide best cooling performance. The fin construction can straight be applied for the Mounting base concept, because the cooling is conducted in similar manner in both cooling element concepts.

5 Testing

5.1 Simulations

The purpose of the simulations is to test thermal performance of the cooling elements. Three variables, air flow, heat load and ambient temperature are tested in the simulations to get a wider picture of their cooling abilities. Simulations are made under the standard conditions defined in the Chapter 4.2.2 to enable comparison between the elements. The simulation results are analysed and a suggestion is made whether a compact thermosyphon is suitable for replacing conventional heatsink in cooling of power electronics.

The air flow simulations are conducted to know how the thermosyphon reacts on the increase or the decrease of the air flow blown through the condenser. Knowing this is highly important because the amount of air travelling through the condenser might reduce through time due to clogging of the condenser with dust. The amount of air blown through the cooling elements strongly affects the temperatures in which the thermosyphons operate. Increased air flow typically decreases the temperatures in the cooling element and decreased air flow increases the temperatures in the cooling element. It is especially important to know how steeply the temperatures rise when the cooling air travelling through the condenser decreases. For example, if one of the two blowers used in the converter module breaks, it would be highly beneficial if the thermosyphon could keep the semiconductor undamaged until the fault is repaired.

The heat load simulations measure how the thermosyphon reacts to the increase of the heating power. The temperatures in the thermosyphon are assumed to increase linearly as the heating power is raised, yet this may not be the case. Should the thermosyphon operation reach dryout, the heat transfer coefficient reduces dramatically and thus increases the temperatures in the cooling element exponentially. Dryout is explained in the Chapter 3.5. The angular coefficients of the temperature curves respect to heat load, in other words the heat resistances of the cooling elements, determine how well the cooling element transfers the heat to the surroundings. An ideal cooling element has a heat resistance of 0 in which case the temperatures in the cooling element and semiconductor would be the ambient temperature of 40 ^{0}C.

In the case of having a thermosyphon that performs better than the Reference heatsink, it is also possible to estimate with this temperature curve the amount of extra heat the thermosyphon is able to withstand until the temperatures have risen to the same level as with the Reference heatsink. It is particularly important to know if the cooling elements are able to cool higher heat loads more efficiently than the Reference heatsink, because that would create a possibility to increase power load converted through each semiconductor. Increasing the power load would result in more cost efficient power modules and would save space in the customers' production facilities.

The variation in the ambient temperature tests how well the cooling concepts adapt to changing conditions outside of the frequency converter module. The outdoor temperature affects the temperatures inside the thermosyphon as it determines a great deal of the operation conditions inside the thermosyphon. The frequency converters can operate in surrounding temperature range between 0 ^{0}C and 50 ^{0}C [26], which imply that the thermosyphon should be able to operate under these conditions. Even though the standard ambient temperature is 40 ^{0}C, the thermosyphon should operate predictably with linear increase in the thermosyphon temperatures as the ambient temperature increases. The coldest temperatures may result in subcooling the coolant and the highest temperatures in superheating. It is especially important to ensure that superheating does not take place, since it would cause the temperatures in the thermosyphon to rise in an uncontrollable manner.

5.2 The testing errors

The simulation and testing results have a certain margin of error that needs to be considered when analysing the results. This thesis conducts only simulations but error margins need to be defined for the experimental measurement results when validating the simulations in the following chapter. The chapter discusses whether the COTHEX thermal simulation program, COTHEX Designer, is able to predict the thermal performance of thermosyphon technology accurately by comparing standard COTHX measurement data to its simulation results. The simulation results should reach the same values as the measurement data within the error margins. Therefore, the simulation and measurement errors need to be defined when comparing the results.

When it comes to Icepak modelling, some simplifications had to be made. The simulation model in the Icepak had to be simplified and the grid had to be made coarser in some places in the converter due to limitations in the computational resources. Without the simplifications the model would have been too complicated to simulate. The simplifications decrease the accuracy of the simulation results, which means that the air flow, pressure and temperature distribution in the module become less accurate.

Another simplification concerns the fins of the Thermos and Heatsink COTHEX cooling concepts. They can be very thin in reality, but the Icepak simulator can only build a mesh of a certain density. If the fins are constructed into the simulation as too thin, the simulator will fail to mesh them and therefore, the fins will not be in the grid. This would mean that the simulator does not take them into account when calculating the flow directions, pressure drops and heat dissipation. Should the fins not be represented in the mesh, the program will calculate the situation as if the fins were not in there. Therefore, the fins have to have a certain thickness for the mesh to notice them. Thick fins create simulation results with higher pressure drops and lower air flows through the condenser than what would be possible in reality. Additional simplification made to the fins is that the louvers were not simulated for similar reasons regarding the mesh, resulting smaller pressure drops and less turbulence than in reality.

Icepak simulation program itself is predicted to have an error of 3 % even with an accurate model with an accurate grid mesh [29]. The main sources or error in Icepak modelling are lack of convergence and inappropriate numerical models, such as turbulence models, radiation modelling and discretization schemes [30]. These simplifications and sources of error generate the total error generated in the Icepak simulations. The total error is estimated to be 6 % for pressure drop, air flow and temperature. The uncertainty of the simulations is depicted with the error bars in the figures that present simulation results for the operating points of the cooling systems and their cooling elements.

COTHEX Designer has an error of some degree to its predictions of the cooling element performance and the level of error is determined in the following chapter. The simulation results of standard COTHEX is compared to results acquired in testing of the standard COTHEX. By using an error of approximately 5 % the results of the standard COTHEX simulations match quite accurately with the testing results and therefore the 5 % error margin is used in the COTHEX Designer simulations.

The measurements of the standard COTHEX have some errors due to limitations in the measurement devices. Errors in the measurements are created in the current generator and thermocouples. The error for the heat load consists of the current generator's error for the voltage level and the current level. The error for the voltage is in the current generator 0.25 % and error for the level of current is 1.0 % [31]. The system error for the thermocouple is +/- 2.2 ^{0}C or +/- 0.75% depending on which of the errors have a larger value at the measured point [32]. The heat load measurements are dependent on the use of multiple testing devices that all generate error and therefore the errors accumulate.

The accumulation of error concerns also the simulations. When simulating the thermal performance of the cooling element concepts with COTHEX Designer, the errors of the simulation results with Icepak have to be taken into account as well. The generated air flow and pressure drop simulated with Icepak have an influence on the thermal performance simulation results with COTHEX Designer. The total error, in other words uncertainty, of the measurements and simulations' results is calculated with a variance formula, which is the sum of individual errors in quadrature. This variance formula is stated in the equation 54:

$$\Delta f = \sqrt{\sum_{i=1}^{n} \left(\frac{\partial f}{\partial x_i} \Delta x_i\right)^2} \quad , \tag{54}$$

where Δf is the total uncertainty of the parameter, x_i is the variable with an error of Δx_i and $\frac{\partial f}{\partial x_i}$ is the partial derivative of the parameter with respect to the variable x_i.

According to equation 54 the uncertainty for the heat load directed to the semiconductor chips is 1.1 % in the following Chapter 5.3. The cables connecting the

current generator to the semiconductor terminals create some systematic error due to their thermal resistance that create heat in the cables. However, this systematic error is so small that it can be ignored in this study.

Equation 54 calculates a total error of 8 % for the temperature of the Thermos and Heatsink COTHEX thermosyphons when considered the errors of Icepak modelling (6%) and COTHEX Designer modelling (5%). The Reference heatsink and Mounting base are first calculated operating points with Icepak and then their temperatures are calculated in their operating points. Therefore, the air flow rate and pressure drop contribute to the simulation of the temperatures of the cooling elements. With an error of 6 % for each parameter, the equation 54 calculates the Reference heatsink and the Mounting base thermosyphon total error of 10.4 % for the temperature. The heat load and ambient temperature are fed in to the simulation programs as known quantities and therefore they do not generate any error in the simulations.

5.3 Validation of the simulations

Thermosyphon technology has proved to be an efficient cooling technology for the semiconductor cooling and a cooling method based on thermosyphon technology has been developed for the frequency converter usage by ABB product development and is presented in the patent EP 2031332 A1 [8]. It can be called standard COTHEX and frequency converters utilising this thermosyphon technology are under the process of bringing the product in to manufacturing.

The standard COTHEX acts as a substitute to heatsink, however, it cannot be used directly to replace the heatsink because of its structure as seen in Figure 3 in Chapter 2.2. It requires a flat planar space through which the fan blows air perpendicularly compared to the baseplate of the cooling element. The heatsink instead needs a cuboid shaped space through which fan blows air parallel compared to the baseplate of the cooling element. The standard COTHEX application used in the frequency converters has proved to be functional and even more importantly, testing has proved that the simulations predict thermosyphon thermal performance quite accurately, which means that the simulation software, COTHEX Designer, for the thermosyphon design studied in the thesis can be used to predict its thermal performance. This chapter validates the use of COTHEX Designer in this thesis by comparing the simulation and testing data of the standard COTHEX together.

Both the simulations and testing results of the standard COTHEX followed the guidelines discussed in the Chapter 5.1, although the ambient temperature in this test was 50 ^{0}C. This change does not have an effect on the prime goals of the testing though. The simulations and the testing results of the standard COTHEX measure the cooling performance of the standard COTHEX in different semiconductor heat loads.

The simulations for the standard COTHEX were made with COTHEX Designer. The structure of the frequency converter using standard COTHEX cooling is designed differently. The cooling fan in it is designed to blow air only through the cooling element condenser and therefore other objects in the frequency converter do not generate any pressure drop. This results that fan blows all of its air through the condenser and there is no need to simulate air flow and pressure drop distribution in the converter module. Therefore, Icepak was not needed when simulating the standard COTHEX cooling performance.

When conducting the tests, heat was generated in the IGBT chips of the semiconductor. The heat is generated by converting electricity in the IGBT chips into heat in the manner explained in Chapter 2.1. A current generator fed the IGBTs current over a small voltage, which generated heat according to the equation 1. The IGBTs were attached to the generator in series creating a closed circuit. The heat was transferred inside the cooling element to its condenser and the fan air flow conveyed the heat out of the test module.

Temperature sensors were drilled inside the semiconductor baseplate under different IGBT chips as seen in Figure 32. The simulation result temperatures however, are given at the surface of the semiconductor baseplate. There is a thickness of length s between these measurement points in the semiconductor baseplate and therefore, the simulation results need to be adjusted so that the results can be compared together. The temperature inside the semiconductor baseplate in the simulation case is calculated from the simulation results with equation 6 to match the testing results.

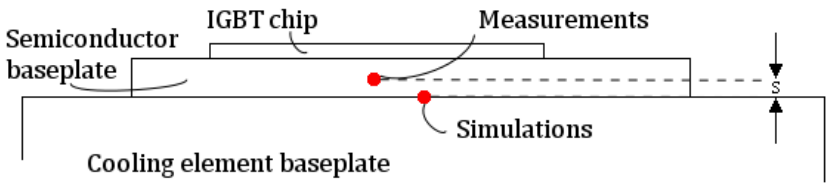

Figure 32. Measurement and simulation points in the simulation validation case

The simulations and testing results of the standard COTHEX are presented in Figure 33. As can be seen in Figure 33, the temperature curve of the simulations follows the temperature curve of testing rather well. An error margin of 5 % for the simulation results will suffice to make a match between all measurement points at specified heat loads within error margins except for one measurement point at the heat load of 4400 W.

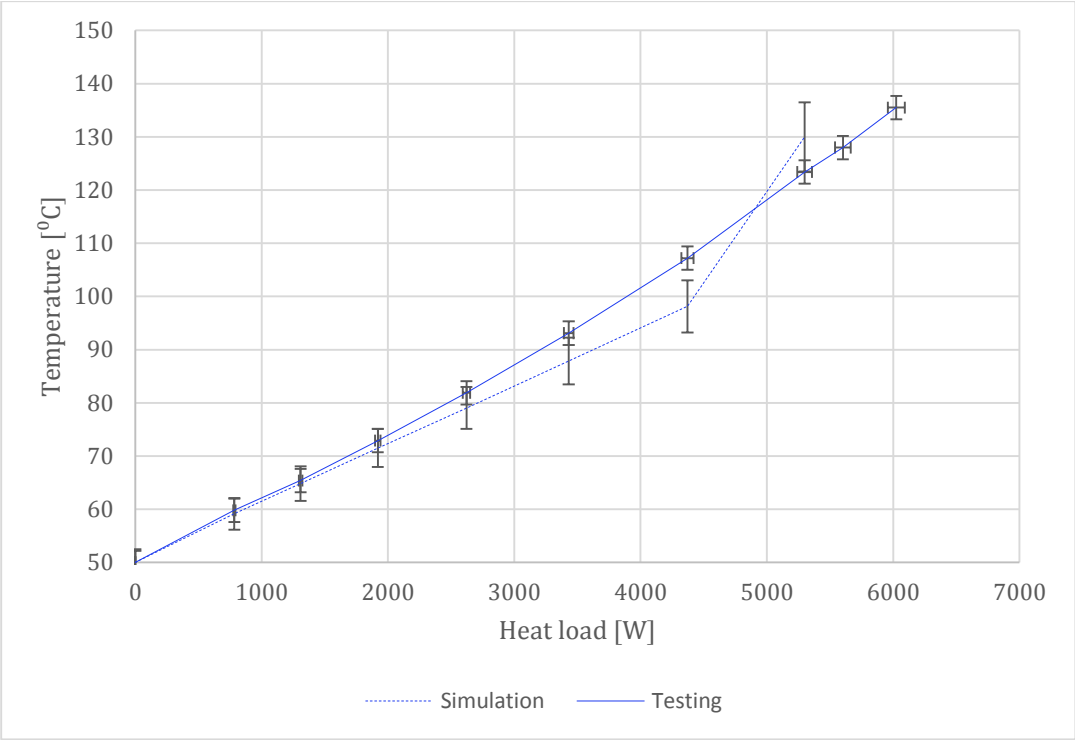

Figure 33. The simulated and tested semiconductor baseplate temperatures of the standard COTHEX

The simulations estimate a slightly smaller thermal resistance than what it is in reality. The thermal resistance of the simulations before the heat load of 4400 W is approximately 11.2 ^{0}C/kW and the thermal resistance of the testing at the same measurement point is 12.3 ^{0}C/kW. This means that with one kilowatt of heat load simulations predict 1.1 ^{0}C smaller temperatures than what it is in reality. Thermal resistance of the simulations increases significantly at heat loads higher than 4400 W, which means that the simulations predict that coolant is at its superheated state after reaching the heat load. It seems not to be the case, however. The superheating of the coolant never occurs according to the temperature curve of the testing due to the fact that the curve's thermal resistance never increases significantly. As stated before, the simulations do not predict reaching critical heat flux accurately, but otherwise the simulation results seem to match the testing results quite accurately. Therefore, the simulations can be considered to produce credible results within the error margins.

6 Results

6.1 Simulation results

6.1.1 Backgrounds

The thermal simulations regarding the cooling elements studied in this thesis are made both with the Icepak and COTHEX Designer. COTHEX Designer is preferred as it is able to calculate the boiling and condensing phenomena unlike Icepak, but Icepak is needed to simulate the thermal performances of the Mounting base thermosyphon and the Reference heatsink. The Reference heatsink is simulated using Icepak because it requires no coolant circulation and therefore can be simulated in typical thermal simulation case for electronics. The Mounting base has to be simulated with Icepak because the lamel fin structure in the thermosyphon application cannot be simulated with COTHEX Designer.

To be able to solve the temperature curves for the Mounting base thermosyphon concept with Icepak, some assumptions had to be made. The boiling inside the baseplate's evaporator channels increases the heat transfer in the baseplate and the increased heat transfer can be taken into account by defining a thermal resistance R for the baseplate. The baseplate is typically made of an aluminium alloy AA-3003, which has thermal conductivity of 190 W/mK and by using the equation 6, the thermal resistance of the baseplate without any fluid cooling inside the baseplate is calculated to be 5.7 K/kW. A lower value is used to account the boiling that increases the heat transfer inside the baseplate. COTHEX Designer is needed to estimate the degree how much the thermal resistance of the Mounting base's baseplate would decrease due to boiling.

Thermos thermosyphon has an identical baseplate, which means that the values for thermal resistance COTHEX Designer has produced for Thermos cooling element can be used to estimate thermal resistance of the Mounting base's baseplate. The thermal resistance varies respect to the temperature of the baseplate. The thermal resistance is stated in Figure 34:

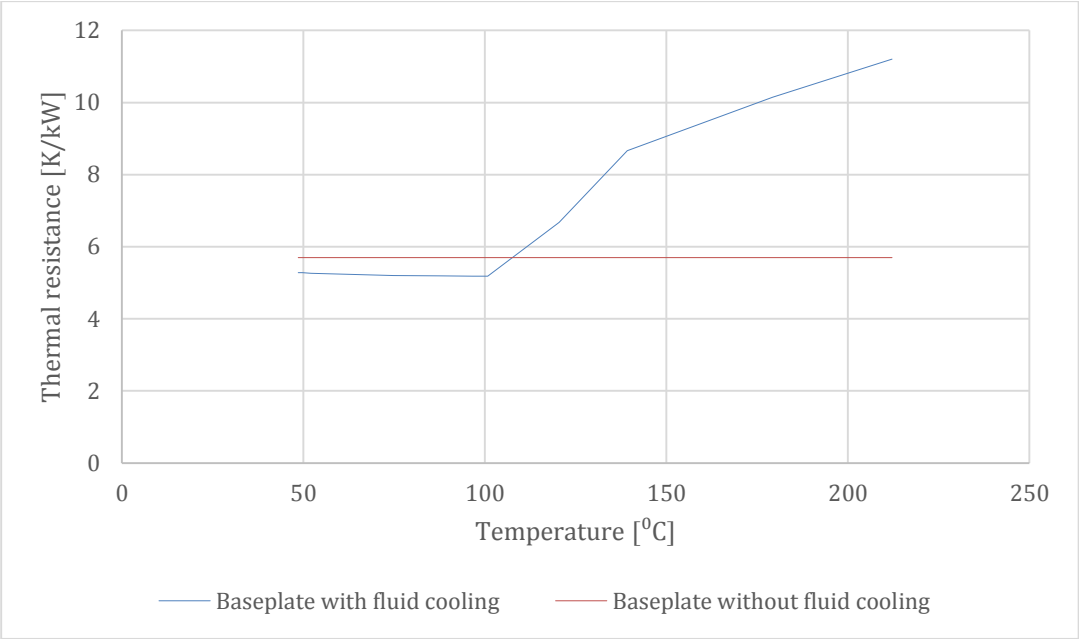

Figure 34. Thermal resistance of the baseplate in Thermos application

The figure shows that liquid cooled baseplate in Thermos application has lower thermal resistance than the baseplate without liquid cooling if the temperature of the baseplate is below 110 °C. Therefore, the Mounting base has potential to cool more efficiently than the conventional heatsink, which has no fluid cooling in its baseplate, at temperatures below 110 °C. The thermal resistance of the liquid cooled baseplate is inserted into the Mounting base Icepak simulation case to give an estimation on how much the Mounting base cooling element improves cooling respect to the conventional heatsink cooling.

The simulation programs have some thermodynamic differences between them that need to be considered when analysing the results. One major difference is how the simulation programs handle power sources. Different approaches for the diffusion of heat from the IGBT chips to the baseplate are used and as a result the COTHEX Designer calculates consistently higher junction temperatures, which means it is not reasonable to compare the junction temperatures of the cooling elements. The temperatures in the baseplates of the cooling elements are steadier and less prone to systematic differences between the simulation methods. Therefore, the mean temperatures of each cooling concept baseplates are used as comparison values.

6.1.2 Operating points

Pressure resistance curves for the converter module and cooling element are calculated for all of the cooling concepts and the method's for this are discussed in the Chapter 4.2.3. The simulations produced resistance curves that determined how much pressure drop the cooling elements and the converter modules as a whole created when a certain amount of air flow was passed through the module. These system resistance and cooling element pressure drop curves were simulated with Icepak to indicate how much

air passed through the condenser of the cooling elements. The pressure drop curves enable prediction of the cooling elements' thermal cooling performance as the standard air flow passing through the fins of cooling element can be determined.

The results of the Icepak simulated system resistance curves for each cooling concept are shown in Figure 35:

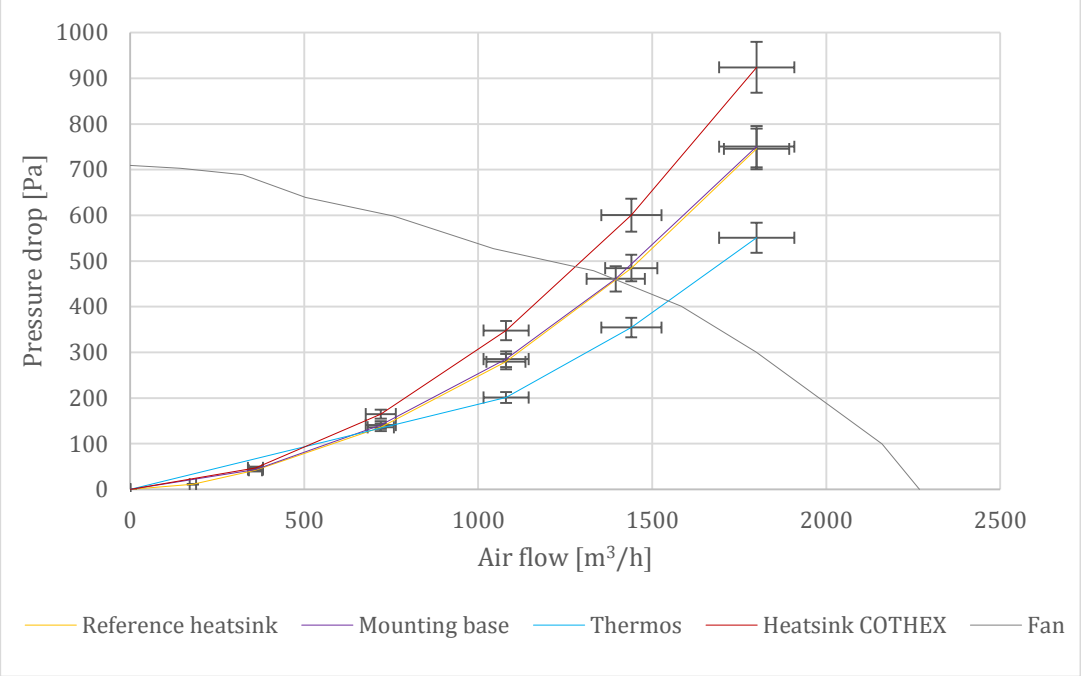

Figure 35. The system resistance curves of the cooling concepts

As seen in the figure, the converter module with Reference heatsinks and Mounting base thermosyphons create similar system resistance curves. The reason for this is that the Mounting base and the Reference heatsink have a similar structure. The Mounting base had the same fin thickness and fin pitch as the Reference heatsink, because such fin structure had been studied to create best cooling performance in the given frequency converter usage. Thermos and Heatsink COTHEX have both very different kind of structures and therefore create different amounts of pressure drop. As a result their converter modules' system resistance curves differentiate as well.

The system resistance curve for the module with Thermos element generates lowest amount of pressure drop as a function of air flow. The whole system pressure of the converter module can be calculated as a sum of generated pressure drops. Because the only difference between the simulation cases is the cooling elements, one can assume that Thermos element creates the least amount of pressure drop respect to air flow compared to the other cooling elements. For the same reasons, Heatsink COTHEX can be assumed to generate biggest amount of pressure drop.

The pressure drop itself cannot completely predict the amount of air travelling through the cooling element condenser, because the cross-sectional area of the condenser contributes as well. Therefore, the individual pressure drop curve and the operating point

for each cooling element are quite different. The operating point of the cooling elements is defined here as the air flow and pressure drop of the cooling element when operating the standard fan on full power in the frequency converter module. The pressure drop curves and operating points of the cooling elements are shown in Figure 36.

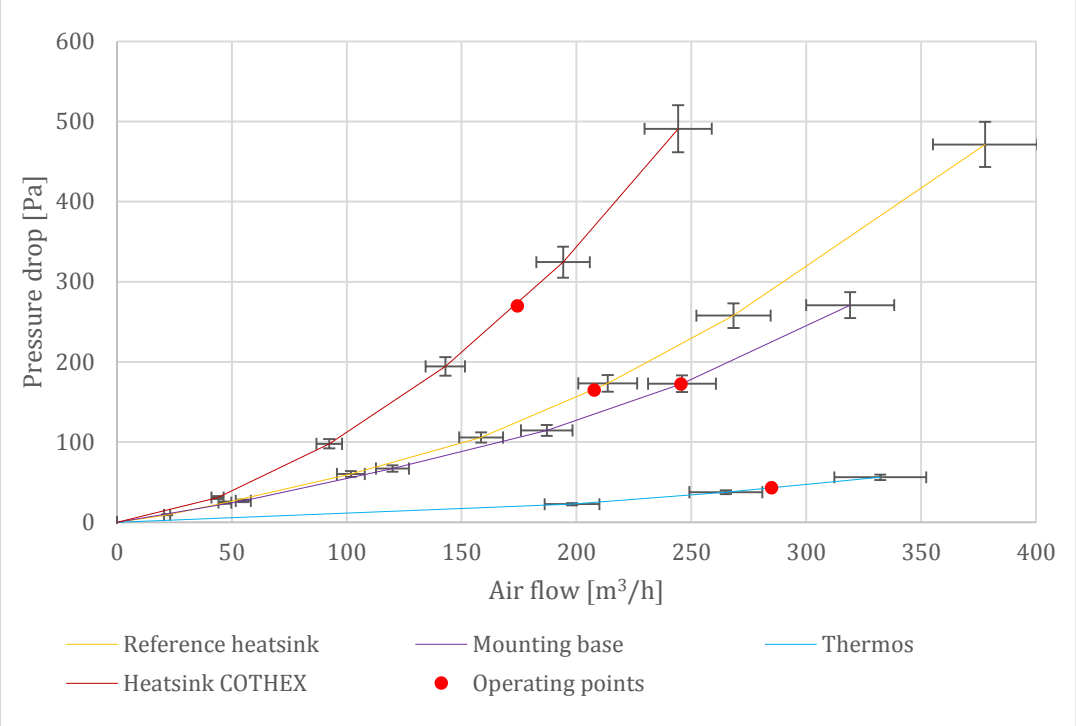

Figure 36. The pressure drop curves of the cooling elements with their operating points

The large pressure drops of the Heatsink COTHEX can be explained with the condenser structure in which the air has to travel a long distance to reach the end of the cooling element. Also the small fin increases the pressure drop. The long travel distance gives the air time to absorb the heat, so it might prove to be a beneficial feature.

Mounting base had the same fin pitch as the Reference heatsink and consequently it generates the same amount of pressure drop with same air flow rates through the converter module. However, it allows more air flow to pass through the condenser than with Reference heatsink. This can be explained with the fact that Reference heatsink has longer condenser fins. Longer fins restrain air from flowing through the condenser and as a result, less air is allowed pass through the condenser with the same amount of pressure drop.

The Thermos cooling concept creates the smallest amount of pressure drop due to the fact that the air travels a very short distance in the cooling fins compared to the other cooling concepts. With inclined fins, the air does not have to shift its course significantly. Should the fins that be placed perpendicularly compared to the condenser MPE tubes like explained in the Chapter 530 about Thermos fin cooling concept, the amount of pressure drop respect to air flow would be significantly higher. However, the inclination of air produces by far the greatest deal of the pressure drop in the Thermos cooling concept with

inclined fins. Should the cooling element pressure drop be further decreased and thus increase the amount of air flow, the only reasonable way to conduct it is to increase the inclination of the fins.

It could be assumed that the element, which allows largest amount of air to travel through the condenser will result the lowest temperatures. This may not be always true, because other factors, such as the structure of the cooling element, the amount of fins and their length in the condenser have a strong impact on the cooling element cooling performance. The relations between the fin structure and the cooling air flow are explained in Chapter 4.2.6 relying on the theories regarding heat transfer from fins discussed in the Chapter 3.3.2. As a result, one cannot predict the cooling performance of the cooling elements only with their pressure drop curves.

The operating points of the cooling elements are defined by using the methods described in the Chapter 4.2.3. The operating points and the temperatures of the cooling elements with standard heat load, air flow and ambient temperature are defined in Table 2. In Table 2, Vis the air flow, which travels through the cooling element condenser, Δp is the pressure drop produced by the cooling element and T is the baseplate temperature of the cooling element in these conditions.

Table 2. The operating points and temperatures of the cooling elements at standard conditions

	$\dot{V}$ [m^3/h]	Δp [Pa]	T [^{0}C]
Reference heatsink	208	165	109
Thermos	285	43	88
Mounting base	246	172	106
Heatsink COTHEX	174	270	119

As can be seen in Table 2, the most promising solutions for the cooling is Thermos cooling concept, because it has the lowest baseplate temperature at the standard conditions. Mounting base seems to improve cooling by small degree compared to the Reference heatsink and Heatsink COTHEX has the lowest cooling performance at the standard conditions.

One noticeable discovery is that the amount of air travelling through the condenser does correlate in this study to the cooling performance of the elements. The elements, which allow large amount of air flow pass through the cooling element, also have low temperature at their baseplate. As matter of fact, the dependency between the air flow and temperature is linear. This strong dependence of the cooling performance to the air flow rate might indicate that cooling air flow is substantially inadequate and much better cooling results would be achieved should higher air flow rates be made available.

6.1.3 Air flow

The simulation results in the standard operating points stated in the previous chapter predict the cooling performance of the cooling elements in typical working situations. It would be beneficial, however, to know how the cooling element operates under conditions that do not match the standard conditions. In typical frequency converter working conditions the ambient temperature might be higher for a period of time. Cooling air flow could also be lower than predicted due to fan malfunction or clogging of the converter module. As time passes, the condenser of the cooling element experiences clogging as well to some degree. Therefore, it is important to study how the cooling elements react to changes in the ambient temperature and air flow rate through the condenser.

The variation in air flow depicts how well the cooling element is able to cool the semiconductor with insufficient amount of air and also estimate the cooling power of the cooling element when given an excessive amount of air. Figure 37 depicts the temperatures of the different cooling elements in correlation to varying air flows through the condenser.

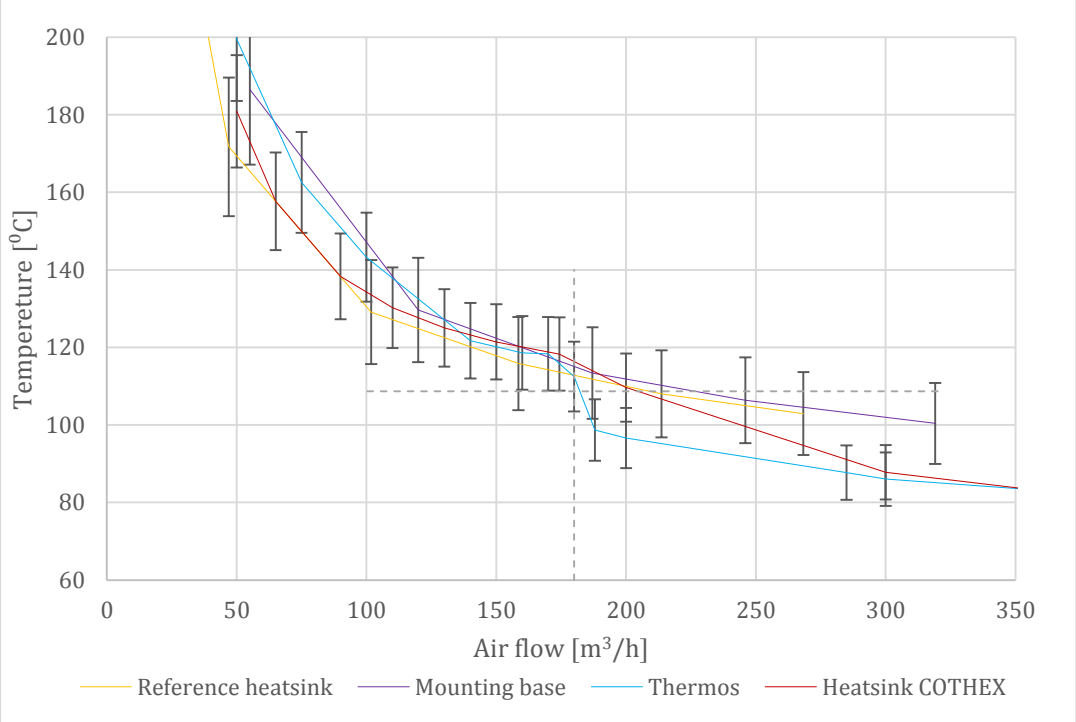

Figure 37. The baseplate temperatures of the cooling elements with different amounts of cooling air flowing through the condenser

The simulations produced baseplate temperate curves as seen in Figure 37. These curves can be iterated equations with which one can predict the cooling performance of the elements at air flow rates out of the range shown in Figure 37. Following equations depict the temperature curves of the cooling element's baseplates:

$$T_R = 88 + \frac{3810}{\dot{V}} \ , \tag{55}$$

$$T_T = 66 + \frac{6180}{\dot{V}} \ , \tag{56}$$

$$T_M = 83 + \frac{5705}{\dot{V}} \ , \tag{57}$$

$$T_H = 67 + \frac{5710}{\dot{V}} \ , \tag{58}$$

where T_R is the temperature of the Reference heatsink baseplate, $\dot{V}$ is the air flow, T_T is the temperature of the Thermos baseplate,T_M is the temperature of the Mounting base baseplate and T_H is the temperature of the Heatsink COTHEX baseplate.

As can be seen in Figure 37, the Reference heatsink has the lowest baseplate temperature of all the cooling elements when the air flow through the cooling element is less than 180 m^3/h. With larger air flow rates the Thermos thermosyphon seems to operate most efficiently. However, Heatsink COTHEX seems to reach better cooling performance than Thermos when the air flow is higher than 360 m^3/h. The baseplate temperature of the Reference heatsink is 109 ^{0}C at its operating point as the grey dashed horizontal line shows in Figure 37. Thermos baseplate temperature falls below this temperature with air flows higher than 180 m^3/h as the grey dashed vertical line shows in Figure 37, Heatsink COTHEX surpasses the cooling performance of the Reference heatsink with air flows higher than 205 m^3/h and the Mounting base with air flows higher than 227 m^3/h.

These results conclude that thermosyphons seem to require some amount of air flow to work properly and in this study the limit is at 180 m^3/h. However, the amount of air required is rather easily achievable. For example, a fan with similar abilities to resist back pressure as the fan used in these simulations can operate only on 50 % of its nominal power to provide sufficient amount of air flow for Thermos thermosyphon to achieve the same cooling performance as the Reference heatsink.

The amount of air flow has been defined to be the biggest bottle neck in the semiconductor cooling. Should there be redundant amount of air flow, the thermosyphon technology would have even greater potential for replacing the conventional heatsinks with thermosyphons. If the cooling elements received infinite amount of air, the temperatures of each cooling element would reach to temperature values that can be seen in the following equations. The equations are derived from the earlier equations 55, 56, 57 and 58:

$$\lim_{\dot{V}\to\infty} T_R = \lim_{\dot{V}\to\infty} \left(88 + \frac{3810}{\dot{V}}\right) = 88 \ , \quad (59)$$

$$\lim_{\dot{V}\to\infty} T_T = \lim_{\dot{V}\to\infty} \left(66 + \frac{6180}{\dot{V}}\right) = 66 \ , \quad (60)$$

$$\lim_{\dot{V}\to\infty} T_M = \lim_{\dot{V}\to\infty} \left(83 + \frac{5705}{\dot{V}}\right) = 83 \ , \quad (61)$$

$$\lim_{\dot{V}\to\infty} T_H = \lim_{\dot{V}\to\infty} \left(67 + \frac{5710}{\dot{V}}\right) = 67 \ . \quad (62)$$

The equations predict that redundant amount of air flow allows the temperature of the Reference heatsink to settle to level of 88 ^{0}C with the standard heat load of 2088 W. All the thermosyphon applications settled into lower temperature levels. This shows the potential of the thermosyphon applications for the cooling of electronic components. Unfortunately the limited space and limited amount of cooling air significantly reduces the cooling efficiency of the thermosyphon applications.

In the case of Thermos, lower air flow rates than 190 m^3/h will lead to significantly decreased cooling performance due to liquid coolant rising to the condenser, in other words flooding. The decrease in air flow rises the temperature of the air leaving the condenser. This is due to the fact that the heat emitted from the condenser needs to stay constant as the equilibrium rule Q_e=Q_c stated in the Chapter 3.5. Therefore, as the air flow rate decreases, the temperature difference between the air that flows into the condenser and the air that leaves it increases as stated in equation 52. As the temperature of the incoming air is the constant temperature of the surroundings, the temperature of the leaving air will increase. The increase in the temperature of the cooling air has a direct effect on the temperature of the coolant. The coolant can only receive heat from higher temperature levels as the second law of thermodynamics states. The temperature level of the coolant has to be higher than the temperature of the air leaving the condenser in order for it to emit heat to the cooling air.

With higher coolant temperatures the enthalpy of evaporation becomes smaller and thus the heat of phase transition decreases. Consequently, the vapour quality change increases as stated in equation 48. As the share of vaporized fluid increases the density of the two-phased fluid degreases, as presented in equation 39. The decrease in the two-phased fluid density increases the frictional pressure drop (equation 45) and consequently, the gravitational pressure drop (equation 44) requires longer section length in the liquid adiabatic section and the condenser section to balance the increased frictional pressure drop. At some point the required section length becomes so long that the liquid rises to the Condenser and it becomes flooded. This means that the liquid in the condenser is subcooled and it reduces heat transfer area meant for condensation. As the condenser heat transfer area becomes smaller, the thermal resistance increases thus increasing the coolant temperature. The flooding occurs with air flow rates lower than 190 m^3/h.

Another fact is that the high coolant temperature generates high system pressure into the loop. As matter of fact, the coolant R134a pressure surpasses its critical pressure p_{cr}=40.6 bar [33] at air flows lower than 140 m^3/h in the Thermos application. When the coolant reaches its critical point, the differences in the material properties between liquid and gas phases cease to exist. This means that the gravity based thermosyphon can no longer circulate the fluid. Therefore, the heat is transferred through the element only with conduction through element's material layers. More of the effects of approaching coolant critical point and its superheating are explained in the Chapter 3.5.

6.1.4 Heat load

Figure 38 depicts how the cooling elements are able to cool the heat generated by the semiconductor. It is particularly important to know if the cooling elements are able to cool higher heat loads better than the Reference heatsink, because that would create a possibility to increase power load converted through each semiconductor.

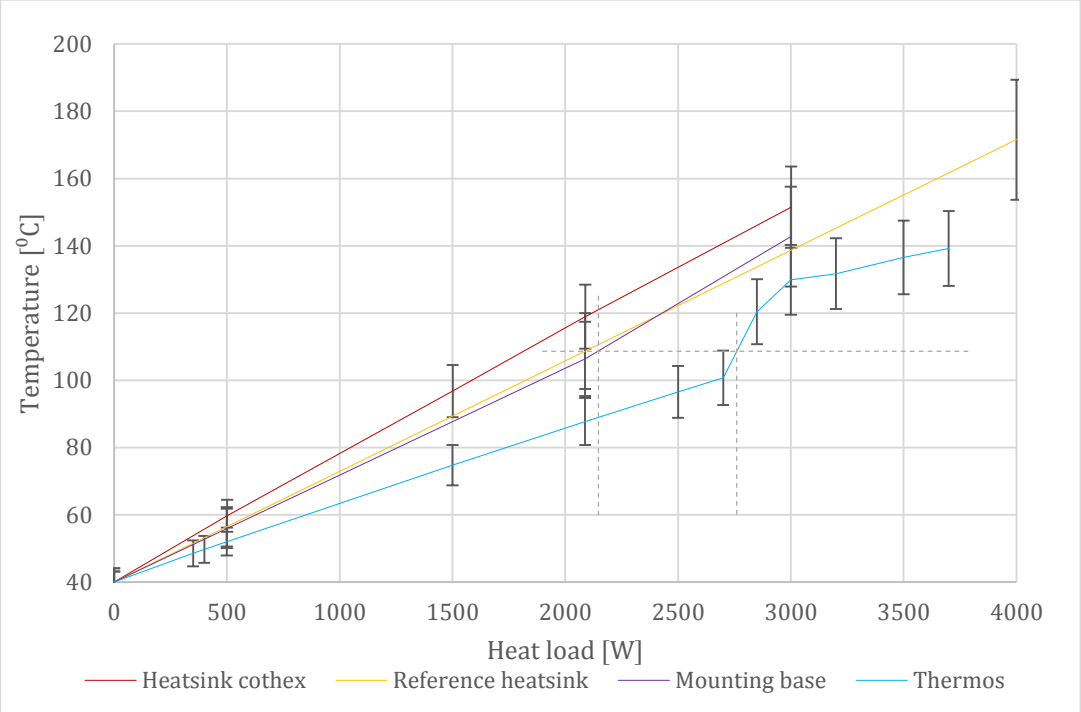

Figure 38. The baseplate temperatures of the cooling elements with variation in heat loads

The temperature of the Reference heatsink at the standard conditions is 109 ^{0}C and it seems that both Thermos and Mounting base have lower temperatures in their operating points. It would be beneficial to learn how much bigger heat loads these elements can endure until their baseplate temperatures reach the same value. The horizontal grey line in Figure 38 predicts the amount of heat load the Thermos and Mounting base cooling elements can cool until they reach the temperature of the Reference heatsink. According to the vertical dashed grey lines Thermos could cool up to 2760 W and Mounting base up to 2145 W before they reach the temperature of the Reference heatsink. This means that Thermos can cool 32 % and Mounting base 3 % more heat than the Reference heatsink at

their operating points. However, the cooling performance of the Mounting base thermosyphon cannot be guaranteed, because the boiling of the refrigerant fluid inside its baseplate was not studied. The result for the Mounting element baseplate temperatures only apply if the assumption that the thermal conductivity of the Mounting base baseplate is the same as with Thermos thermosyphon with different heat loads.

Heatsink COTHEX seems to provide poorest cooling performance. The cause for this is probably that the element creates so much pressure drop that it allows very little air pass through the condenser fins. The amount of air that passes through its condenser is only 84 % of the amount that passes through fins of the Reference heatsink. If the element was provided with bigger amount of air flow, the cooling would improve significantly as predicted in equation 58.

The heat load results in shown in Figure 38 indicate that Thermos element has the lowest thermal resistance. The temperature difference between the baseplate and surrounding are lowest with this element, although the baseplate temperatures seem to increase rapidly after reaching the heat load of 2700 W. The thermal resistances of the cooling elements are calculated from the results according to the equation 6 and they are presented in Figure 39:

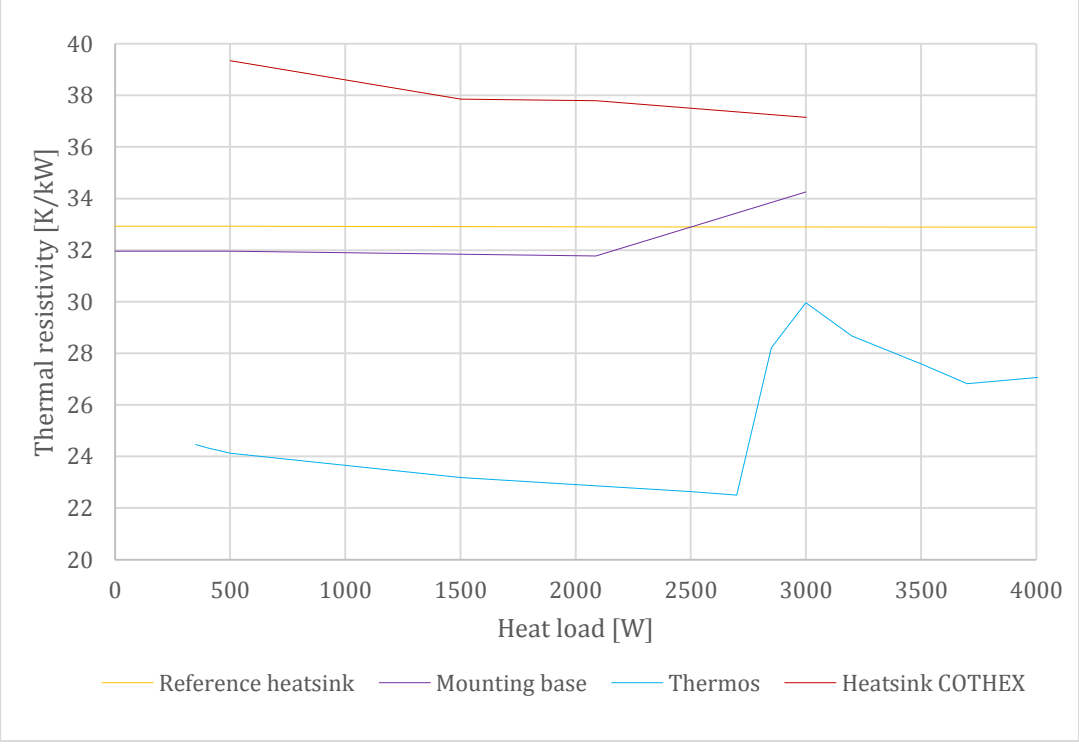

Figure 39. Thermal resistivity of the cooling elements

The lowest thermal resistance can be reached using the Thermos thermosyphon as predicted. It has its best thermal transfer abilities with heat load of 2700 W. However, with higher heat loads the thermal resistance seems to increase rapidly and therefore, heat loads higher than 2700 W should be avoided. One might think the rapid increase of thermal resistance occurs due to thermosyphon superheating as explained in the Chapter

3.5 about the fluid states. However, this is not the case with Thermos cooling element. With higher heat loads than 2700 W, the condenser becomes flooded with subcooled coolant and consequently is not able to transfer heat as efficiently. As a result of this, the added heat load increases the thermal resistance dramatically. The reasons for the flooding of the condenser can be explained with behaviour of the section pressure drops in the loop discussed in the Chapter 3.5.

When the heat load increases, the vapour quality change increases as stated in equation 48. An increase in the heat load raises temperature of the coolant. This decreases the evaporation enthalpy and hence decreases the heat of phase transition at higher temperatures. The decrease in the heat of phase transition also contributes to generation higher amounts of vaporization. The simulation results of the air flow concluded that increase of the vaporization eventually leads to flooding of the condenser. The flooding occurs in Thermos application with heat loads higher than 2850 W. As the condenser heat transfer area becomes smaller, the thermal resistance increases.

The coolant R134a pressure surpasses its critical pressure in the Thermos application at heat loads higher than 3500 W. When the coolant reaches its critical point, the differences in the material properties between liquid and gas phases cease to exist. Without the differences in the densities of coolant material, gravity based thermosyphon can no longer circulate the fluid and the heat is transferred through the element only with conduction. The effects of approaching coolant critical point and its superheating are explained more thoroughly in Chapter 3.5.

To avoid flooding in the condenser, the condenser should either be more effective, for example by having more heat transfer area, or the condenser and liquid adiabatic section should be longer in total to provide longer section length. When considering the restrictions given for the space that the thermosyphon is given, the only possible ways to improve the structure is to increase the liquid adiabatic section and thus, make sure that flooding does not reach to the condenser area or by installing a pump. These kinds of improvement ideas for the construction of Thermos thermosyphon are discussed in Chapter 6.2.2.

6.1.5 Ambient temperature

Figure 40 shows how the variation in the ambient temperature affects the temperatures in the cooling concepts.

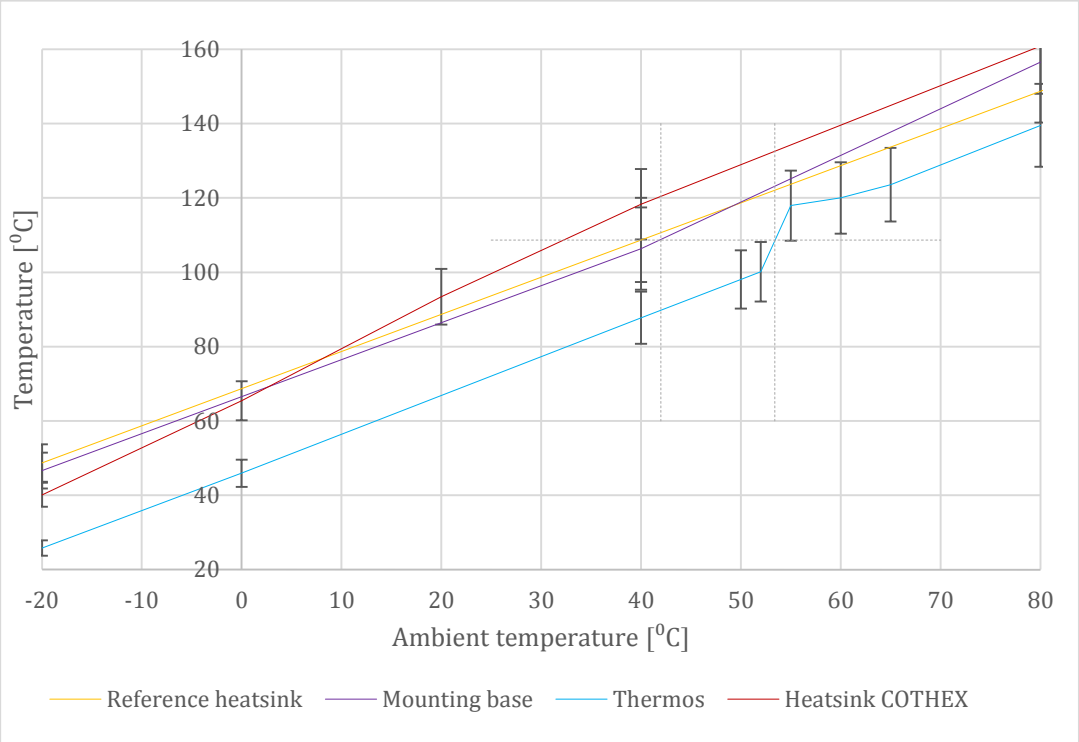

Figure 40. The baseplate temperatures of the cooling elements with variation in ambient temperature

It seems that the Thermos operates the best in whole range of ambient temperatures and the Mounting base works little bit better than the Reference heatsink at temperatures below 50 ^{0}C. Heatsink COTHEX operates best at low temperatures but its thermal resistance seem to increase rapidly with higher ambient temperatures. Heatsink COTHEX has better cooling performance than the Reference heatsink at temperatures below 8 ^{0}C. Good cooling performance at low temperatures does not give much benefit though, because the baseplate temperatures are at rather low level anyway.

The thermal resistance of both Thermos and Mounting base elements seem to increase when reaching higher temperatures than 50 ^{0}C. The increase in thermal resistance can be explained with condenser flooding and reaching coolant critical point. With high ambient temperatures the temperature of the leaving air is naturally high as well. As already stated in the air flow simulation results the increased temperature of the cooling air increases the temperature of the coolant. With higher coolant temperatures the enthalpy of evaporation becomes smaller and thus the heat of phase transition decreases. This eventually leads to flooding of the Condenser for the same reasons as in the air flow and heat load variation simulations and are explained in the Chapter 6.1.3. The condenser of the Thermos element becomes flooded at ambient temperatures 55 ^{0}C.

The coolant R134a pressure surpasses its critical pressure in the Thermos application at temperatures higher than 65 ^{0}C. As explained in the previous chapter, when the coolant reaches its critical point, thermosyphon applications can no longer transfer heat with fluid circulation.

6.2 Concept selection

6.2.1 The selected concept

The best cooling concept is chosen based on the cooling performance of the cooling element. The conditions in which the cooling elements are compared together are explained in Chapter 4.2.2 and the results based on that presented in the previous chapter. The cooling abilities were determined by using simulation programs Icepak and COTHEX designer. The benefits and disadvantages of the winning concept are studied more in detail in the following chapter

All of the simulation results show that Thermos concept generates most efficient results. It seems to operate at approximately 20 ^{0}C lower temperature than the competing concepts at the standard conditions and it can be safely operated under conditions that are in the frequency converter operating range. Therefore, Thermos is selected as the best concept to replace the conventional finned aluminium heatsink.

6.2.2 Benefits and disadvantages of the concept

The winning concept in thesis is Thermos thermosyphon concept. It provides the best cooling performance in the whole frequency converter operation range and allows to widen the operation range even further. The semiconductor temperatures are the lowest with Thermos thermosyphon with heat loads up to 2700 W and it is able to cool at ambient temperatures up to 50 ^{0}C when the fan is operated at full power. In addition, Thermos has provided some benefits that are typical for thermosyphon cooling elements, such as even temperature distribution at the cooling element baseplate. However, Thermos also has some disadvantages, such as condenser flooding and manufacturing costs.

Thermos experiences one significant challenge when it comes to the structure of it. The condenser of the element reaches all the way down to the bottom parts of the cooling element and as a result of that part of the coolant is stratified to the bottom parts of the condenser MPE tubes in liquid form. This is not favourable situation as the liquid will become subcooled due to condenser fins absorbing the heat from the coolant and emitting it to the surroundings. The condenser MPE tubes should be filled with vapour instead to provide well-functioning device. Picture a. in Figure 41 shows the stratification of the coolant in Thermos element.

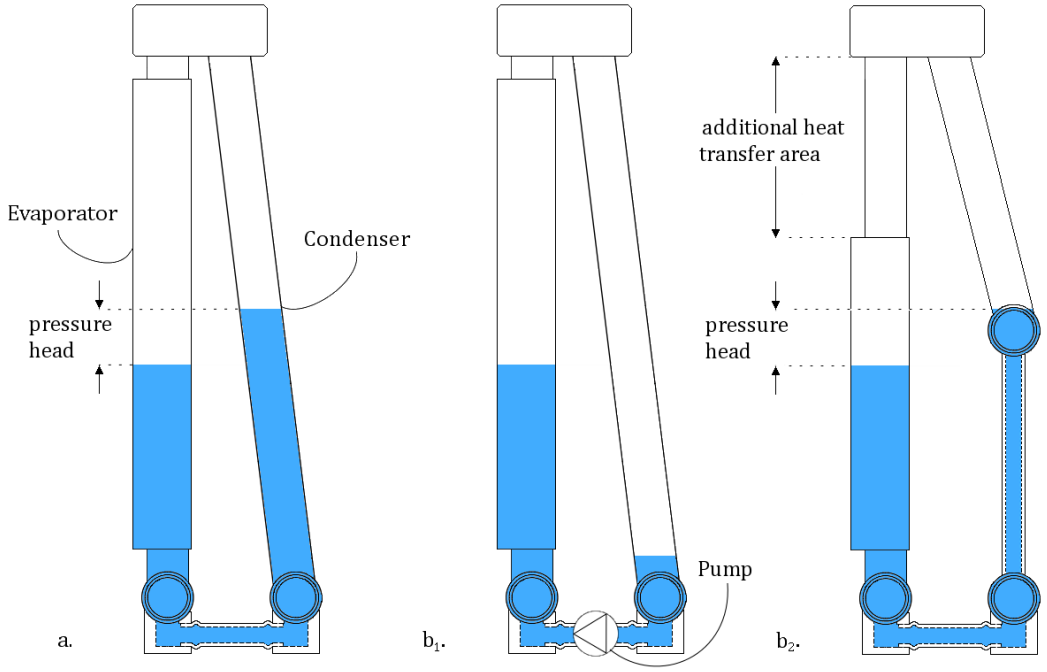

Figure 41. Stratification of liquid in Thermos; a. with original structure and b_1. with pump and b_2. construction only with effective heat transfer area

The pressure head between the evaporator and condenser liquid levels is due to frictional pressure drop generated in the pipe walls and at curves, expansions and shrinkages of the loop. The simulation results do not take into account the condenser flooding and therefore the results indicate Thermos performance without the condenser flooding. The coolant in liquid form in the condenser MPE tubes decreases heat transfer out of the cooling element dramatically and therefore a solution to this should be provided. Storing the liquid in the condenser should be avoided for several reasons.

Experimental measurements conducted in ABB research team concluded that condenser practically does not transfer heat out of the flooded area in the condenser and hence, the area does not dissipate any heat out of the element. The reason for poor heat transfer is that heat transfer coefficient for convection from liquid to the condenser fins is widely smaller than heat transfer coefficient for condensation of the two-phase fluid. As stated in Figure 2 in Chapter 2.2, heat transfer of condensation from two-phase fluid to the condenser fins is 10 to 100 times larger than with the convective heat transfer of liquid. Therefore, the flooded condenser area can be seen as lost heat transfer area and only the parts of the condenser in which vapour condensates contribute to heat transfer.

Another reason for avoiding storing of the coolant in liquid form in the condenser is that it creates great temperature differences over the evaporator baseplate. The liquid in the condenser becomes highly subcooled due to heat transfer to the fins and because the convective heat transfer to the subcooled liquid at the evaporator has higher thermal resistance than in evaporation, the baseplate temperature increases drastically as predicted in equation 6 in Chapter 3.4.1.

The final disadvantage for fluid storage in the condenser is that the lost heat transfer area increases air pressure drop and thus lowers the amount of air flow through the condenser. The effective area creates pressure drop as well, but simultaneously heat is transferred out of the condenser. The flooded condenser area hinders the air flow with no gain and therefore placing fins on such area is useless.

The problem of having subcooled liquid in the condenser can be solved in two ways. One way is to add an external force that keeps the liquid out of the condenser and pumps it to the evaporator tubes. This would mean that an additional pump would have to be installed into the element. One major benefit of using thermosyphon technology in the semiconductor cooling was that no external forces would be needed in the cooling. The heat entering the cooling system is supposed to work as a natural pump and circulate the coolant in the loop. The major disadvantage of using a pump in the thermosyphon application is that it requires electricity and it needs to be replaced repeatedly and thus the expenses of using the thermosyphon increase. Picture b_1. in Figure 41 depicts the gravitational stratification of the fluid in the Thermos element when pump is used to keep the liquid out of the condenser MPE tubes.

Another solution is to rely on the effective heat transfer area of the element. The lowest point of the condenser should be at same level as the surface of the liquid, because all parts of the condenser that are flooded practically do not transfer any heat. The element should not generate pressure drop for the air flow at element parts in which heat is not transferred to ensure highest possible air flow rate passing the effective heat transfer area. Therefore, pipes connect the condenser to the bottom manifolds. The liquid surface in the condenser is at the level of evaporator added by pressure head. Consequently, heat transfer area diminishes radically as the bottom of the condenser is located higher. Effective heat transfer area can be increased by minimizing the baseplate length and adding fins between the MPE tubes on top of the baseplate before the top manifold. Picture b_2. in Figure 41 depicts the gravitational stratification of the fluid in the Thermos element when only the effective area of heat transfer is used.

With filling ratio of 55 % the heat transfer area of the condenser is about 48 % smaller than in the original solution, however, if the additional heat transfer area is put into use, the effective heat transfer area is only 9 % smaller than the original condenser area. Even without the additional heat transfer area, the b_2 Thermos element has a good probability to function better than the Reference heatsink, because it has 32 % more heat transfer area than the Reference heatsink and it generates less pressure drop, thus ensuring more air flow through the condenser.

Even the pipes in the picture b_2 cannot completely prevent condense flooding. Condenser may become flooded due to increase in the frictional pressure drop in the loop, which increase the pressure head in the liquid adiabatic section. As explained in the simulation result chapters, the frictional pressure drop increase with as air flow rates decrease or when heat loads and ambient temperatures increase. Therefore, the cooling element structure and the coolant filling ratio should be determined in such way that

there is room for the liquid to rise in the liquid adiabatic section. More studies are needed to define the optimal filling ratio and condenser length for the Thermos cooling element and they are discussed in the following chapter about future development ideas.

Thermos has a structure that is easy to manufacture. Both the cost of manufacturing the Thermos cooling element and making the initial investment to acquire tools is rather small, however, the manufacturing costs are higher than with the Reference heatsink. If the price of the Reference heatsink is stated as x, the Thermos would cost depending on the amount of manufactured yearly between 2.1x and 3x. The tooling investment would increase the price of the cooling elements by some degree. If considered that the tooling investment is paid in the prices of the cooling elements in one year, the cost of single Thermos cooling element would be between 2.2x and 4.1x for that year. The manufacturing costs of Thermos seem rather high compared to the Reference heatsink, but it should also be taken into account that their costs compared to the manufacturing costs of a whole frequency converter are small.

Thermos will achieve the same cooling performance as the Reference heatsink with only air flow of 180 m^3/h. This means that a with similar abilities to resist back pressure as the fan used in the frequency converters can operate only at 50 % of its nominal power to provide sufficient amount of air flow for Thermos to achieve the same cooling performance than with the Reference heatsink. Another benefit is that the clogging of the condenser fins will not create problems. For example, let us assume that the clogging will prevent air from flowing through the cooling element condenser and allows only 80 % to travel through of the nominal air flow rate. At the standard conditions this would raise the Thermos element baseplate temperature by 5 ^{0}C according to the equation 56.

Thermos will achieve the same cooling performance as the Reference heatsink with heat load of 2760 W. This means that more power can be converted in the semiconductors with the same sized cooling element. The semiconductors may also be operated at wider heat load range without risking of damaging them. Thermos also allows the working conditions to be at higher temperature levels than before. At standard conditions Thermos reaches the same baseplate temperatures as the Reference heatsink at ambient temperature of 55 ^{0}C. This advantage originates from the general good cooling performance of the element however, not from abilities to cool efficiently at high ambient temperatures. On the contrary, the thermal resistances of all studied thermosyphon structures increased at higher ambient temperatures and decreased in lower ambient temperatures. The reason for this can be found in the coolant material properties and its behaviour in the loop. The same problems occur if the heat loads reach too high or air flow rates are too low. These problems are discussed in the previous chapters regarding simulation results.

The thermal simulations revealed one major benefit in the thermosyphon cooling technology. It is evident that the temperature distribution in the baseplate is more even with thermosyphon applications than with heatsinks. The reason for this is that the heat transfer is more efficient in the solutions where refrigerant absorbs and transfers heat out of the baseplate rather than where all heat is only conducted out of the baseplate.

Therefore, it can be said that the thermal resistance between the semiconductor chip and the cooling element baseplate is often smaller in the thermosyphon solutions than in the heatsink solutions. However, one must keep in mind that the total thermal resistance of the whole cooling element determines element's cooling performance and yet, efficient heat transfer in the cooling element baseplate gives many advantages. Figure 42 presents the temperature distribution in the baseplates of the Reference heatsink and Thermos at the standard conditions.

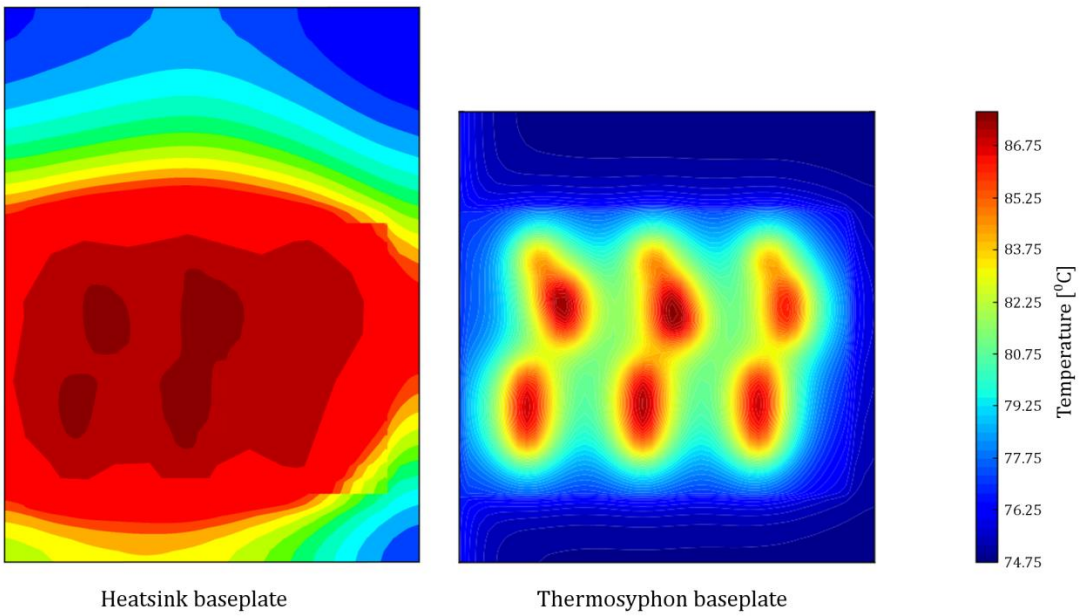

Figure 42. Temperature distribution in the baseplates of the Reference heatsink and Thermos

Due to higher thermal resistance, more heat seems to travel along the baseplate in vertical direction in the heatsink cooling element than with thermosyphon element. This means that the chips located in the lower parts of the semiconductor heat the chips located in the upper parts. Consequently, these chips suffer from higher temperatures than the lower chips and are in bigger risk of breaking. For example, the temperature difference between the coolest and hottest chip in the heatsink cooling concept is 12 ^{0}C whereas it is 7 ^{0}C with the Thermos cooling concept. The big temperature difference between the chips also results that the hottest chips age at faster pace and therefore they perform less ideally. This increases leakage current in the chips.

The temperature difference itself will create thermal stress between the components inside the semiconductor and inside the components as well. The constant change in temperature inside a chip or between components will cause strain and fatigue their material. The higher the temperature difference is, the faster the components will age due to thermal stress. For example, the largest temperature difference inside an IGBT chip in the heatsink cooling concept is 17 ^{0}C and it is only 5 ^{0}C with the Thermos cooling concept. Additionally, high changes in the temperature at the semiconductor will pump thermal grease out of the layer between the semiconductor and module baseplates. This

means that air will replace the areas where grease no longer exist and further increase junction temperature due to lower heat transfer. That is why it is essential to have smallest possible thermal resistance between the semiconductor and cooling element baseplate to allow an even temperature distribution in the semiconductor and cooling element baseplate.

7 Future development ideas

Some improvements can be made to the Thermos cooling element concept. Defining the most feasible structure for the Thermos cooling element to replace a conventional heatsink is about optimizing the structure to allow highest possible air flow rate to pass the condenser and to have the largest possible heat transfer area at the condenser with most effective fluid circulation at the thermosyphon loop. These features could still be improved further to develop even more effective cooling element.

The bottleneck of the current Thermos solution lies on the restricted heat transfer area at the condenser and the shape of the cooling element could be developed in such way that the effective heat transfer area of the condenser could be increased even further. The effective heat transfer area is strongly dependent on the filling ratio of the coolant. For example, if the structure in picture b_2 in Figure 41 was used, the condenser effective area could be increased by reducing the filling ratio. Smaller filling ratio will directly decrease the liquid length and thus the condenser could begin from a lower point and hence, effective heat transfer area can be increased. Figure 43 depicts the effects of decreasing coolant filling ratio.

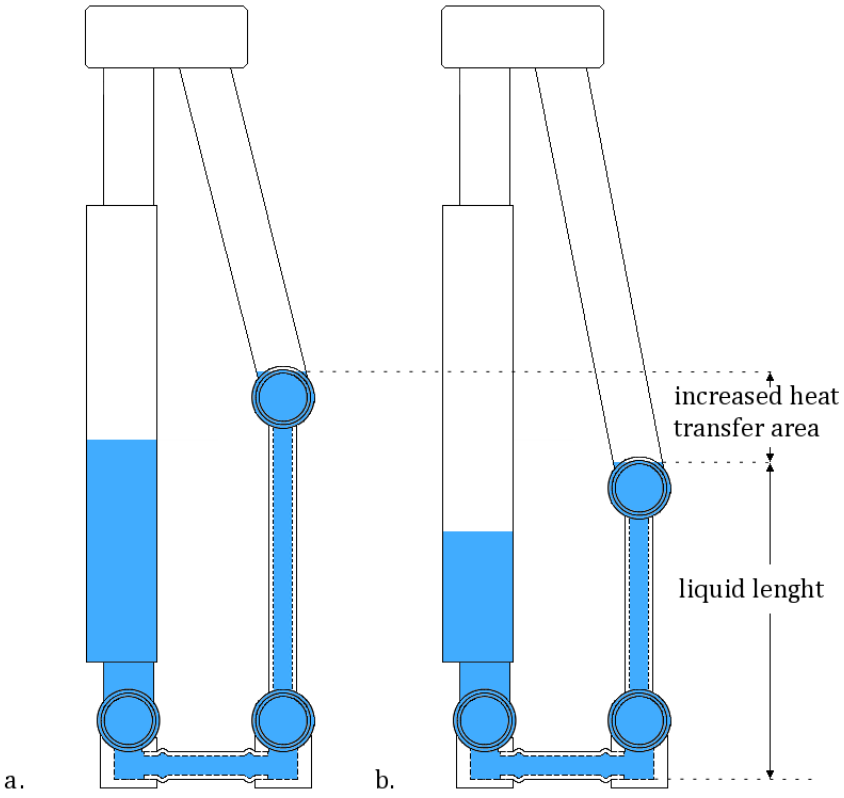

Figure 43. Higher filling ratio in the picture a. and lower filling ratio in the picture b.

Decreasing the filling ratio from the chosen 55 % might prove out to be effective. However, very small filling ratios may cause dryout and increase the cooling element temperature and especially temperature difference at the baseplate. Therefore, it would be beneficial to define an optimum filling ratio that cools the semiconductor most efficiently.

Another improvement made to the Thermos element concerns the structure of its fins. The structure of the condenser fins can further be developed by optimizing the degree of inclination to of the fins in the Thermos cooling element condenser reach better cooling performance of the cooling element. The basic idea of the optimization is that the optimization has to be done between increasing air flow through the cooling element and having maximum amount of fins in the condenser.

Increasing the angle of inclination in the fins will reduce the created amount of pressure drop at the element as the air flow has to shift its course much less when travelling through the condenser. The decrease of pressure drop leads to increase of the air flow rate. This will result in greater heat transfer in the condenser area and thus, better cooling performance. On the other hand, high inclination in the fins means that less fins fit into the condenser structure and the fins become longer in length. Having smaller amount of fins in the condenser decrease the amount of heat transferred in the cooling element. However, longer fins will increase the fin efficiency as the air has more time to absorb heat from the fins.

This study was made to find a solution to a very specific case. A solution was found to replace a conventional heatsink of certain size within a certain operating condition. It would be beneficial to know if Thermos cooling elements can replace heatsinks of other sizes and could Thermos elements be optimized to operate at even more severe conditions. Optimization of cooling element to operate at more severe conditions, such as higher heat loads and lower air flows, means that coolant type needs to be reselected. It is important that the coolant type is selected according to the conditions the cooling element operates in and the air flow rate, ambient temperature and heat load subjected to the cooling element have a great influence on cooling abilities of the coolant. Therefore, the selected coolant type R134a should be changed as the coolant R134a reached its critical point at rather low temperatures and thus, loses its ability to transfer heat. Another coolant, which has its critical point at higher temperature should be selected if the cooling element were used outside of Thermos operation range. As this study can guarantee success for replacing the Reference heatsink at standard conditions, it would be beneficial to know how well Thermos can replace heatsinks of other sizes and structures as well.

These kind of new studies would improve Thermos cooling performance and gain knowledge on the chances of replacing any kinds of heatsinks to thermosyphons and would gain much benefit when improving cooling of electronics.

8 Conclusions and recommendations

There were two criteria defined in the objectives that determine whether a successful thermosyphon cooling concept was found to replace conventional heatsink in cooling of semiconductor devices. Naturally, the cooling performance of the thermosyphon would have exceed the cooling performance of the heatsink, but also the thermosyphon structure would have to fit into the same space and be cooled with air, which flows in same direction as with the heatsink. These requirements allow the heatsink to be replaced directly with a thermosyphon without having to make any alternations in the application it is used in. Thermos cooling concept was found to fulfil these criteria and so it can be stated that a successful thermosyphon based cooling concept was found and patented.

Thermos proved out to work best of all the studied thermosyphon cooling concepts. It has the best thermal performance at most of the conditions regarding heat load conveyed into the element, air flow travelling through the condenser of the element and ambient temperature it operates in. At the standard conditions, which resemble frequency converter's typical usage, the temperature of Thermos element's baseplate was 18 °C lower than the baseplate of the second best concept, the Mounting base. Additionally, it was 21 °C lower than the baseplate of the same size conventional heatsink, which is called the Reference heatsink. However, the thermal performance of Thermos concept did not surpass the cooling performance of the Reference heatsink at all study points. In the air flow simulation tests Thermos gave better cooling performance with air flow rates over 180 m^3/h. This indicates that if a very low amount of air is provided, a conventional heatsink may convey heat better than a thermosyphon. However, a fan operating on 50 % of the nominal power in frequency converter usage would provide sufficient air flow rate for the thermosyphon to surpass the cooling performance of conventional heatsink.

Condenser flooding has proved out to be problematic in the Thermos design. It was discovered that the area in the condenser, in which the coolant is in liquid form, does not transfer heat and can be seen as lost heat transfer area. In fact, the flooded area causes major problems due to the fact that the liquid emits heat to the fins and becomes subcooled. Consequently, the subcooled liquid produces highly uneven temperature distribution to the baseplate due to higher thermal resistivity in the baseplate. Therefore, I suggested a new Thermos element design in which the condenser is redesigned in such way that it does not gather any liquid in the condenser. Redesign and adding more effective heat transfer area between the baseplate and top manifold result that Thermos can be constructed in such way that it has only 9 % less heat transfer area than in the original design.

Thermos cooling element may still experience condenser flooding at low air flow rates, high heat loads and high ambient temperatures. At extreme cases, the coolant may reach its critical point. In such situation the heat transfer of the element becomes unstable and the temperature in the cooling element will rise rapidly, which may lead to material damage. Therefore, it is recommended that the Thermos operates within the standard conditions and exceeds only with maximum of one condition parameter from the limits

of standard conditions. The absolute operating limit for the maximum amount heat load is 2700 W, which allows the Thermos concept to dissipate 29 % more heat than the Reference heatsink. The operating limit for the minimal amount of air flow travelling through the cooling element is 190 m^3/h, allowing the converter be operated with 33 % less air flow. Furthermore, the ambient temperature should always be less than 50 °C. If the cooling element is operated within the standard conditions without exceeding the operating limits, the cooling element can be operated without a risk of overheating the semiconductor chips.

The manufacturing costs of the thermosyphon technology are estimated to be from two to four times higher than with the conventional aluminium heatsinks. However, it is important to note that the improved cooling performance offers many benefits that increase the value of the converter. Improved cooling provides lower temperatures and more even temperature distribution at the baseplate of the cooling element and consequently, decelerates aging of semiconductor's components and lessens the need for their maintenance. Additionally, semiconductors will have wider operation range because the heat loss they cause while in operation is dissipated more efficiently. Further studies should, however, be conducted regarding the economic viability of implementing thermosyphon technology.

Replacing a conventional heatsink of size 186 x 86.5 x 250 mm with Thermos thermosyphon will improve significantly the cooling of semiconductor device in the studied ACS880 frequency converter usage. Furthermore, Thermos is designed in such way that it can be used to replace of other conventional heatsinks of similar sizes only with moderate modification in its design. This thesis concentrated to study the possibility of replacing the conventional heatsink with a thermosyphon from the technical point of view and therefore, the study can be said to have been successful.

References

[1] R. Viswanath, V. Wakharkar, A. Watwe and V. Lebonheur, “Thermal performance challenges from silicon to systems,” *Intel Technology Journal*, no. Q3, 2000.

[2] X. Perpiñà, M. Piton, M. Mermet-Guyennet, X. Jordà and J. Millán, “Local thermal cycles determination in thermosyphon-cooled traction igbt modules reproducing mission profiles,” *Microelectronics Reliablity,* vol. 47, no. 9-11, pp. 1071-1076, 10 2007.

[3] S. S. Kang, “Advanced Cooling for Power Electronics,” in *International Conference on Integrated Power Electronics Systems*, Nuremberg, 2012.

[4] M. M. Shah, “A general correlation for heat transfer during film condensation inside pipes,” vol. 22, 1979.

[5] Y.-J. Chag and C.-C. Wang, “A generalized heat transfer correlation for louver fin geometry,” *International Journal of Heat and Mass Transfer,* vol. 40, no. 3, pp. 533-544, 2 1997.

[6] D. Chrisholm, “Void Fraction during Two-Phase Flow,” *Journal of Mechanical Engineering Science,* vol. 15, no. 3, pp. 235-236, 6 1973.

[7] J. E. Guyer, D. Wheeler and J. A. Warren, “FiPy: Partial Differential Equations with Python,” *Computing in Science & Engineering,* vol. 11, pp. 6-15, 6 2009.

[8] B. Agostini and B. Yesin, “Heat exchanger for power-electronics components”. Switzerland Patent EP 2031332 A1, 4 3 2009.

[9] H. D. Baehr and K. Stephan, Heat and Mass Transfer, 2 ed., Springer, 2006.

[10] F. P. Incropera, D. P. Dewitt, T. L. Bergman and A. S. Lavine, Fundamentals of Heat and Mass Transfer, 6 ed., John Wiley & Sons, 2006, p. 1024.

[11] F. P. Incropera and D. P. Dewitt, Fundamentals of Heat and Mass Transfer, 4 ed., John Wiley & Sons, 1996, p. 886.

[12] B. Agostini and B. Yesin, “Heat exchange device”. Switzerland Patent US 20090266514 A1, 29 10 2009.

[13] L. Chen, Y. S. Tian and T. G. Karayiannis, “The Effect of Tube Diameter on Vertical Two-phase Flow Regimes in Small Tubes,” International Journal of Heat and Mass Transfer , London, 2006.

[14] B. Agostini and A. Bontemps, “Vertical flow boiling of refrigerant R134a in small channels,” no. 26, 2004.

[15] R. Revellin and J. Thorne, “A new type of diabatic flow pattern map for boiling heat transfer in microchannels,” vol. 17, pp. 788-796, 2007.

[16] G. F. Hewitt and D. N. Roberts, Studies of Two-Phase Flow Patterns by Simultaneous X-Ray and Flash Photography, London: Defense Technical Information Center, 1969, p. 28.

[17] D. Papini and A. Cammi, "Modelling of Heat Transfer Phenomena for Vertical and Horizontal Configurations of In-Pool Condensers and Comparison with Experimental Findings," *Science and Technology of Nuclear Installations*, vol. 2010, p. 16, 2010.

[18] O. P. Bergelin and A. E. Dukler, "Characteristics of flow in falling liquid films," vol. 48, 1952.

[19] K. Tripplet, S. Ghiaasiaan, S. Abdel-Khalik, A. LeMouel and B. McCord, "Gas liquid two-phase flow in microchannels. Part I: twophase flow patterns," vol. 25, p. 377–394, 1999.

[20] B. Agostini and B. Yesin, "Modeling of a gravity driven two-phase loop," Baden-Daettwil, 2008.

[21] B. Agostini, D. Kearney and F. Agostini, "Electro-magnetic device comprising a cooling arrangement including a specifically arranged thermosyphon". Patent EP2682957 A1, 8 1 2014.

[22] T. K. and R. L. , "Mounting base". Finland Patent EP 2383779 B1, 12 9 2012.

[23] "Thermal Conductivity," 2014. [Online]. Available: http://www.engineeringtoolbox.com/thermal-conductivity-d_429.html. [Accessed 5 2014].

[24] A. L. Woodcraft, "Predicting the thermal conductivity of aluminium alloys in the cryogenic to room temperature range," vol. 45, no. 6, pp. Pages 421-431, 2005.

[25] "Raaka-aineet," 27 5 2014. [Online]. Available: http://porssi.taloussanomat.fi/commodities/. [Accessed 27 5 2014].

[26] L. v. A. drives, "ABB industrial drives ACS880, multidrives 1.5 to 5600 kW Catalog," ABB, 2014.

[27] G. Zyhowski and A. Brown, "Low Global Warming Fluids for Replacement of HFC-245fa and HFC-134a in ORC Applications".

[28] S. Gustafsson, "Corrosion properties of aluminium alloys and surface treated alloys in tap water," Sapa Technology, Uppsala, 2011.

[29] W.-D. Kuan, Y.-W. Hsueh, H.-C. Lien and W.-P. Chen, "Integrating Computational Fluid Dynamics and Neural Networks to Predict Temperature Distribution of the Semiconductor Chip with Multi-heat Sources," in *Third International Symposium on Neural Networks*, Chengdu, 2006.

[30] E. Öztürk and İ. Tarı, "A Road Map For Cfd Modelling Of Forced Cooled Packages," in *ASME International Mechanical Engineering Congress and Exposition*, Chicago, 2006.

[31] Ametek, “Programmable Power Supplies & Electronic Loads Catalog,” Ametek, San Diego, 2013.

[32] “Thermocoupleinfo,” REOTEMP Instrument Corporation , [Online]. Available: http://www.thermocoupleinfo.com/. [Accessed 2014 7 10].

[33] B. Agostini and M. Habert, “Compact Thermosyphon Heat Exchanger for Power Electronics Cooling,” *Journal of Energy and Power Engineering,* no. 7, pp. 972-978, 31 5 2013.

Appendix 1. The Zero Equation Model – Mixing Length Model

The viscosity of the fluid is changed (from a constant value) to one defined by:

$$\mu_t \equiv \rho l_m^2 S ,$$

where ρ is density [kg/m^3] and
l_m is the distance across which turbulent mixing takes place (size of turbulent eddies).

The distance across which turbulent mixing takes place is defined as:

$$l_m = min\,(0.419y, 0.09W) ,$$

where y = distance from wall and
W = maximum dimension of the computational domain.

S is the modulus of the mean rate of strain tensor, defined as:

$$S \equiv MOD\left(2S_{ij}S_{ij}\right) ,$$

where the mean strain rate is given by:

$$S_{ij} = \frac{1}{2}\left(\frac{du_i}{du_j} + \frac{du_j}{dx_i}\right) .$$

The fluid conductivity, k_t, is then defined as a function of the turbulent viscosity μ_t, specific heat c_p, and the Prandtl number, Pr_t as follows:

$$k_t = \frac{\mu_t c_p}{Pr_t} .$$

Pr_t is 0.9 away from the wall and near the wall an empirical equation is used to increase Pr_t.